University of Stellenbosch

Masters Thesis

Hydraulic Model Investigation of Sediment Control Measures at Low Weir River Diversion Works

Author:
LJ du Plessis

Supervisor:
Prof GR Basson

A thesis submitted in fulfillment of the requirements for the Masters degree in Hydraulic Engineering

at the

Department of Civil Engineering

March 2015

Declaration of Authorship

I, L.J. du Plessis, declare that this thesis and the work presented in it are my own. I confirm that:

- This work was done while enrolled for a Masters degree at the University of Stellenbosch.
- Where any part of this thesis has previously been submitted for a degree or any other qualification at this University or any other institution, this has been clearly stated.
- Where I have consulted the published work of others, this is always clearly attributed.
- Where I have quoted from the work of others, the source is always given. With the exception of such quotations, this thesis is entirely my own work.
- I have acknowledged all main sources of help.

Signed: _____

Date: _____

UNIVERSITY OF STELLENBOSCH

Abstract

Engineering Faculty
Department or Civil Engineering

Masters Degree

Hydraulic Model Investigation of Sediment Control Measures at Low Weir River Diversion Works

by L.J. du Plessis

Rivers are one of the earth's major readily available sources of fresh water. Abstractions from rivers are however not without problems. Firstly, river flow is variable and to deliver a constant yield is difficult. Secondly, rivers transport sediment which will be included in the diverted flow. Sediment control at diversion works have been studied for many years and this study attempts to gain further knowledge on certain sediment control features of diversion works.

Sediment control at diversion works and abstraction works is crucial to prolong the life of the mechanical components like pumps and turbines. A Commonly used diversion works design is one with a low weir and a graveltrap. The weir dams water for abstraction, which is of importance in South Africa with its variable rainfall and river flow.

The study focused on the following design features of diversion works: (1) the intake angle, which is the angle at which the structure is pushed into the river, (2) the intake opening height above a datum, (3) the river flow range where sediment is sufficiently scoured from the graveltrap and (4) the efficiency and river flow range of sediment flushing through a sluice gate at the graveltrap.

A Physical model study was conducted in the laboratory of the University of Stellenbosch, which consisted of designing the diversion works that were to be tested. The designs were based on guidelines from previous studies, case studies and hydraulic principles. The above mentioned features (1-4) were studied at three structures with prototype weir sizes of 2.5 m, 3.5 m and 4.5 m. The river was modelled as a straight rectangular channel with a loose bed surface, which was simulated with crushed peach pips. Sediment was also fed into the system with a conveyor belt feed system.

Pumps were used to abstract water and sediment through the intake opening, during the diverted sediment tests. Flow was diverted at a specific flow rate for each structure. The diverted

sediment was caught and weighed. Each structure was designed to divert sediment through one of three intake opening heights, to determine whether a higher intake opening sufficiently reduces the amount of diverted sediment. The self-scour efficiency at the graveltrap was determined with a sediment level survey in the graveltrap. From the survey a *clearance flow* was determined, which is the minimum river flow that clears the intake opening of sediment along its complete length. It was also determined what intake angle induces secondary flow which results in the lowest clearance flow. The sediment flushing through the sluice gate was evaluated by recording the time it takes a full graveltrap to be flushed clean at various river flow rates. The maximum river flow at which the graveltrap still flushes efficiently was determined for each structure.

It was found that between the 30^0, 45^0 and 60^0 intake angle that were tested, the 60 ^{0} angle yields the lowest diverted sediment ratio (DSR) over the range of structures as well as river flows tested. The tests yielded a river flow at each structure where the DSR is at minimum. During the self-scour tests of the graveltrap, it was determined that a 45^0 intake angle promotes better self-scour at the graveltrap. To promote both features, a 45^0 intake angle is suggested, as it reduces diverted sediment and has a lower risk of issues due to too large flow constriction.

The intake opening height was evaluated with analysis of diverted load and concentration. The conclusions on the intake opening vary between structure sizes. In the case of the smallest structure, with a 2.5 m weir height, the improvement observed for intake openings higher than the first (lowest) were variable. In the case of the 3.5 m weir structure, the results showed three consecutive intake openings could be feasible. In the case of the 4.5 m weir structure, less improvement was observed between the highest two intakes. Flood frequency should determine whether an intake opening with top-of-inlet of 1.6 m or 3.3 m above the minimum operating level should be designed.

It was observed during the sediment flushing tests that submergence of either the graveltrap wall and/or the downstream water level affects the flushing efficiency. y_3/y_2, which is the downstream flow depth over the contracted flow depth under the sluice gate of the graveltrap, was evaluated as an indicator of efficient flushing. The study found that a good guideline would be to flush during river flows where $y_3/y_2 < 1$, while also ensuring the flow over the graveltrap wall entrains the sediment in the graveltrap.

A figure which plots the downstream flow depth over sluice gate opening size was developed to serve as an operational guideline to efficient sediment flushing. The figure shows zones of efficient and non-efficient flushing. Further, the observed sediment flushing and self-scour ranges at each structure are also represented graphically.

The fact that there was designed for a specific river scenario and also the lack of varied model sediment size, limits the applicability of the findings and conclusions.

STELLENBOSCH UNIVERSITEIT

Opsomming

Fakulteit van Ingenieurswese
Departement van Siviele Ingenieurswese

Meesters Graad

Hydraulic Model Investigation of Sediment Control Measures at Low Weir River Diversion Works

by L.J. du Plessis

Riviere is van die aarde se hoof, maklik beskikbare bronne van vars water. Onttrekking uit riviere is wel nie sonder probleme nie. Eerstens is rivier vloei wisselvallig en om 'n konstante lewering te handhaaf is moeilik. Tweedens, vervoer riviere sediment wat ingesluit sal wees in die uitgekeerde vloei. Sediment beheer by uitkeerwerke word al vir baie jare bestudeer en hierdie studie poog om verdere kennis te verkry oor sekere sediment beheer funksies van uitkeerwerke.

Sediment beheer by uitkeerwerke en onttrekkingswerke is noodsaaklik om die lewensduur van meganiese komponente soos pompe en turbines te verleng. 'n Algemeen toegepaste uitkeerwerke ontwerp is een met n lae keerwal en gruisvangkanaal. Die keerwal dam water op, wat nodig kan wees om die lewering te handhaaf, veral met Suid-Afrika se wisselvallige reënval en rivier vloei.

Die studie het gefokus op die volgende ontwerp funksies van uitkeerwerke: (1) die inlaathoek, wat die hoek is waarteen die struktuur in die rivier ingedruk is, (2) die inlaatopening hoogte bo 'n datum, (3) die rivier vloei reeks waar sediment voldoende uitgeskuur word uit die gruisvangkanaal uit en (4) die effektiwiteit en rivier vloei reeks van 'n sediment spoel aksie deur 'n sluishek in die gruisvangkanaal.

'n Fisiese model studie was onderneem in die laboratorium van die Universiteit van Stellenbosch, wat bestaan het uit die ontwerp van die uitkeerwerke wat getoets sou word. Die ontwerp is gebasseer op riglyne van vorige studies, gevallestudies en hirouliese beginsels. Die bogenoemde funksies (1-4) was bestudeer by drie strukture met prototipe keerwal hoogtes van 2.5 m, 3.5 m en 4.5 m. Die rivier was gemodelleer as 'n reguit, reghoekige kanaal met 'n los bed oppervlakte, wat gesimuleer is met fyngemaakte perske pitte. Sediment was ook in die sisteem ingevoer met 'n vervoerband voer sisteem.

Pompe was gebruik om water en sediment te onttrek deur die inlaatopening tydens die uitgekeerde sediment toetse. Vloei was uitgekeer teen 'n spesifieke vloeitempo vir elke struktuur. Die uitgekeerde sediment was gevang en geweeg. Elke struktuur was ontwerp om sediment uit te

keer deur een van drie inlaatopening hoogtes, om te bepaal of 'n hoër inlaatopening hoogte die hoeveelheid uitgekeerde sediment voldoende verminder. Die self-uitskuur effektiwiteit van die gruisvangkanaal was bepaal deur 'n sediment vlak opmeting in die gruisvangkanaal. Vanaf die opmeting was 'n *skoonmaak vloei* bepaal, wat die minimum rivier vloei is wat die inlaatopening skoon maak van sediment oor die totale lengte. Dit was ook bepaal watter inlaathoek veroorsaak sekondêre vloei wat die laagste skoonmaak vloei oplewer. Die sediment spoel aksie deur die sluishek was geëvalueer deur die tyd wat dit neem om 'n vol gruisvangkanaal skoon te spoel, teen verskeie rivier vloeitempos te bepaal. 'n Maksimum rivier vloei waarteen die guisvangkanaal steeds effektiewelik skoon spoel was bepaal vir elke struktuur.

Dit was bevind dat tussen die 30^0, 45^0 en 60^0 inlaathoeke wat getoets is, lewer die 60^0 hoek die laagste uitgekeerde sediment verhouding (USV) oor die reeks van strukture, asook rivier vloeitempos wat getoets is. Die toetse het 'n rivier vloei opgelewer by elke struktuur, waar USV 'n minimum was. Gedurende die self-uitskuur toetse was dit bepaal dat 'n 45^0 inlaathoek beter uitskuur in die gruisvangkanaal bevorder. Om beide funksies te bevorder word 'n 45^0 inlaathoek voorgestel, omdat dit ook uitgekeerde sediment verminder en 'n laer risiko van probleme as gevolg van te groot vloei vernouing het.

Die inlaatopening hoogte was geëvalueer met analise van die uitgekeerde sediment lading en konsentrasie. Die gevolgtrekkings oor die inlaatopening hoogte varieer tussen struktuur groottes. In die geval van die kleinste struktuur, met 'n 2.5 m keerwal hoogte, was die verbetering wat waargeneem was by inlaatopeninge hoër as die eerste (laagste) inlaat, wisselvallig. In die geval van 'n 3.5 m keerwal struktuur het die resultate getoon dat drie opeenvolgende inlaatopeninge kan uitvoerbaar wees. In die geval van 'n 4.5 m keerwal struktuur was minder verbetering waargeneem tussen die hoogste twee inlate. Vloed frekwensie moet bepaal of 'n inlaatopening hoogte met 'n bokant-van-inlaat vlak van 1.6 m of 3.3 m bo minimun bedryfvlak moet ontwerp word.

Dit was waargeneem dat gedurende die sediment spoel toetse dat versuiping van die gruisvangkanaal muur en/of die stroomaf watervlak die spoel effektiwiteit beïnvloed. y_3/y_2, wat die stroomaf vloeidiepte oor die vernoude vloeidiepte onder die sluishek van die gruisvangkanaal is, was geëvalueer as 'n indikator van effektiewe spoel aksie. Die studie het bevind dat 'n goeie riglyn sal wees om te spoel tydens rivier vloeie waar $y_3/y_2 < 1$ is, terwyl dit ook verseker moet word dat vloei oor die gruisvang kanaal sediment meevoer in die gruisvangkanaal.

'n Figuur wat die stroomaf vloeidiepte teenoor die sluisopening grootte plot was ontwikkel om te dien as 'n bedryfsriglyn tot effektiewe spoel aksie. Die figuur toon zones van effektiewe en nie-effektiewe spoel aksie aan. Verder is die waargeneemde sediment spoel aksie en self-uitskuur reekse van elke struktuur ook grafies voorgestel.

Die feit dat daar ontwerp is vir 'n spesifieke rivier scenario asook die gebrek aan variërende model sediment grootte, beperk die toepasbaarheid van die bevindings en gevolgtrekkings.

Acknowledgements

I would like to thank the following people:

Prof. Gerrit Basson, thank you for all the guidance and knowledge you gave me in the last two years. I will be a better engineer due to your lessons.

Christiaan Visser, who foresaw my every possible mistake, thank you for your open door and practical advice.

The laboratory staff and especially Johann Nieuwoudt and Iliyaaz Williams, with whom I spent the bulk of my time, thank you for your time, your patience, your humour and your advice.

My family, thank you for your everlasting belief that I could actually finish the project.

Contents

List of Figures

List of Tables

Abbreviations

DDR	**D**iverted **D**ischarge **R**atio
DS	**D**iverted **S**ediment
DSR	**D**iverted **S**ediment **R**atio
LNW	**L**ow **N**otch **W**eir
MOL	**M**inimum **O**perating **L**evel
SF	**S**ediment **F**lushing
SS	**S**elf **S**cour

Symbols

b_r	width of river
b_d	width of diverted flow
b_p	width of pocket (dividing walls
B	top width of river
C	concentration
Cd	concentration of diverted sediment
d	particle diameter
d_{50}	median particle diameter
D	depth of flow
g	gravitational acceleration
G	sediment transport capacity g/s
u	flow velocity
$\overline{u}$	average flow velocity
u_*	shear velocity
u_c	mean critical velocity
u_{*c}	critical shear velocity
Q_d	Diverted flow (Design abstraction)
Q_c	critical flow causing sediment transport
r_c	radius of curvature
Re	Reynolds number
S	longitudinal slope of river
w	settling/fall velocity
w	width of the river
v	local flow velocity
y	distance measured from the water surface
y_0	flow depth
ρ	density of water
ρ_s	density of sediment

ν	kinematic viscocity
τ	shear stress
Δh	super elevation of water level due to flow around a bend
ω	unit stream power

Chapter 1

Introduction

1.1 Background and Motivation of Study

Water is life, and the management of it ensures it is distributed to where the demand is. In South Africa water is mainly used for irrigation (62% of harnessed fresh water, DWAF (2004)), but also for domestic use, mining, industrial, power generation and some commercial forestry.

The earth's sources of fresh water are lakes, rivers, groundwater and polar ice, of which only the lakes and the rivers are readily available sources. Raudkivi (1993) states that rivers are globally the major source of water to meet the various demands, due to the fact that they are more evenly distributed. The problem related to rivers as a water source is their variability of flow. South Africa, which is predominantly semi-arid, has low average annual rainfall on a global scale (450 mm/a compared with 860 mm/a, DWAF (2004)). The rainfall is also extremely seasonal and even variable within a season, resulting in rivers with mostly low water levels and sporadic high flows. The nature of the rivers drastically limits the amount of water that could be abstracted without damming. This is the first problem with river abstraction in South Africa.

Natural rivers carry sediment in form of bedload or suspended load (discussed in Chapter 2) with origins either from overland flow or in-stream sediment which is re-entrained if the river has the carrying capacity.

During abstraction of river water, sediment will be included in the diverted flow with a range of resulting difficulties. The sedimentation of the diversion works should be avoided and sediment will cause damage in the form of abrasion and cavitation to the machinery (pumps or hydro turbines).

Another sediment related issue is reservoir sedimentation, which is an especially problematic issue in South Africa, enough so to disregard future developments of large reservoirs. Due to

water scarcity, this might not be feasible, but diversion and abstraction works with no (or low) weir should be promoted. The diverted flow can be discharged into an off-channel reservoir where sediment is excluded at the abstraction works (Basson and Rooseboom, 1997).

River diversion structures are used to divert flow from the main watercourse for the purpose of abstraction. The purpose of the abstracted water determines the flow rate necessary, which then together with the characteristics of the river (flow and sediment characteristics) determines the design of the river diversion structure. Irrigation, industrial (cooling water), abstraction for run-of-river hydropower and off-channel storage (including pumped-storage hydropower schemes) are examples of water uses that require large water diversion and abstraction. The structures necessary for such diversion require a weir to create enough water head above the intake structures to ensure the water demand is met.

The importance of the exclusion of sediment is clear, and has been vastly discussed, but this research project attempts to gain further knowledge specifically on the structure, and especially on structures designed for larger diverted flows. A structure with a weir allows damming of water to allow larger abstractions, but with the various sedimentation problems mentioned above. The proposed methods of mitigation are (1) use of the optimum intake angle to induce secondary currents which will push sediment laden flow away from the intake (refer to Chapter 3.3.2.2). Method (2) is intake heights on different levels, closing and opening as the water level rises and drops. This will allow the clearer water in top flows to be abstracted while excluding sediment laden bottom flows. Further, investigations of the flushing of a graveltrap through sluice gates would determine the range of flows where graveltrap flushing is efficient and at what point the graveltrap scours sufficiently with the sluice gate closed. If the graveltrap is clean it would reduce the amount of local sediment abstracted through the intake opening.

1.2 Objectives

The research aims to investigate methods of sediment exclusion at diversion works. All tests were conducted on structures consisting of a weir and a graveltrap ,seen in Figure 1.1.

The objective of the study is to investigate the following features of the diversion works structures:

- The effect of the intake angle on diverted sediment and scour from the graveltrap, with the purpose of finding a optimum intake angle.
- The effect of intake opening height on diverted sediment, to determine whether and at which size structure higher inlets are relatively efficient.

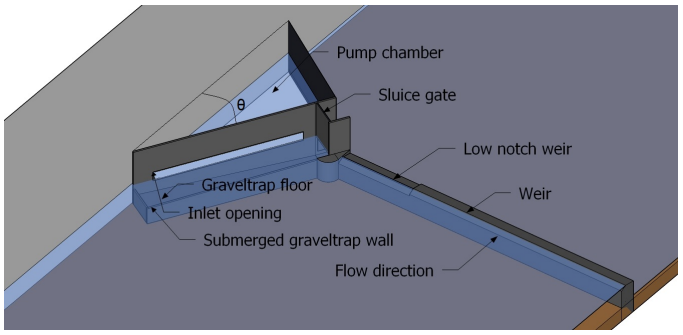

FIGURE 1.1: Diversion works designed for physical model tests

- The sediment flushing (with water level draw down) efficiency and range through the sluice gate of the graveltrap.
- The river flow range where self scouring of the graveltrap sufficiently clears the intake opening.

The features were tested at three different weir heights, with different diverted flows, intake opening dimensions, diverted flows and graveltrap dimensions. The effects of the above mentioned features were tested per structure and compared between structures.

1.3 Method

The research is conducted with a literature study on river flow and sediment characteristics in South Africa, sediment transport theory and formulae, river hydraulics with focus on secondary flow and river regime theory. River diversion was studied with focus on its basic principles, the river flow and sediment related issues and finally various river diversion structure designs, features and placement with the purpose of sediment control.

Physical model tests were conducted on river diversion works at the University of Stellenbosch Hydraulics Laboratory. The model is based on a river scenario applicable to South African rivers, i.e. the Orange River. The river is modelled as a straight, 3 m wide, rectangular channel with an erodible boundary.

A 200 mm layer of sediment (size graded crushed peach pips) were placed on the floor of the channel and sediment was fed into the system with a conveyor-belt system.

Three diversion structures with weir heights of 2.5, 3.5 and 4.5m were designed to divert 1, 5 and $10 m^3/s$, respectively, and scaled with the Froude similarities.

The sediment diversion tests consisted of testing each structure at three intake angles (30^0, 45^0 and 60^0), as well as at three opening heights which were specific for each structure. At each

structure the diverted flow (Q_d) was kept constant, whilst the channel flow (Q_{riv}) was varied from low to flood flows.

Sediment flushing through the graveltrap was evaluated in terms of flushing time necessary to flush the full graveltrap sufficiently clean. The sediment flushing tests were conducted for each structure at each intake angle, from low flows up to the flow determined to be ineffective.

The self scouring efficiency of the graveltrap was determined by means of a graveltrap survey along the length of the graveltrap. The graveltrap was filled to the invert level of the lowest intake opening before the initiation of the test. The remaining levels were surveyed post each increased flow. The flow that sufficiently cleared the intake opening along its complete length was recorded as the *clearance flow*. This was determined for each structure at each angle.

1.4 Chapter Overview

The study consists of six chapters. Chapter 2 is a literature study, covering the characteristics of river flow and the alluvial sediment in South Africa. Chapter 2 also includes study of river hydraulics with focus on the understanding of secondary flow and river regime theory.

Chapter 3 is also a literature study, with focus on river diversion. The basic principles is covered, including the issues observed worldwide and specifically in South Africa. Finally Chapter 3 discusses applicable river diversion works and features, including its placement and design.

The methodology of the experimental investigation of this study is discussed in Chapter 4. It covers the design guidelines, process, physical limitations and assumptions of the physical model study. A summary of the test conditions and a description of the procedures are also included in Chapter 4.

Chapter 5 presents the results of each test, as well as an analysis of the results. Chapter 6 summarises the findings and conclusions of the study and recommendations for further research that arose from the study is mentioned in Chapter 7.

The test result data is tabulated in Appendix A. In Appendix B the pump calibration and accuracy tests are tabulated along with the determination of the wet-to-dry sediment weight factor used in the testing. The prototype sediment size, represented by the model sediment mixture calculation is shown in Appendix C.

Chapter 2

Literature Study : River Flow and Sediment Behaviour

2.1 Introduction

This literature study was conducted to understand aspects of alluvial river flow, specifically in South Africa, to understand its effects on water diversion and abstraction. The sediment characteristics were studied accordingly with focus on its origin and transport, which is dependent on the river flow hydrology, the geology of the catchment and land use.

It was found that various techniques have been developed to use topography and river hydraulics to cope with the complexity of South African alluvial rivers. Sediment dynamics, river bend hydraulics, secondary flows, sediment distribution and velocity profiles are important in river diversion works and has been thoroughly discussed by the likes of Vanoni (1975), Raudkivi (1993), Bouvard (1992) and Yang (1996). The WRC (Water Research Commission) reports by Brink *et al.* (2006) and Basson (2006) focussed on South African conditions and applications. Recently, Brink (2004) and Van Heerden (2012) conducted studies on the optimum placement within a river bend.

2.2 South African River Flow

To be able to study river diversion, it is crucial to understand river flow and sediment transport in South Africa. South African rivers are known to be extremely variable and seasonal, due to the extreme difference in rainfall during the wet and dry seasons. The variability also extends beyond seasonality, where critical low flows can occur for years and in turn can change into flood flows in minutes of heavy rainfall. The high variability of rainfall increases variability

in sediment loads which makes the design of river diversion works highly complex. To worsen the situation in South Africa, the positions of urban developments are generally not located close to our main watercourses (DWAF, 2004). Historic developments were driven by industries (mining) and political influence (DWAF, 2004). Thus, the demand of quite a few developed areas in the country exceeds the available yield within that region. This forces the complex abstraction and large scale transfers of water across catchments (DWAF, 2004).

2.3 Sediment Characteristics in South Africa

Significant sediment transport in alluvial rivers occur during floods and in South Africa it was observed that transported sediment consists of approximately 20% sand, 40% clay and 40% silt with relatively fine sands of 0.2 to 0.5 mm deposited after floods (Brink *et al.*, 2006). Rooseboom (1992a) states that the inland rivers of South Africa carry mainly particles smaller than 0.2 mm. Note that in mountainous catchments, the rivers will be able to carry sediment with a larger bedload fraction compared to the inland rivers. This is explained by Raudkivi (1993), who discussed the influence of bed slope on grain distribution with reference to sediment entrainment. It is stated that decrease of bed slope causes the decrease of mean particle size and an increase in uniformity of the grain size. Table 2.1 shows the particle size classification according to the BS 1377 (1975).

Table 2.1: Soil classification according to the BS 1377 (1975)

Very fine clay	0.00024-.0005 mm	Very coarse sand	1-2 mm
Fine clay	0.0005-0.001 mm	Very fine gravel	2-4 mm
Medium clay	0.001-0.002 mm	Fine gravel	4-8 mm
Coarse clay	0.002-0.004 mm	Medium gravel	8-16 mm
Very fine silt	0.004-0.008 mm	Coarse gravel	16-32 mm
Fine silt	0.008-0.016 mm	Very coarse gravel	32-64 mm
Medium silt	0.016-0.031 mm	Small cobbles	64-128 mm
Coarse silt	0.031-0.062 mm	Large cobbles	128-256 mm
Very fine sand	0.062-0.125 mm	Small boulders	256-512 mm
Fine sand	0.125-0.250 mm	Medium boulders	512-1024 mm
Medium sand	0.250-0.5 mm	Large boulders	1024-2048 mm
Coarse sand	0.5-1.0 mm	Very large boulders	2048-4096 mm

According to Rooseboom (1992a), storms add silt and clay (limited by the amount available) to the river from its catchment, via overland sheet flow. The particles are carried via minor streams, where the carrying capacity is sufficient to carry the entrained load, to major river courses where the carrying capacity exceeds the necessary amount. Thus, the sediment concentration is generally not limited by the carrying capacity, but rather by the availability of sediment. If a catchment released all of its silt and clay during a storm, the amount that ends up in the river during that storm and the next (with a depleted catchment) will differ drastically.

Estimation of fine sediment loads can be made from average annual data, if available. Records exist from prior 1970, but the design of diversion structures require longer data records. If local data is not available, Brink *et al.* (2006) recommends estimates based on regional sediment yields developed by Rooseboom *et al.* (1992b), but only for smaller abstraction works. Fine sediment concentrations observed during floods can vary annually from 20 000 mg/l to 60 000 mg/l during an extreme flood (Brink *et al.*, 2006).

2.4 Sediment Yield

The yield indicates the observed and estimated amount (mass) of sediment that is carried by the river over a specified time (normally a year). Sediment yield, which is dependent on the flow, is very hard to estimate when considering that very long records (at least five years of daily measured data and more measurements during floods) are necessary to be able to include the impacts of floods (which can increase the yield up to thirteen times the mean annual yield (Brink *et al.*, 2006)). Secondly, the influence of deforestation, land degradation and overgrazing on sediment yield is tough to predict, which in turn makes it difficult to estimate the future yields.

Currently annual sediment yields are observed to be between 100-400 ton/km^2/a, with a maximum of 1000 km^2/a in the Eastern Cape (Brink *et al.*, 2006). Methods to determine sediment yield are either the sediment yield map based on statistical regional approach by Rooseboom *et al.* (1992b), surveys of sediment deposits or sediment load-discharge rating curves.

Msadala and Basson (2009) developed analytical methods of sediment yield prediction and also evaluated the strengths and weaknesses of numerical modelling of sediment yield. The study found that both empirical and probabilistic methods can be used as a decision making tool in feasibility studies. It is also specified which method to use in which regions of South Africa.

Numerical models have proven to be powerful tools for detail designs in water resource management, but need to be validated with site specific data records which is not always available.

2.5 Sediment Transport

Sediment transport theory and its predictive equations are of high importance to the engineer of diversion structures. It explains the natural state of a river, as well as the changes to the natural state post construction of diversion works. Also, sediment transport knowledge enables us to design better functioning diversion works, due to better understanding of i.e. flushing of sediment through sluice gates. With sediment transport knowledge, erosion and scour can be

controlled and even used as a design feature, i.e. the placement of diversion structures in a bend where maximum scour occur. The river bend phenomenon will be discussed in Chapter 2.7.

Sediment transport occurs only where water flows over an erodible bed. Sediment is transported in one of two methods, either only by rolling along the river bed or in co-operation with sediment in suspension. The two load types are called bedload and suspended load, respectively. A third mode of transport, called the wash load, differs from the two main transport modes, in that the the sediment is introduced into the river from overland flow where it then stays in suspension and is normally not entrained by the river flow like the other two methods. Wash load consists of fine silt and clay and is normally not of significant quantities (Raudkivi, 1993). In South Africa however, this is not the case, as discussed in Chapter 2.3.

2.5.1 Particle Entrainment

Particle entrainment is governed by the balance between the forces applied by the fluid, of drag and lift (equations 2.1 and 2.2), and the self weight of the particle (equation 2.3). The friction force (natural resistance) is related to the self weight of the particle. The parameters are defined in the list of symbols or defined explicitly at equations when and where they are applied only at specific equations.

$$F_D = \frac{1}{2}\rho C_D \frac{\pi d^2}{4}(\alpha u_*)^2 \tag{2.1}$$

$$F_L = \frac{1}{2}\rho C_L \frac{\pi d^2}{4}(\alpha u_*)^2 \tag{2.2}$$

$$W = \frac{\pi d^3 g}{6}(\rho_s - \rho) \tag{2.3}$$

where:

C_D is the drag coefficient.
C_L is the lift coefficient.
α is the shear velocity coefficient.

2.5.2 Shear Resistance Approach

With focus on bed- and suspended load there will naturally be flows over an erodible boundary where sediment transport does not occur, or rather does not yet occur. Thus, there should be a point in stream flow where the increasing energy from the flow will be enough to move particles from their current position. Raudkivi (1993) and Chadwick *et al.* (2004) describes this as the

threshold of movement, where the particles which lie on a rough surface has a natural resistance to movement due to its shape and position between its surrounding particles. This is a shear resistance between the surface of the particle to be moved and its stationary surrounding. The factors like particle position are probabilistic, but when a particle is prominent on the bed and thus not affected by its surroundings, the self weight (equation 2.3) of the particle is the sole stabilising force, which opposes movement. The concept of viscous flow introduces a shear stress (equation 2.4) in fluids based on the weight component of water, acting in the direction of flow. In laminar flow, the shear stress increases linearly from the water surface to a maximum (τ_0) at bed level. At some point a critical shear stress (τ_c), induced by the flow of water, will be enough to initiate particle movement. The first method of transport to occur is bed load and with increasing shear stress (increasing fluid velocity), particles will be entrained creating suspended load as well. Refer to Figure 2.1.

$$\tau_0 = \rho g y_0 S \tag{2.4}$$

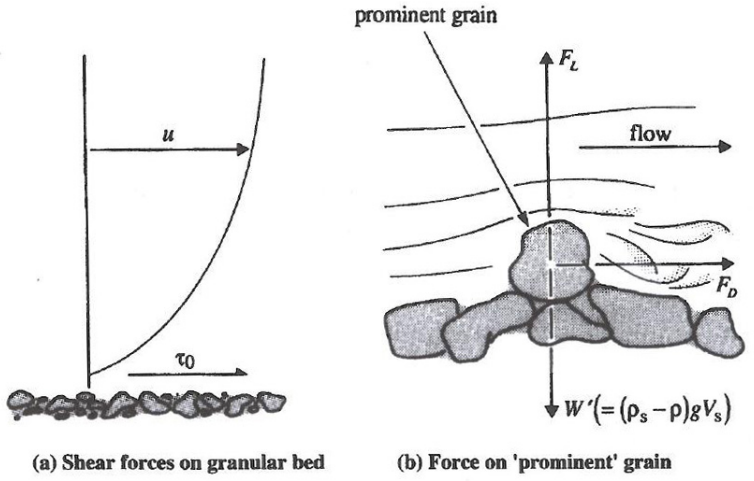

FIGURE 2.1: Particle Entrainment Forces (Chadwick *et al.*, 2004)

With the assumption of uniform sediments in unidirectional uniform flow and average levels of turbulence, the Shields curve (Figure 2.2 plots the entrainment function (2.5) against the Reynolds number (equation 2.6) (Raudkivi, 1993).

$$\theta_c = \frac{\tau_c}{\rho g(S_s - 1)d} = \frac{u_{*c}^2}{g(S_s - 1)d} \tag{2.5}$$

where:

$$S_s = \frac{\rho_s}{\rho}$$

$$Re_* = \frac{u_* d}{\nu} \tag{2.6}$$

where:

$$u_* = \sqrt{\frac{\tau_0}{\rho}} = \sqrt{\frac{\rho g y_0 S}{\rho}} = \sqrt{g y_0 S}$$

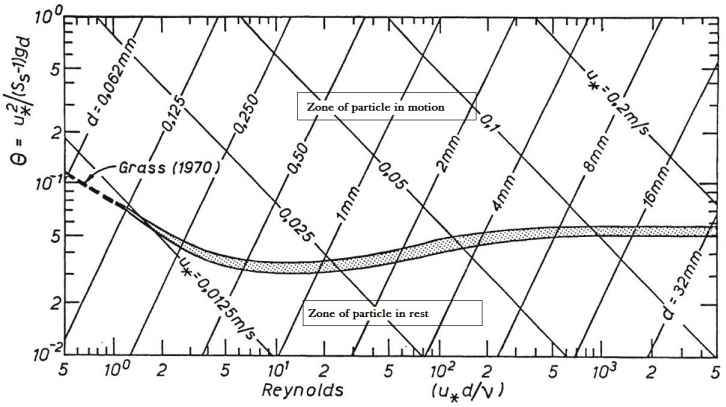

FIGURE 2.2: Shields Curve: Sediment entrainment as a function of the Reynolds number. The shaded bands indicates the spread of data used; the dashed lines envelope most of the published data. (Raudkivi, 1993)

Note that the velocity gradient (and thus the shear stress) in turbulent flow conditions differ from laminar conditions, due to eddying motion. In turbulent flow conditions, shear stress develop through eddie movement, as described by Rooseboom (1992a), who also developed mathematically the average shear stress over the cylindrical eddie (in clear water, with a rigid bed). In practice such as river flow, we deal mainly with turbulent flow.

2.5.3 Critical Velocity Approach

This approach refers to the relationship between a so-called *critical velocity* and particle entrainment. The known earliest development of this approach was done by Hjulstrom (1935), which delivered a curve plotting velocity versus particle diameter. a Simple equation (2.7) for the mean critical velocity (u_c) at a given elevation, incorporating the logarithmic velocity distribution is shown in Raudkivi (1993). Yang (1973) used drag and lift forces, combined with the logarithmic velocity distribution to develop the equations (2.8 and 2.9) for the mean critical velocity (U_c) over the depth of flow.

$$u_c = 5.75 u_{*c} log(y/y') \tag{2.7}$$

where:

y' is the elevation at which the velocity is zero according to the log-distribution.

u_{*c} is the shear critical velocity.

$$\frac{U_c}{w} = \frac{2.5}{log\left(\frac{u_* d}{\nu}\right) - 0.06} + 0.66 \tag{2.8}$$

when:

$$1.15 < \frac{u_* d}{\nu} < 70$$

and reducing to

$$\frac{U_c}{w} = 2.05 \tag{2.9}$$

when:

$$\frac{u_* d}{\nu} > 70$$

2.5.4 Unit Stream Power Approach

Stream power theory was evaluated by Bagnold (1966), who reasoned that the rate of energy (measured as stream power per unit area) dissipation that occurs while transporting sediment can be related to sediment transport capacity. The power available in a stream of unit length is given by equation 2.10 and for a unit width of that stream reduces to equation 2.11 (incorporating equation 2.4).

$$Power = \rho g Q S \tag{2.10}$$

$$\omega = \frac{Power}{flow\ width} = \rho g y_0 \overline{u} S = \tau \overline{u} \tag{2.11}$$

Rooseboom and Mulke (1982) used the stream power concept to describe sediment entrainment. Equation 2.12 shows the stream power per unit volume (unit length and width). Ultimately the study yielded relationships describing the entrainment threshold, for rough turbulent flow (equation 2.13) and smooth turbulent (as well as laminar) (equation 2.14). Figure 2.3 (also called the Modified Lui Diagram) shows these relationships graphically with measured data from Yang (1973).

$$(\rho_s - \rho) g w \tag{2.12}$$

$$\frac{\sqrt{gDS}}{w} = 0.12 \tag{2.13}$$

when:

$$\frac{\sqrt{gDS}}{\nu} > 13$$

$$\frac{\sqrt{gDS}}{w} = \frac{1.6}{\frac{gDS}{\nu}d} \tag{2.14}$$

when:

$$\frac{\sqrt{gDS}}{\nu} < 13$$

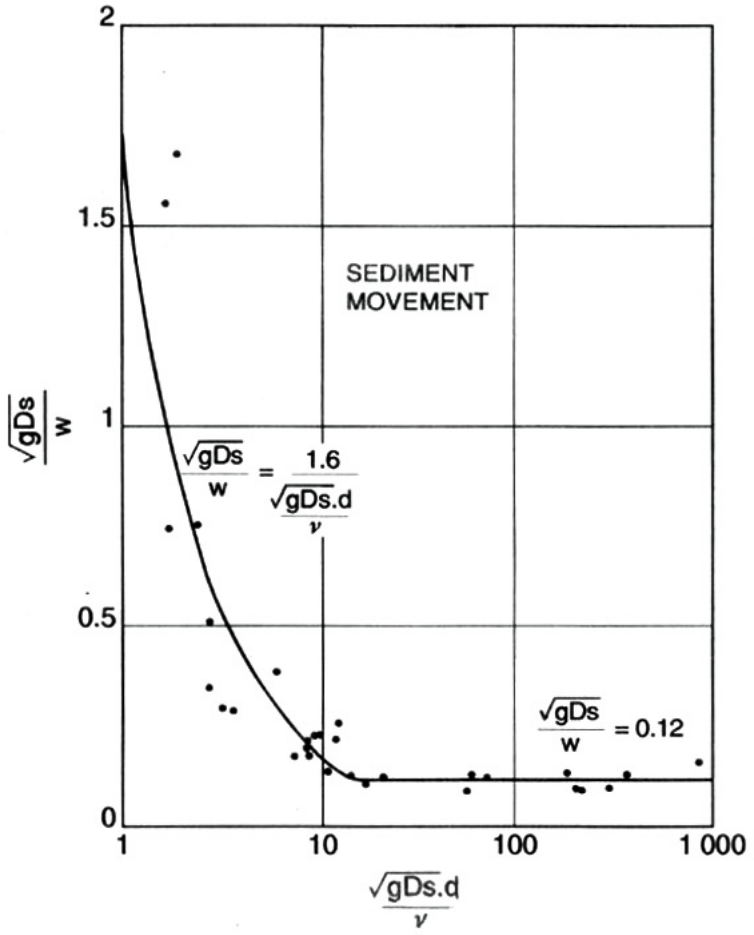

FIGURE 2.3: Modified Lui Diagram (Rooseboom and Mulke, 1982)

2.5.5 Probabilistic Nature of Particle Entrainment

The initiation of movement of a sediment particle is dependant not only on the factors which can be simplified and averaged in such a way so that they can be applied in mathematical relationships. Various factors which are not a certainty in each situation influence whether a particle will be entrained or not. Yang (1996) mentions the following probabilistic factors: particle position in relation to other particles with different grain sizes; particle position in

relation to bed forms like ripples and dunes; and the instantaneous strength of turbulence, along with the orientation of the particles at that moment.

2.5.6 Turbulent Sediment Transport Theories

There are a vast amount of sediment transport equations, which predict bedload, suspended load or total load. It has been observed that specific transport equations are more popular in certain parts of the world. Sediment transport equations are known to be inaccurate and site specific coefficients are incorporated to yield acceptable answers. Also, the theories all assume uniform sediment particles and steady, uniform flow, equilibrium conditions. This is in reality not the case.

Basson and Rooseboom (1997) reviewed the following generally used equilibrium sediment transport equations:

- Engelund and Hansen(1967)
- Ackers and White (1973)
- Unit Stream Power, the modified Lui diagram (Yang (1973), Rooseboom (1992a))
- Gravitational Power Theory (Velikanov (1954), Dou(1974), Zhang(1959))
- van Rijn (1984) methods

Basson and Rooseboom (1997) highlights the successful predictions in South Africa, achieved with the unit stream power equations developed by Yang (1973) and Rooseboom (1992a).

The Van Rijn equations, which are based on empirical data, are unique in the sense that they include the change in bed roughness and energy dissipation for different flow regimes and sediment transport.

All of the methods above still excluded the fine sediment transport processes. Basson and Rooseboom (1997) mentions the in-practice methods of predicting the fine sediments transport specifically in reservoirs:

- Diffusion equation
- Sediment transport equations, re-calibrated with fine sediment data.
- Combinations of the diffusion equation and re-calibrated sediment transport equations.

2.6 Vertical Distribution of Suspended Sediment

It is now understood that if energy in the stream is sufficient, particles will be entrained and if the energy is further increased, particles will be suspended. The concentration of the suspended sediment will vary vertically across the stream. If the particles are small enough (in relation to the energy of the stream), like the wash load in South Africa, the particle distribution could be near homogeneous. Larger particles, which is more detrimental in the diverted flow, could be excluded by diverting the water at heights above the stream bed where the sediment concentration is less.

The Rouse (1937) equation (2.15) expresses the vertical distribution of the amount of sediment as a C/C_a ratio, which is the sediment concentration a height (y) above the bed related to the sediment concentration at a height equal to the bedload layer thickness (a) above the bed.

$$\frac{C}{C_a} = \left(\frac{D-y}{y}.\frac{a}{D-a}\right)^Z \tag{2.15}$$

where:

κ is the von Karman coefficient.
C is the sediment concentration a distance y above the bed.
C_a is the sediment concentration at a reference distance a above the bed.

The value of Z (equation 2.16) determines the variability of the vertical distribution. As Z increases, suspended transport decreases and vertical distribution variability increases. Basson and Rooseboom (1997) (among other mentioned by them and Yang (1996)), replaced the variable Z with Z_1, which modified the equation to be applicable to coarse particles and not only fines. Z_1 is not defined.

$$Z = \frac{w}{\kappa\sqrt{gDS}} \tag{2.16}$$

2.7 River Bend Hydraulics

When river flows around a bend, a secondary flow is formed in the transverse direction. The secondary flow (also known as spiral flow) moves at the top/open boundary towards the outer bank of the bend and at bed level towards the inside bank (Figure 2.4). This mechanism scours sediment from the outer bank and bed and transports it towards the inside bank. This is very a noticeable feature of alluvial rivers. Sediment rejection at an intake is enhanced by structure placement at the outer bank of a bend. This chapter attempts to discuss the basic

theory of this occurrence, described by Minikin (1920), Bridge and Jarvis (1982), Avery (1989), Raudkivi (1993) who has more in-depth literature studies on the topic. Recently Brink (2004) and Van Heerden (2012) also conducted physical model studies on the scour position in a bend.

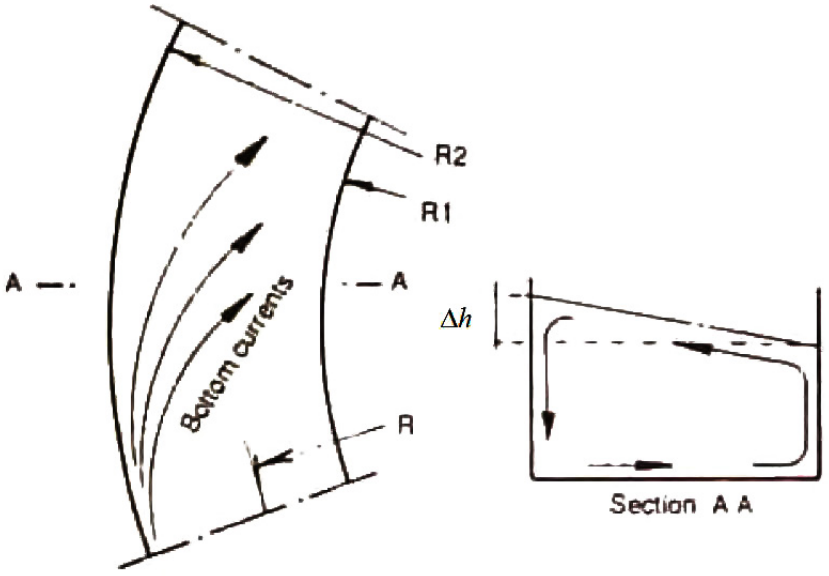

FIGURE 2.4: River bend: spiral flow (Bouvard, 1992)

2.7.1 Curvlinear Flow and the Initiation of Secondary Flow

When water flows around a bend a centrifugal acceleration is generated across the width of the stream. The combination of the centrifugal accelerations across the stream an increase in elevation of the water level at the outer bank. This elevation is determined with equation 2.17 (Bouvard, 1992).

$$\Delta h = \int_{R_1}^{R_2} \frac{v^2}{gR} dR \tag{2.17}$$

where:

v is the local velocity.
Δh is the super-elevation at the outer bank.
R_1 is the inner radius.
R_2 is the inner radius.
R is the radius of the local streamline.

The velocity and thus also the resulting centrifugal acceleration is assumed to be zero at the banks of the river. The elevated water level causes an increase in hydrostatic pressure on the

outer bank, which results in a transverse flow at the bottom of the bed (Figure 2.4). The transverse bottom flow scours sediment away from the outer bank and carries sediment towards the inside of the bend.

2.7.2 Position of Fully Developed Secondary Flow, Maximum Scour and the Proposed Position of Diversion Works

A River can bend between 0^0 and 180^0 and secondary flows will develop in any bend. There is a point within the bend where it is said that the flow is fully developed, where the scouring at the outer bend is at its greatest extent. Raudkivi (1993) developed an equation 2.18, relating to Figure 2.5, which showed that secondary flows only fully develop at 30^0 into a bend.

$$\theta = 1.5\frac{C}{\sqrt{g}}\frac{D}{r} \tag{2.18}$$

where:

C is the Chezy coefficient.
r is the radius of curvature.
y_0 is the depth of flow.

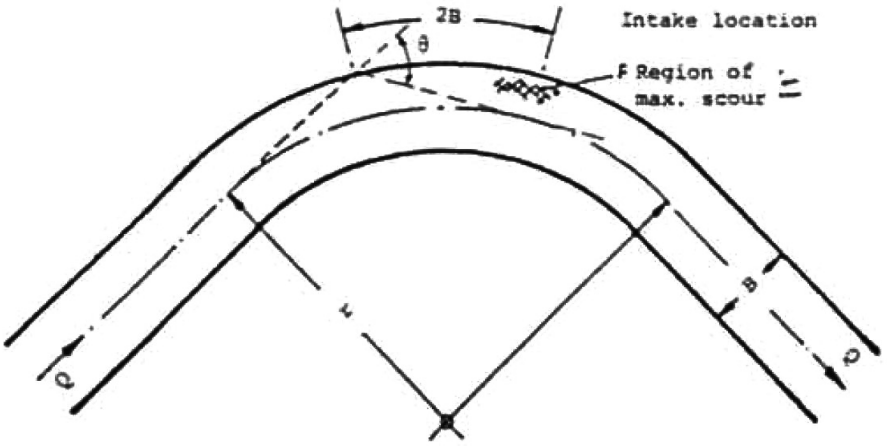

FIGURE 2.5: Position of developed secondary flow (Raudkivi, 1993)

Choudhary and Narasimhan (1977) and Bridge and Jarvis (1982) studied the strength of the secondary flow, as well as the position of developing, maximum intensity and decaying zones. The strength of spiral flow is represented as a percentage ratio of the radial velocity to the mean velocity of the stream flow (Choudhary and Narasimhan, 1977).

The secondary flow initiates scouring at the outer bank of a bend. In physical model studies, the position of a diversion works, is determined by determining the position of the deepest scour

hole in the bend (Brink (2004) and Van Heerden (2012)). The shape and position of the deepest scour hole is affected by the sediment and water discharge, radius of curvature (r_c), angle of the bend, stream cross section and the slope of the energy gradient (Shen (1971) and Raudkivi (1993)). A radius of curvature to width ratio (r_c/w) ranging between 3 and 15.2 (largest ratio tested by Brink (2004)) is popularly related to the scour position. As mentioned, the intake position and the maximum scour position is linked and Brink (2004) found that Table 2.2 works well over a range of r_c/w ratios. Table 2.2 relates the central angle of the bend to the optimal intake location.

TABLE 2.2: Central angle of bend and optimal intake location (SC (Sediment Committee) and CHES (1992), cited in Brink (2004))

Central angle of bend (^{0})	<45	60	90	120	150	180
Optimal location of intake (^{0})	0	45	60	80	95	110

2.7.3 Flow Velocity Characteristics Around a Bend

Flow around a bend has two significant effects on the streamlines of the flow. (1) The position of the maximum flow through the bend (start, centre and exit) moves. Bridge and Jarvis (1982) showed that as generally known, the maximum velocity moves from close to the inside bank at the start of the curve, to near the outer bank downstream of the apex of the bend. There is however the possibility that when the river is in flood and water level is above the bankfull level, the position of the maximum velocity moves to the inner bank.

(2) Due to secondary currents, the velocity vector deviates from its normal right angle to the stream cross-section. The vector is angled towards the outer bank, at an angle δ, which is simply determined with equation 2.19 (Bridge and Jarvis, 1982). Bridge and Jarvis (1982) also showed that equation 2.20 accurately determines the deviation angle, where k is a constant with a value close to 10. The deviation angle is a good indicator of spiral flow strength.

$$tan\delta = \frac{v_z}{v_x} \tag{2.19}$$

where:

v_z is the local transverse velocity.
v_x is the local stream-wise velocity.

$$tan\delta = \frac{kD}{r} \tag{2.20}$$

where:

k is a constant with a value close to 10.
r is the local radius of curvature.

2.8 River Regime

River regime is a concept linked to river morphology, which is a branch of geomorphology. River morphology is the study of the formation of river features on mega scale (longitudinal slope of a river reach), macro scale (cross-sectional shape) and meso scale (bed features i.e. ripples and dunes). Beck (2003) states that a river in regime is one that *" has obtained a long-term stable configuration, with only minor adjustments "*. Adjustments refer to changes of cross-sectional shape (width and depth), longitudinal slope and channel patterns. The adjustments are a result of the water discharge, sediment load and sediment characteristics.

2.8.1 Dominant Discharge and Bankfull Discharge

Water discharge is mentionable above other morphology affecting factors, due to its greater influence. The morphology of a river is formed over a long period where a range from low to flood flows influences the shape. It is generally understood that one discharge could form the same channel as the range of flows. This *one* flow is the dominant discharge.

The simplest definition of bankfull discharge is the discharge that results in a water level which is at the tops of the banks of the main channel, before the flow goes onto the floodplains. Denys (2006) did a thorough study on the interaction zone between the main channel and the floodplain, with focus on sediment deposition on the floodplain.

For the purpose of this study, it should be noted that bankfull flow and dominant discharge is not the same and both can be linked to a recurrence interval. Beck (2003) discusses the existing definitions of both terms, as well as the difficulties in determining each.

2.8.2 Regime Equations

When considering the three basic degrees of freedom of a river (width, depth and slope) and the factors that influence them, namely: water discharge, sediment load and channel roughness, it is possible to describe the stable state of a river in regime. Beck (2003) did a study on the then existing regime equations and found that previous equations were all empirically determined, meaning that they are applicable only to the conditions which resulted the data from which they were determined. The aim of the study was to determine analytical regime equations for

South African conditions. Coefficients that simplify the equations were added and calibrated with cross-sectional data from 59 South African sites. The study yielded equations 2.21 and 2.22, which are valid for the ranges summarised in Table 2.3. It was found that the 1:10 year recurrence flood is the dominant discharge and is correctly applied in the regime equations.

$$B = 4.034 {Q_{10}}^{0.365} S^{-0.228} {d_{50}}^{0.053} \tag{2.21}$$

$$D = 0.071 {Q_{10}}^{0.374} S^{-0.154} {d_{50}}^{-0.02} \tag{2.22}$$

TABLE 2.3: Ranges of parameters, applicable in equations 2.21 and 2.22 (Beck, 2003)

Parameters	**Range**
Discharge, Q_{10} (m^3/s)	68 - 5200
Width, B (m)	22 - 351
Average, Depth D (m)	0.51 - 5.9
Hydraulic Radius, R (m)	0.49 - 6.4
Slope, S	0.00015 - 0.07198
d_{50} (mm)	0.005 - 0.5

Chapter 3

Literature Study : River Diversion with Focus on Sediment Control

3.1 Introduction

The purpose of water abstraction from a river is to meet a demand of a user, be it for basic human needs, agriculture, industrial or energy supply. The diversion works have to deal with the characteristic complications of river flow. The two main complications are (1) abstracting a constant yield with variable river flow and (2) dealing with the sediment that is entrained in the flow. Dealing with sediment is a multi-faceted issue, where both the preservation of the river and the maintenance of the diversion works are of importance.

This chapter aims to review the studies on diversion works and sediment control at the diversion works, but with definite focus on the diversion works identified as commonly used in South Africa, and which was the object of the physical tests. Avery (1989), Bouvard (1992) and Raudkivi (1993) discussed all aspects concerning design and operation of diversion works. Brink *et al.* (2006) and Basson (2006) were written to resolve the issues still experienced in South Africa and discussed all the relevant types of diversion works.

3.2 Sediment Related Issues at River Diversion Works

3.2.1 Reservoir Sedimentation

Reservoir sedimentation has been a problem worldwide and it has been found that reservoirs in semi-arid areas with high sediment yield ratios are exceptionally prone to reservoir sedimentation. The issues are of hydraulic as well as environmental nature.

In South Africa some extreme cases have been observed: the Mbashe weir in the Eastern Cape silted up within 2 years of completion (Wallace (1994), cited in (Basson and Rooseboom, 1997)) and a reservoir basin survey of the Welbedacht reservoir on the Caledon river, conducted by the Department of Water Affairs (Basson and Rooseboom, 1997) showed 85% of its capacity was lost within 20 years. The link between fine sediments and reservoir sedimentation can be drawn by the following observation: A reservoir wall slows upstream flow velocity to such an extent that coarser sediments are settled a distance upstream of the dam wall, but due to the small settling velocity of the fine material, the fine sediments are carried towards the dam and a fraction will be deposited against the dam wall or weir (Basson and Rooseboom, 1997), (Rooseboom, 1992a). The build-up of fine (cohesive) sediments is difficult to flush out (Basson, 2006). Where the deposited sediments are coarser, i.e. at the Lavey run-of-river hydropower plant on the Rhone River in Switzerland, the sediment could be flushed out more effectively across the length of the weir (Bieri *et al.*, 2011). The siltation of dams is a problem which is almost impossible to prevent or manage and Basson and Rooseboom (1997) recommends off-channel storage as the long-term sustainable solution to the control of sediment in reservoirs.

Weirs across rivers, used to dam water for abstraction, are generally lower than dam walls of reservoirs, but still suffer the same consequences caused by siltation.

3.2.2 Diversion of Sediment

Suspended sediment will be diverted and abstracted through the intake of the diversion works, where after the particles will either remain in suspension and continue downstream (to pumps/turbines), or if the diverted flow velocity is slow enough, sediment will be deposited in the pump chamber or diversion canals (Avery, 1989).

Particles in suspension will cause damage (in the form of abrasion and cavitation) to the mechanical parts of the pumps or turbines of the intake works. Impellers will erode, bearings and seals wear down, and other moving parts like gates and valves are also affected (Avery, 1989).

Raudkivi (1993) states that for heads over 50 m (on hydropower turbines), the grain size diverted should be less than 100 μm and when the head reaches over 200m, the silts and clays would cause significant damage. According to Raudkivi (1993), the cavitation damage reaches a maximum at diverted sediment concentrations of 25 g/l.

If sediment carrying capacity (flow velocity) reduces past the intake, sediment is deposited in the pump chamber, which will cause damage to the pumps at start-up (Basson, 2006). In gravity systems, like irrigation schemes, the deposit in the canal system will decrease the capacity of the canal (Avery, 1989).

Sediment deposition is not only an issue upstream (or at) the diversion works, but also downstream at water treatment works where the removal of large quantities of particulates increases the size (and thus the capital cost) of the treatment works. The same issues exist at run-of-river hydropower works, where sediment deposition in upstream channels, but also downstream chambers and penstocks of such diversion works is considered unwanted and an issue that should be managed (Van Heerden, 2012).

Due to weir sedimentation, the inlet to the diversion canal or pump chamber can be partially blocked, causing the diverted sediment to increase due to the constant source of sediment accumulating at the inlet.

The siltation of the diversion works should be avoided and can be done by i.e. adding a sluicing channel along the inlet. Figure 3.1 shows parallel boulder and gravel traps which are effectively sluice channels that were designed to trap and flush different sizes of sediment. Without these sluice gates the intake openings might have been completely blocked or sediment would accumulate at the invert of the opening.

3.2.3 Effects on River Morphology

River regime, as explained in Chapter 2.8 is a stable state of a river, in terms of width, depth and longitudinal slope. A Structure like a dam or a weir across the river reduces the flow and sediment load in the river downstream of the dam, ultimately changing the river morphology. Upstream, the effect of slower flow velocities reduces the sediment carrying capacity, resulting in sedimentation.

A Weir divides the river in to an upstream and downstream reach, with adverse effects on both sides.

Upstream the backwater effect initiates the formation of a delta. Sediment will continue to deposit at the weir where the velocities are slow. The weir will ultimately silt up to its crest

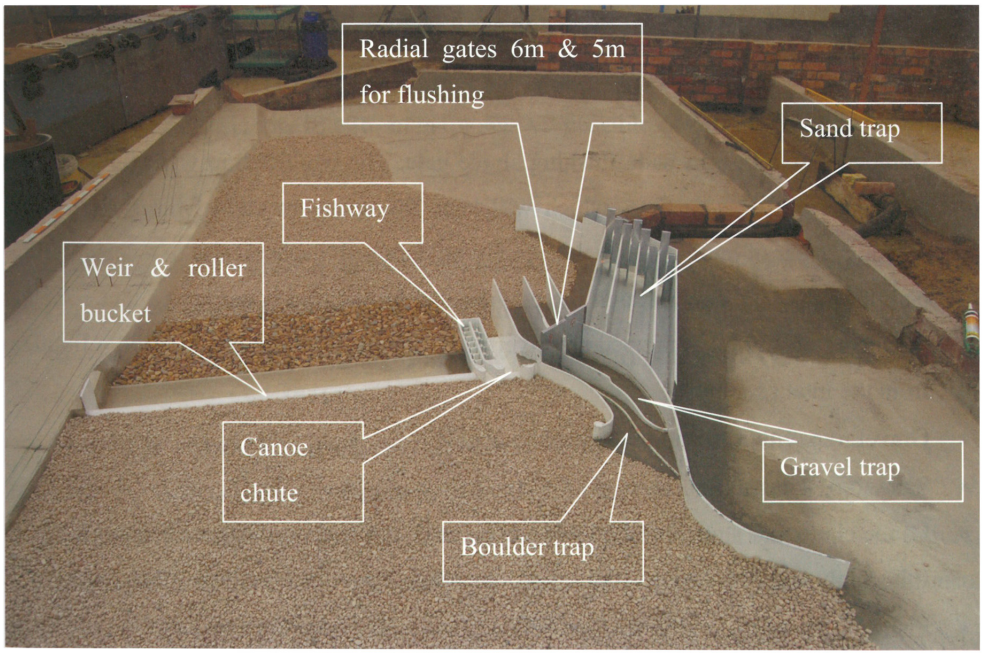

FIGURE 3.1: Berg River Supplement Scheme diversion works model (Basson, 2006)

level, where after the initial slope of the river will re-establish. The backwater region continuously moves backward until the new stable condition is reached. This process alters the reach drastically, vegetation is lost and the riparian zone needs to re-establish. The groundwater level is also affected by the damming. (Raudkivi, 1993)

Petts and Pratts (1983) found that downstream of the weir net degradation will take place due to the lower amount of sediment in the flow that is passed over or through the weir. The flow that passes over will have sediment carrying capacity, but with a low sediment concentration, resulting in the entrainment of sediment. This is in correlation with Raudkivi (1993), who adds that after a reservoir is silted to the crest, downstream aggradation will initiate. The dynamics of degradation and aggradation is complex and dependant on variables like the flood frequency.

3.3 River Diversion and Abstraction Works

There is a vast amount of different designs of water abstraction works, serving various purposes and dealing with site typographies and sediment characteristics. Trademarks of diversion works are their position (i.e. at river bends), the diversion/intake angle, and the combinations with sediment control features like sluice channels, dividing walls, excluder tunnels, baffles, guide vanes and deflectors (Raudkivi, 1993).

According to Vanoni (1975) there are three principle methods of sediment control:

1. Diverting only clear water and allowing sediment to continue downstream.
2. Diverting water and sediment, without deposition in the diversion works or canal.
3. Diverting as little sediment as possible and removing deposited sediment with the most cost-effective way.

Method 1 is ideal, but difficult to achieve. Method 2 leaves the sediment control to downstream works (i.e. at the water treatment works, which is most likely not designed to handle the high sediment concentration). Method 3 is the most practical option and is adopted in most designs.

Sediment Control is said to be active or passive, where active control is i.e. sluice channels that are opened intermittently, and flush sediment when *activated*. Passive controls, i.e. the diversion angle, merely enhances the secondary flow phenomenon to exclude sediment *passively*.

A Good first distinction is made between diversions (1) with a weir, or (2) without a weir. A second distinction is whether the intake is a frontal, lateral (bank) or bottom intake.

Avery (1989) discusses the choice of intake according to the following factors:

- Function of the intake: Water supply, irrigation, power supply etc.
- Scale of the diversion, in terms of diverted flow size and the range of water depth at which flow must be diverted
- Type of site: Stream, river, canal, lake, reservoir, or coastal locations
- Site features: Flow regime and sediment loads
- Construction of diversion works and constrictions of the site

Basson (2006) proposed the following designs for South Africa:

- A Bank intake (with no weir) located on the outer bank at a stable river bend.
- Diversion works with a low weir, a graveltrap (sluice channel with flushing gates) in front of the intake and pump canals/sand trap that can be flushed, located on the outer bank at a stable river bend.
- A Barrage on a river with large gates across the river, located on the outer bank at a stable river bend.
- An Intake, combined with a deep sand pit and jet pumps to clean the pit.

- Sand pump systems with infiltration gallery

Note that the Basson (2006) WRC report solely recommends lateral diversions and sand pump systems. Frontal and bottom intakes are merely mentioned in this study, but the focus is on lateral intake systems.

3.3.1 Diverted Flow and Diverted Sediment

3.3.1.1 Factors Affecting the Size of the Diverted Flow

Guidelines (or limitations) on the amount of water that is diverted from a river or stream are dependant first of all on the available flow, Q_{riv}, but also on the sediment transport requirements and ecological constraints. If the river flow is less than the flow inducing bedload transport (Q_c), no sediment can be diverted and all of the river flow, except the amount necessary for ecological reasons, can be diverted (Raudkivi, 1993). If sediment transport is active, sediment will be diverted and the river regime will be affected downstream of the diversion (as discussed in Chapter 3.2.3).

The diversion capacity is popularly measured as a ratio of the diverted flow to the river flow, Q_d/Q_{riv}, also called the Diverted Discharge Ratio (DDR). Avery (1989) suggested DDR of 66% to 77% for rivers in England. DDR for Chinese rivers should be lower, at 45% to 50% according to Tan (1996). Raudkivi (1993) stated that an empirical guideline is that DDR should not be more than 50%.

3.3.1.2 Diverted Sediment

The amount of sediment that is diverted is measured as a ratio of the sediment transport rate in the diverted flow (G_d) over the sediment transport rate in the oncoming river (G_{riv}), and is called the Diverted Sediment Ratio (DSR).

The adverse effects of sediment in the diverted flow have been discussed in Chapter 3.2.2. Generally it makes sense to minimise the DSR, but Avery (1989) mentions that some diverted sediment may be allowable, considering the maximum grain size as well. The quality standard of the water is set by the uses. If the diverted flow is used for irrigation on porous soil, sediment in the diverted flow could be beneficial (Raudkivi, 1993).

The foremost method of DSR control is the positioning of the intake in the river, especially in bends, as discussed in Chapter 2.7. Figure 3.2 shows the test findings of Habermaas (1935) as summarised by Moyosi (1965), showing the effect of the diversion channel position.

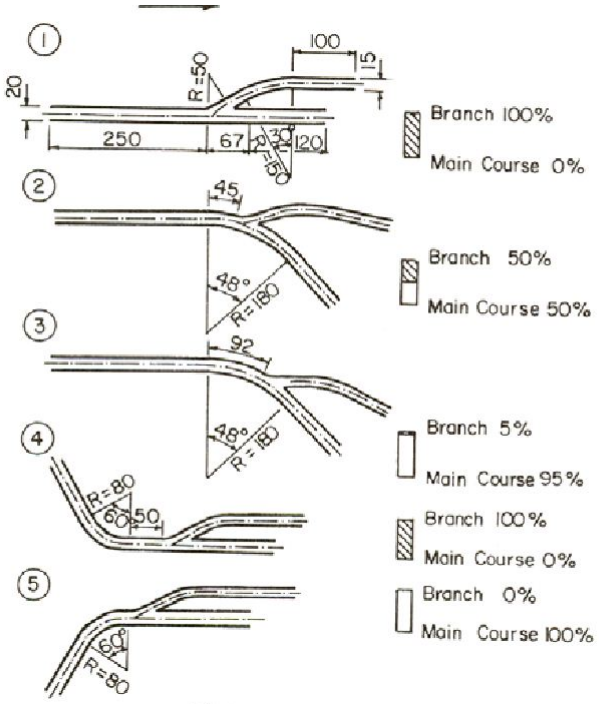

FIGURE 3.2: Findings of Habermaas (1935) on the diversion channel position (Moyosi, 1965)

The other factors are the diversion/intake angle, intake type and the sediment excluding techniques/features. Figure 3.3 compares the DSR of a lateral and a frontal intake, versus the DDR. In this case, the frontal intake diverted less sediment at any DDR.

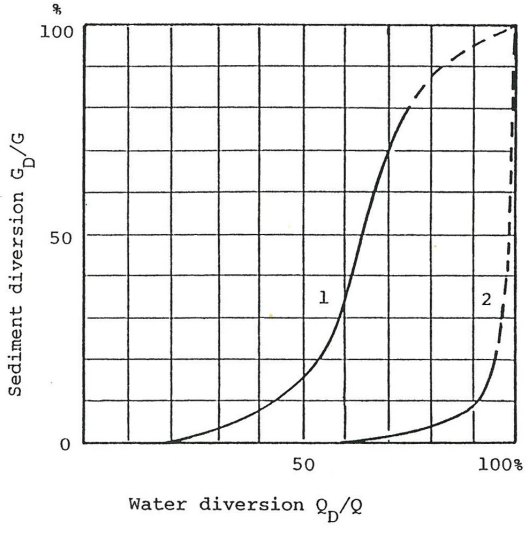

FIGURE 3.3: Comparison of sediment diversion by lateral (1) and frontal (2) intakes under the same condition (Raudkivi, 1993)

3.3.2 Intake Location and Angle

3.3.2.1 Location

The location of the intake is the first mitigation method of the two main complications, (1) abstracting a constant yield with variable river flow and (2) dealing with the sediment that is entrained in the flow.

The intake should be located on a reach with stable river banks. Considering diversion works with no weir or dam, the intake should be located where it can be determined to a certainty that the main flow will not move away from the intake. On braiding and meandering river reaches, prediction of the main channel is difficult and could result in flows not entering the intake.

Utilising the river bend phenomena (Chapter 2.7). The position into the bend can accurately be determined with Table 2.2.

3.3.2.2 Diversion - and Intake Angle

Studies on the angle of diversion, referring to a lateral diversion with an angle (θ) between the main channel and the diverted channel (Figure 3.4) have resulted in varying recommendations.

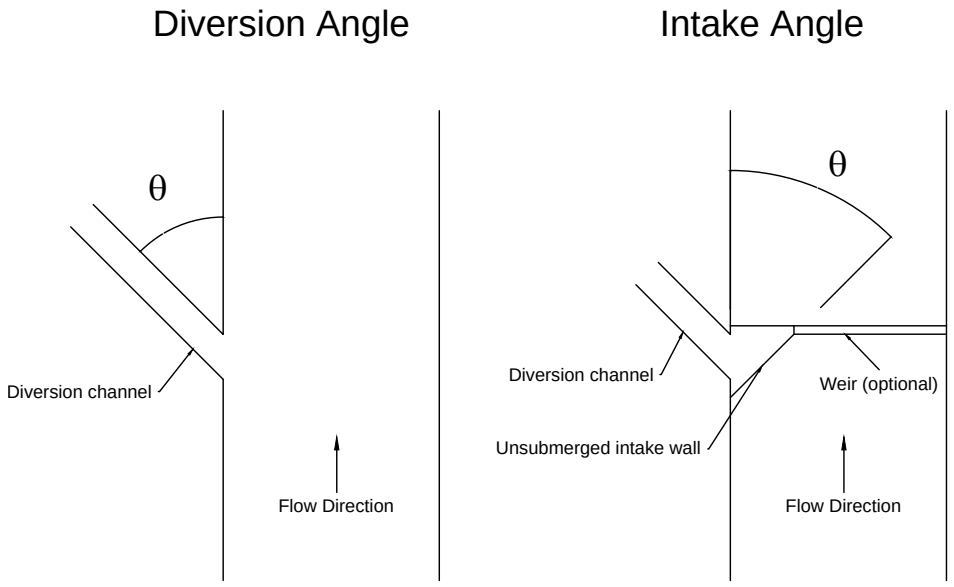

FIGURE 3.4: Comparison and definition of diversion angle and intake angle

Bulle (1926) showed that the diversion angle has a small influence on the diverted sediment ratio (DSR) and that the angle is dependent on the DDR and the intake location. This concept is shown in Figure 3.2.

Avery (1989) stated that the angle is dependent on the DDR, river width, diversion channel width and other factors. Angles smaller than 45^0 are recommended.

Brink (2004) studied the velocity profiles for three diversion angles (25^0, 35^0 and 50^0), from which he also concluded that there is no optimum diversion angle, but made the following observations:

- DDR increases with diversion angle
- DDR decreases with Froude number of the river flow
- The diversion angles tested did not influence the secondary flow pattern in the bend

Note that the Brink (2004) tests were conducted, simulating a river diversion channel with no structure obstructing flow in the river and the amount of flow diverted was measured, instead of controlled.

Van Heerden (2012) tested the *angle of diversion structure*, which has a different meaning than diversion angle seen in Figure 3.4, but could be related. From now on there will be referred to the angle tested by Van Heerden (2012) as the *intake angle*. The *intake angle* is not the angle between the main river and the diversion channel, but rather the angle at which the intake structure is set into the river. Assuming a diversion channel continues downstream of the intake and is set at a right angle to the intake, Figure 3.4 depicts the scenario that relates the diversion and intake angle. For the case of diversion works with a weir, the angle between the weir and the diversion works is the complimentary angle to the intake angle.

If the diversion angle is increased, it would not necessarily (i.e. Brink (2004)) have any physical effects on the flow in the river. All effects were due to the diversion of flow lines.

The effects of the intake angle should rather be linked to intake designs that induce local secondary currents, like in Figure 3.5. The question: *at what intake angle can the design discharge be abstracted, while minimising the DSR, without other adverse effects?* should be answered.

Van Heerden (2012) disregarded an intake angle that would cause damming and changes in river regime. The study found an optimum intake angle of 30^0.

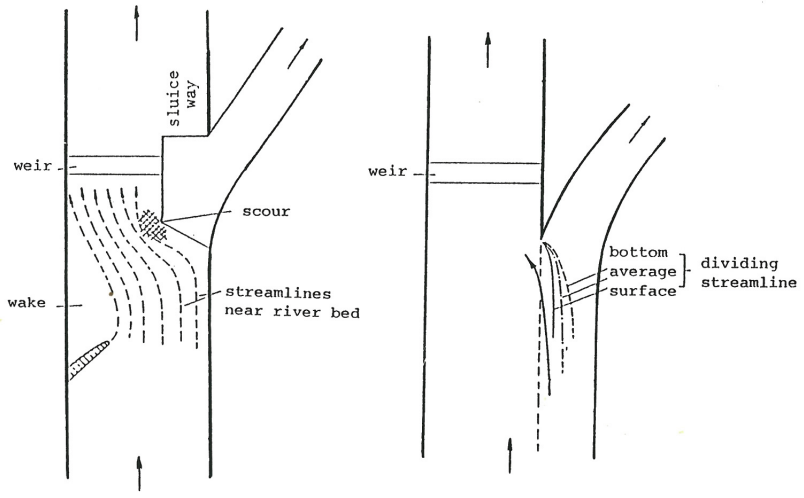

FIGURE 3.5: Diversion works designed to induce local secondary flow (Raudkivi, 1993)

Bouvard (1992) recommends an intake angle between 15^0 and 20^0, and mentions that larger angles could promote secondary currents even more, but should be tested to determine if the angle has any detrimental effects.

3.3.3 River Intakes

3.3.3.1 Frontal and Bottom Intakes

Avery (1989), Bouvard (1992) and Raudkivi (1993) depicts frontal and bottom intakes as applicable on mountain streams. Frontal intakes abstract the clear top flows of mountain streams and bottom flows are installed due to the nature of the sites, making construction of more complex intakes difficult. Both intakes operate with- or without a weir. Figure 3.6 shows a pier-type intake, which is also a form of frontal intake. The bedload will pass over the low sill and clearer water will be abstracted through the screens and. Figure 3.7 shows the bottom intake arrangement for a hydropower plant in the French Alps. Fine sediment and debris, abstracted with the design discharge of 3 m^3/s, is transported to a settling basin, to settle out the sediment and debris.

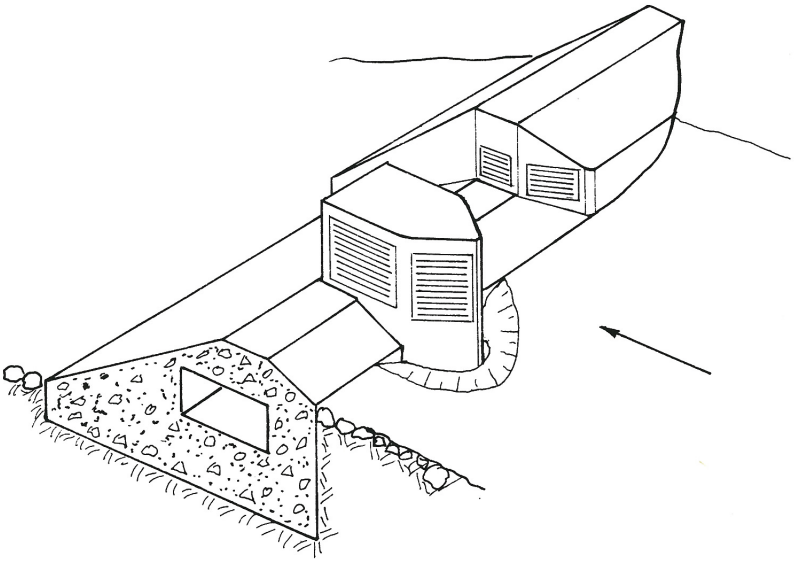

FIGURE 3.6: Pier-type frontal intake (Raudkivi, 1993)

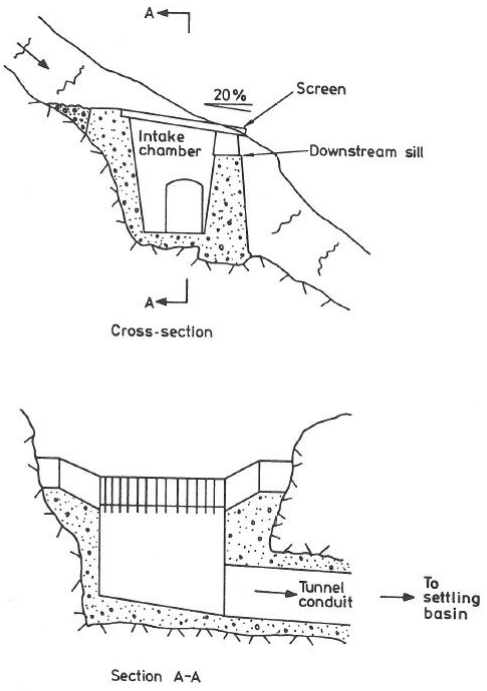

FIGURE 3.7: Bottom intake (Avery, 1989)

3.3.3.2 Lateral Diversion

The lateral diversion is based on horizontal separation of flows, into (1) a diverted flow and (2) the flow that continues downstream along the river channel. Figure 3.8 shows the probable dividing streamline of a 90^0 diversion. The curved streamline induces spiral flow in the same way a river bend would. The curvature has an adverse effect on the sediment intake in this case, where the sediment laden bottom current transports sediment towards the intake. Sediment is deposited downstream of the intake, due to the reduced flow, but scouring against the wall removes the sediment at the wall.

This type of diversion is normally placed on a river reach where mainly sub-critical flow occurs. Supercritical flow in the diversion channel is also avoided by controlling the diverted flow ratio (DDR).

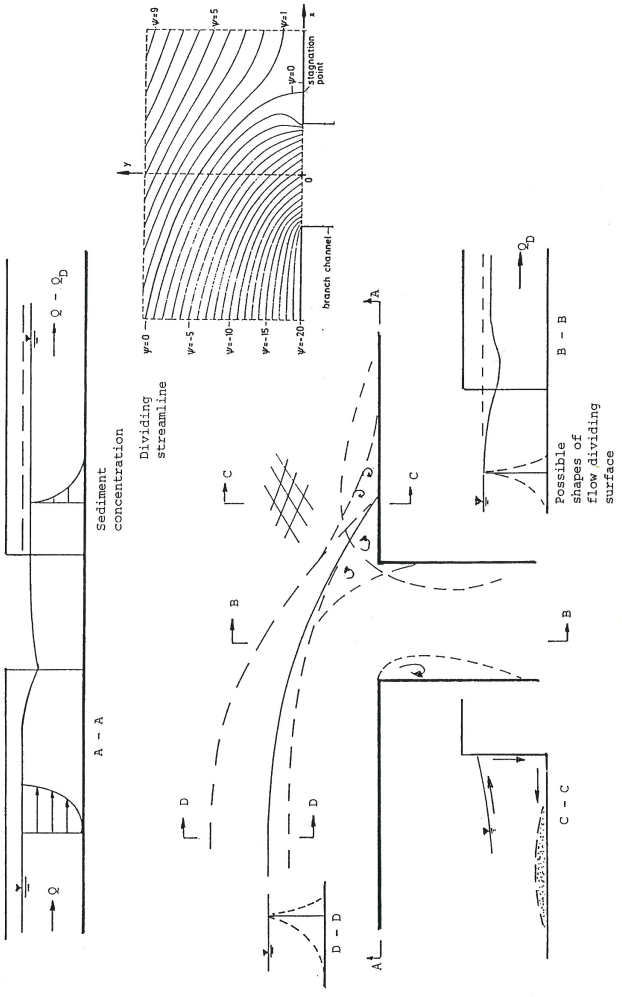

FIGURE 3.8: Schematic layout of a 90 ^{0} lateral diversion (Raudkivi, 1993)

3.3.3.3 Bank Intakes without a Weir

This type of intake is solely dependent on the effects of secondary flow to reduce the diverted sediment. The intake is suitable at locations where the water level is more constant and predictable. If the main channel meanders away from the intake during low flows, no water can be abstracted. Avery (1989) proposes intakes without a weir for abstractions with lower DDR ratios.

If the intake cannot be placed in a river bend, other methods of creating lateral flow at the intake should be applied. Groynes and dividing walls can create lateral flow by means of flow convergence.

Advantages of weir-less intakes are first of all the lower impact on the river regime (Basson, 2006) and secondly the lower construction cost.

3.3.3.4 Bank Intakes with a Weir

Adding a weir is appropriate for larger river abstractions where a constant yield is necessary. The weir creates the necessary head to ensure river abstraction even during low river flows. Raudkivi (1993) gave a guideline of when a weir is necessary according to a factor $Q_{\%}$, which is the specific river flow with the frequency of the project's water demand. If $Q_d/Q_{\%}$ is greater than 0.25, a diversion weir is necessary. The height of the weir is directly proportional to the amount of flow that can be abstracted, at the required yield frequency. The head created by weirs are used to flush the intake works and a sluice channel if applicable. Rooseboom (2002) proposed the typical design with a weir for South Africa, as presented in Figure 3.9.

The features discussed are designed to positively amplify the bend flow phenomena and/or keep the intake clear of sediment by settling and flushing it downstream.

The following features are discussed:

- Gravel sluices
- Side-sluice Arrangement
- Dividing walls
- Guide vanes
- Other approach flow controls

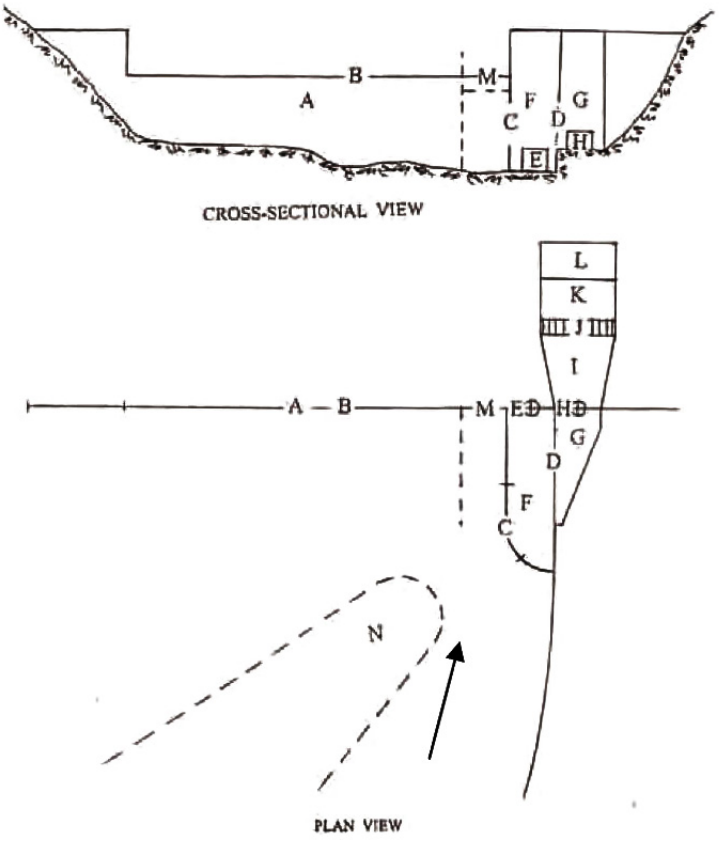

FIGURE 3.9: Typical abstraction works design for SA, as proposed by Rooseboom (2002). A : Weir, B : Spillway, C: Open intake, D: Screen intake, E: Scour gates, F: Scour chamber, G: Collection channel, H: Control gate(s), I: Transition channel(s), J: Vortex suppressor, K: Settling basin, L: Pumps, M: Low notch weir, N: Groyne.

3.3.3.5 Sediment Control Features

Gravel Sluice: This feature consists of a channel, parallel and connected to the intake opening sill/wall, as shown in Figure 3.10. Downstream of the channel a sluice gate is situated, that releases water and sediment back to the river when opened. The channel is normally operated in a alternating two-phase process of deposition and flushing.

During the deposition period, the sluice gate is closed and the velocities in the reservoir are slow enough for bedload and some of the suspended load to settle. A limit to the amount of deposited sediment is set by the height of the intake opening above the bed of the channel. If the sediment reaches the intake opening the sediment will be entrained and transported by the faster velocities through the opening, at which point the channel should rather be flushed if the river flow permits it.

According to Bouvard (1992), channels should be flushed during periods of higher river flow (floods). During periods of flushing, water abstraction should cease to prevent the entrained sediment from being abstracted. Draw down of the reservoir (decreasing the water level) before

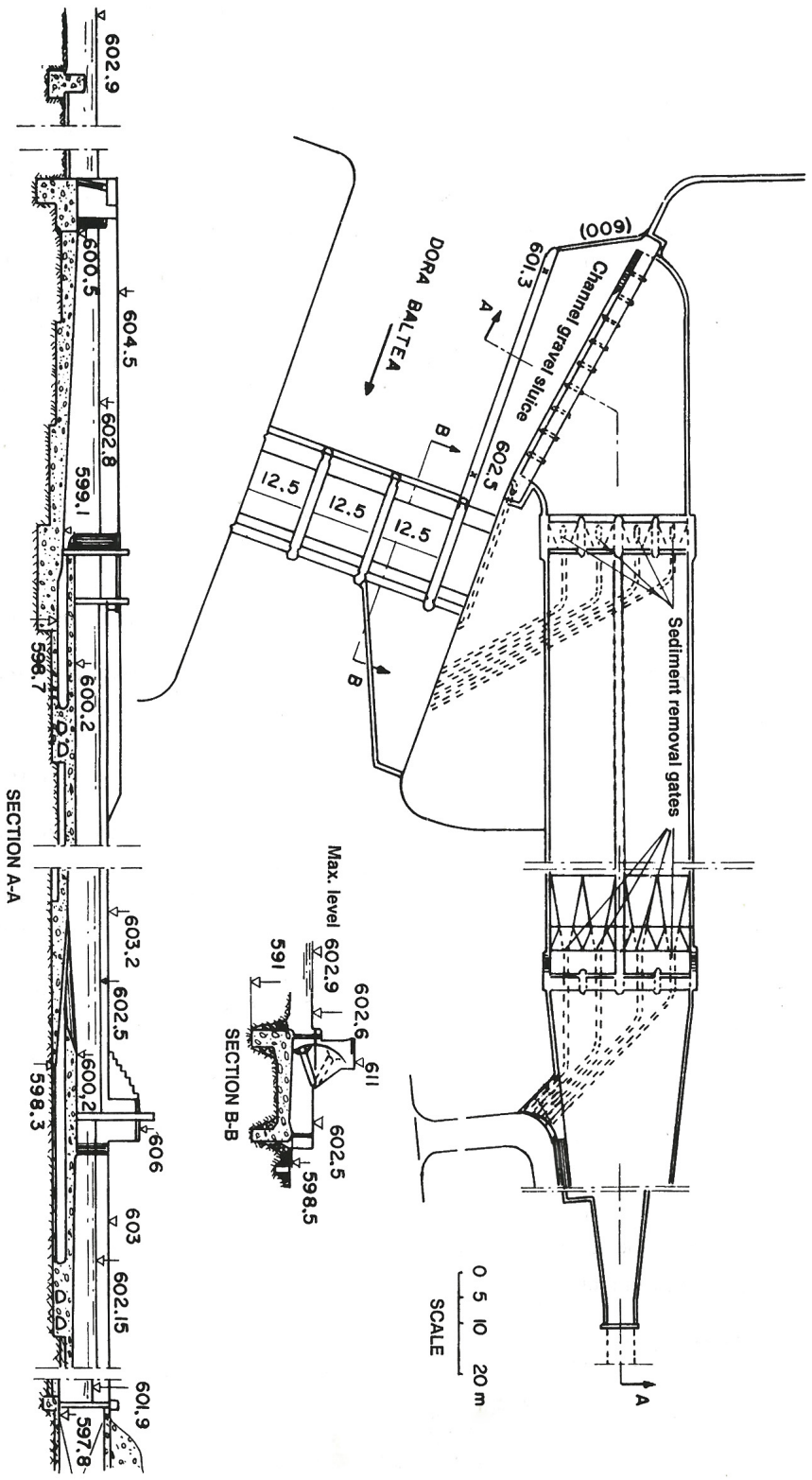

FIGURE 3.10: Dam and water intake on the Dora Baltea, Itlay, including an open-channel gravel sluice (Bouvard, 1992)

flushing creates faster velocities in the sluice channel, resulting in shorter flushing times. The point (Q_{riv}) at which flushing starts to be effective as well as ceases to be effective is not specified.

An optimum sluicing arrangement would flush all the sediment in the sluice by the smallest possible volume of water in the shortest amount of time. However, this often results in negative effects on the downstream river regime and ecology. Bouvard (1992) measures flushing efficiency as either *hydraulic* or *economic* efficiency. Hydraulic efficiency simply relates to the volume of water used to flush a certain volume of sediment, where the more water used, the less efficient the system is flushed. Economic efficiency is concerned with the original purpose of the water used for flushing. If $Q_{riv} \gg Q_d$, the excess water can be used for flushing without a loss of discharge yield.

There are some variations of the gravel sluice arrangement and some additional features have been designed and applied with varying success. The general design features of the gravel sluice are the channel width, channel floor (slope), the sluice channel (training) wall.

The combination of the width and the slope should create supercritical velocities that can entrain and flush the deposited sediment. Basson (2006) recommends flushing velocities of 2 to 4 m/s. Avery (1989) states that the maximum width of the channel can be determined with regime equations (as in Chapter 2.8). According to Bouvard (1992), the channel must be concrete lined and have a slope of at least 1:50, but steeper slopes are designed. The Berg River Abstraction Works at Voëlvlei dam (South Africa) were designed with sluice channel slopes as steep as 1:20 and the Berg River Supplement Scheme abstraction works (Figure 3.1, which were designed to handle high bedloads, has a sluice channel slope of 1:16.7 (Basson, 2006).

The sluice channel training wall can extend above the low-notch weir with the end of the channel open to the main channel, classified by Bouvard (1992) as a *Channel Gravel Sluice*, or it could be a submerged wall, acting as a weir (*Overpour-channel Gravel Sluice*).

The sluice channel wall should extend beyond the intake openings. Figure 3.10 shows an example of an intake on the Dora Baltea River in Italy, featuring a channel gravel sluice. Note the channel converges to a width of 6 m and is fitted with a 6×3.9 m radial sluice gate.

The submerged wall of the overflow gravel sluice forms a closed channel, by connecting with the inlet wall. Thus, water enters the channel by flowing over the submerged wall. The closed channel reduces the sediment that enters the channel, until the sediment builds up to the level of the submerged wall. The flow over the submerged wall should form a separated nappe, entraining sediment at impact (Bouvard, 1992). The wall should have a negative slope, with the level equal or lower than the LNW level where it connects with the weir (dam). The negative slope ensures the bulk of the flow to enter at the upstream end of the channel, creating stronger

longitudinal flow to transport sediment downstream. Basson (2006) recommends the level of the wall should not be so low, that the flow in the gravel sluice submerges the control (gravel sluice wall). Figure 3.11 shows the water intake at the Plan du Lac dam on the Veneon River, consisting of a 4.6 m wide overflow sluice channel with a channel bed slope of 1:50 and negative wall slope of 1:50. The Lebalelo pumpstation on the Olifants River (South Africa) has a similar design, shown in Figure 3.12. The flushing data at the Lebalelo pumpstation was recorded in 2003 documented by Brink *et al.* (2006), is shown in Figure 3.13.

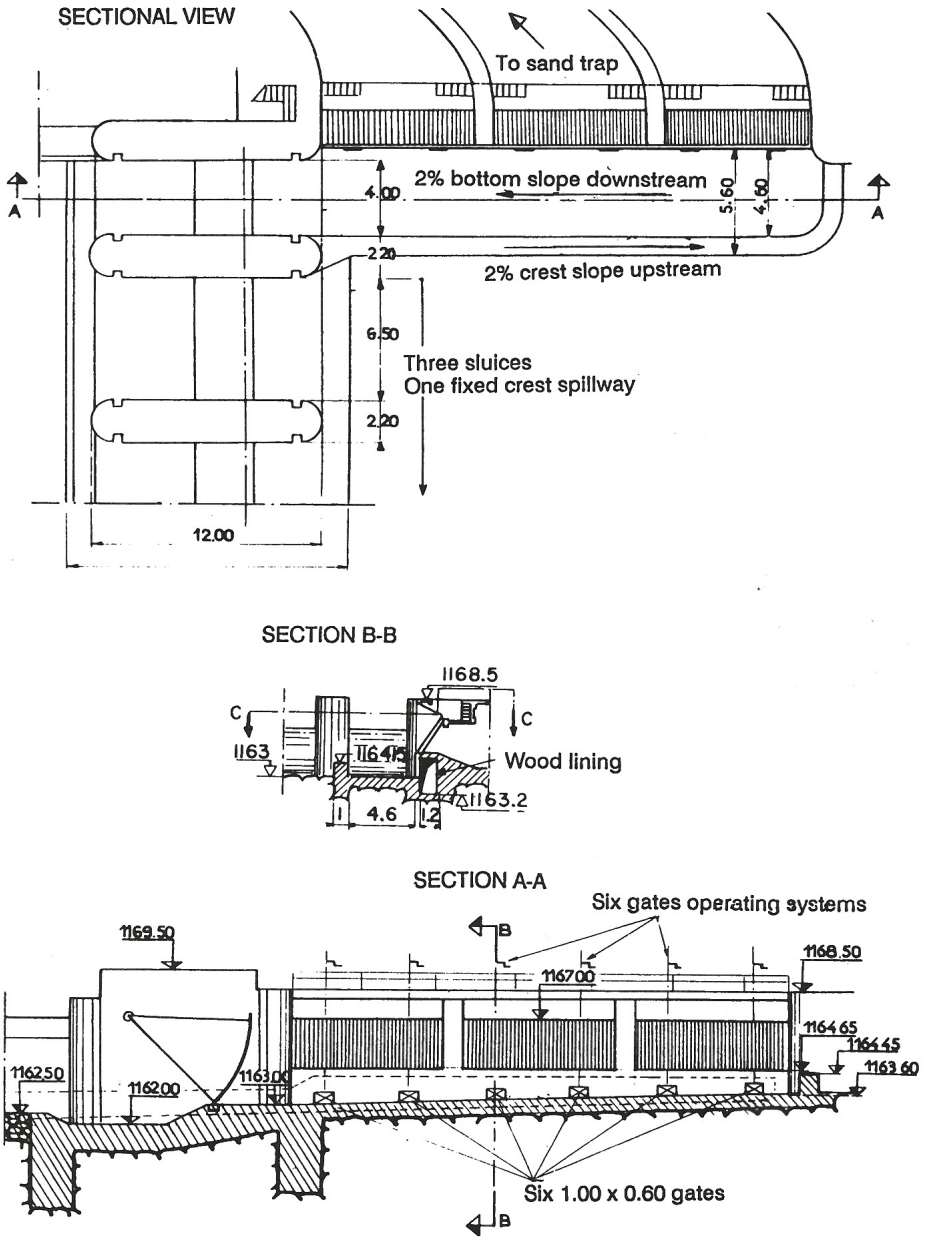

FIGURE 3.11: Plan du Lac dam and water intake on the Vénéon in the French Alps (Bouvard, 1992)

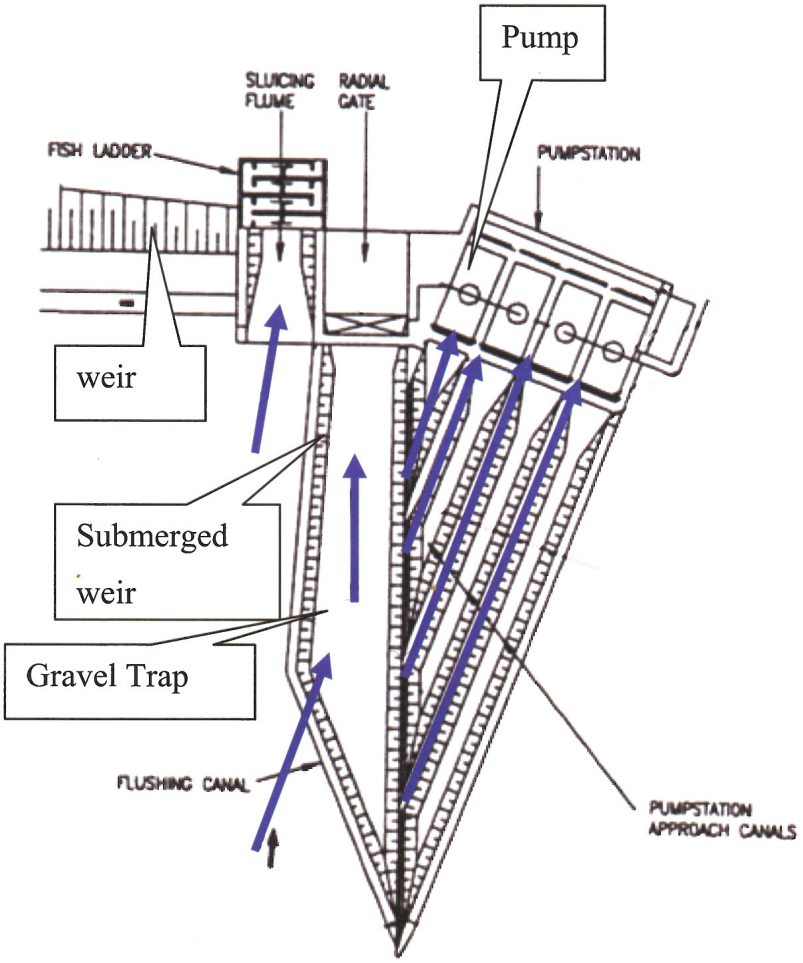

FIGURE 3.12: Lebalelo diversion works on the Olifants River (Brink *et al.*, 2006)

The gravel sluice can be curved to amplify the bend effect. The sediment in the channel moves to the convex side of the curve and the water abstraction is from the clearer concave side. Flows with higher sediment concentrations are flushed through the channel and water with lower sediment concentrations are diverted. Avery (1989) sets the following basic principles for a curved gravel sluice design:

- The approach to the curved channel must ensure that spiral flow forms.
- The diversion canal inlet (from curved sluice channel into downstream works) arrangement should not cause entrainment of sediment.
- Velocities in the curved sluice channel must be able to move all sediment through the sluice gate.
- The width of the curved sluice channel at the entrance point can be determined with regime methods. The channel can be narrowed towards the sluice gate.

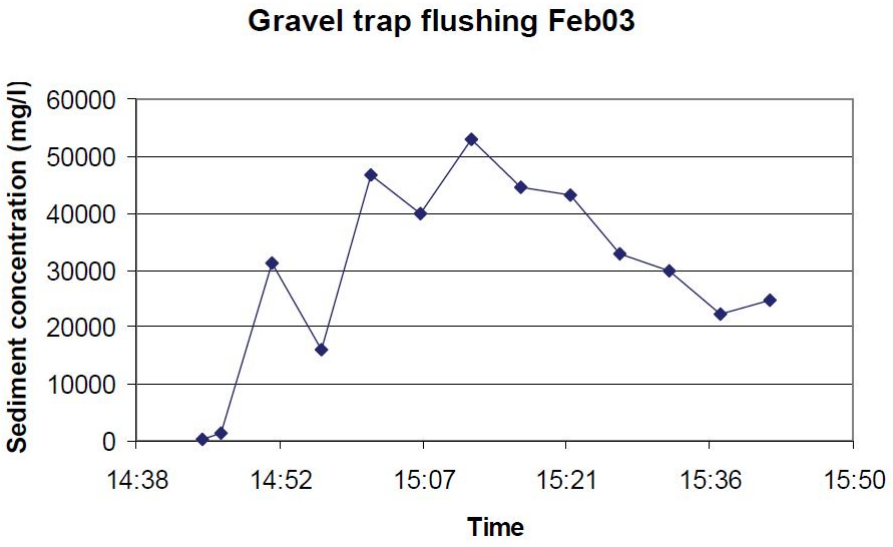

FIGURE 3.13: Flushing data recorded at the Lebalelo diversion works in 2003 (Brink *et al.*, 2006)

An example is the design of the headworks of the Osborne Canal at the Woodston Diversion Dam (Figure 3.14). The sluice channel operates as a *channel gravel sluice*, with the training walls extending above the water level at minimum operating level. The gravel sluice operates continuously, skipping the deposition phase discussed above (Vanoni, 1975). The velocity in the channel is maintained at 2.5 to 3.5 m/s (Avery, 1989), which is in accordance to the recommendation made by Basson (2006). The diversion inlet of the Woodston dam is via a gate operated inlet at the end of the curved channel.

Designs with curved sluice channels are seen in South Africa as well i.e. the Berg River Supplement Scheme diversion works (Figure 3.1).

Side-Sluice Arrangement: This feature consists of a sluicing arrangement, situated downstream of the initial diversion. The second division (sluicing flow) should return a flow with higher concentration than the flow which is continuing downstream to the diversion canal or pump system. This feature is normally added to a bank intake with a weir, as it requires head for flushing. This design is suitable to abstract larger flows.(Avery, 1989)

Avery (1989) saw the initial division as parallel to the flow direction, but his theory could also be applied to a lateral diversion. The basis of a (frontal) initial diversion channel design is river regime theory. Referring to the layout in Figure 3.15, Avery (1989) calculates the width of the river (b_r) with equation 3.1, the width of the flow that is to be diverted (b_d) with equation 3.2 and the width of the diversion channel (b_e) can be calculated with equation 3.3. Here Q_d is the flow abstracted through the intakes plus the flow lost to flushing.

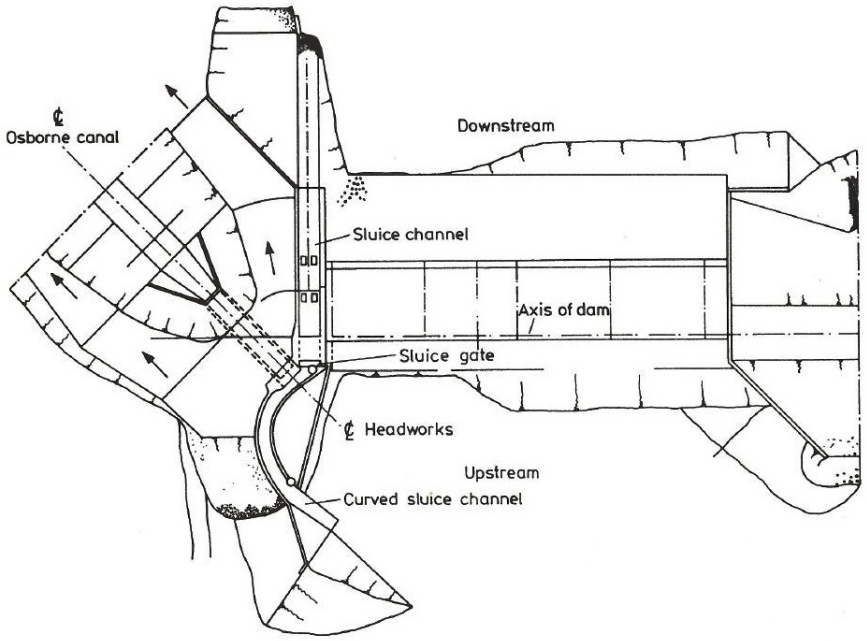

FIGURE 3.14: Osborne Canal at the Woodston Diversion Dam (Avery, 1989)

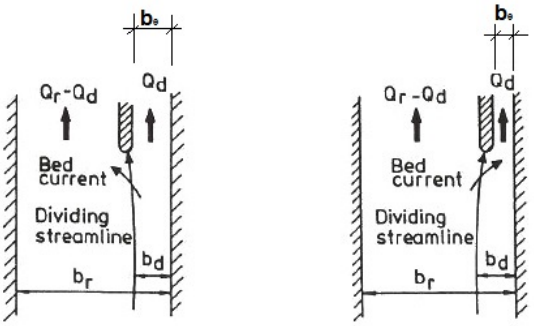

FIGURE 3.15: Initial flow division and the dividing streamline (Avery, 1989)

$$b_r = 5\sqrt{Q_r} \tag{3.1}$$

$$b_d = 5\frac{Q_d}{\sqrt{Q_r}} \tag{3.2}$$

$$b_e = 5\sqrt{Q_d} \tag{3.3}$$

As seen in Figure 3.15, if b_e is too narrow, the flow curvature is towards the channel, increasing the sediment concentration in the first diversion channel and consequently, the abstracted flow.

Figure 3.16 shows the position of the sluicing channel and the dimensioning of such an arrangement. Avery (1989) discussed the design of a *well proportioned* structure, with the most important constraint on the line AB, which must be parallel to the river bank. Further the angle, α should be between 20^0 and 30^0. The rest of the dimensions can be manipulated.

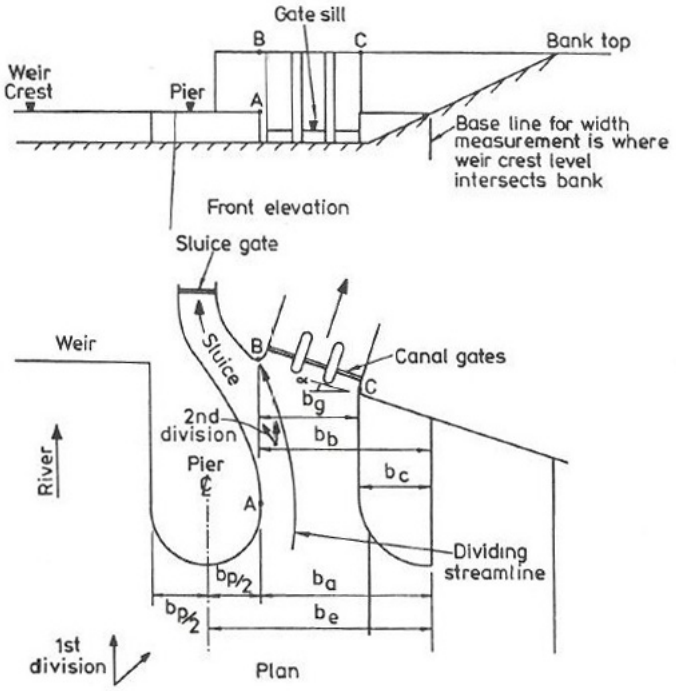

FIGURE 3.16: Second division of flow : a side-sluice arrangement (Avery, 1989)

Other considerations according to Avery (1989) are:

- The pier height should be at weir crest level, to prevent floating debris to accumulate in front of the abstraction intake (the *canal gates*, in Figure 3.16).
- The slope of the sluice channel should create velocities that are able to flush the accumulated sediment.

Dividing Walls Dividing walls are mentionable sediment exclusion features, utilising the flow curvature effect and alternating particle settling and flushing phases. A dividing wall separates the river (as seen in Figure 3.17) into a *pocket* from which water is abstracted and the rest of the river which continues downstream.

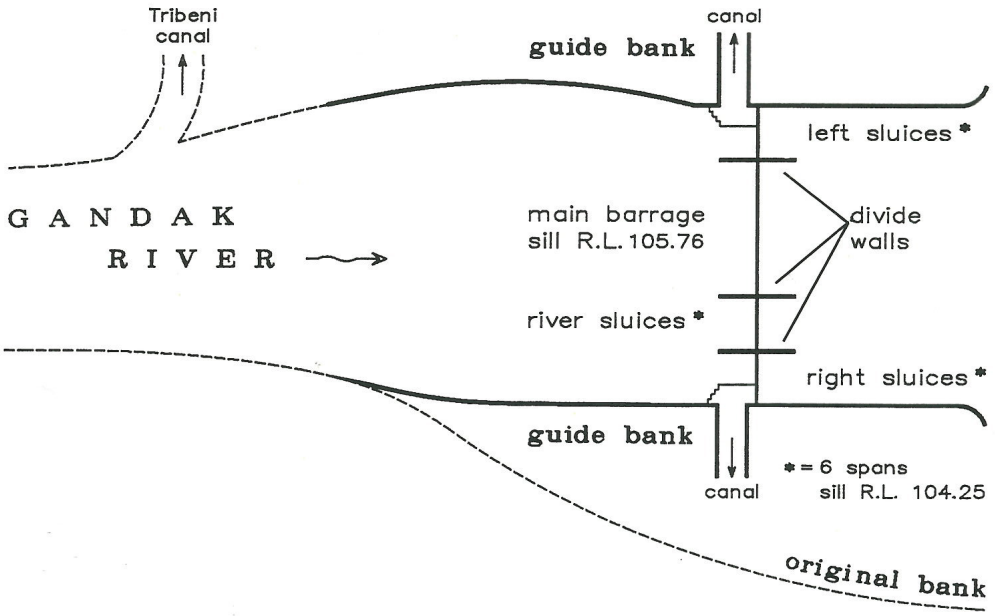

FIGURE 3.17: Dividing walls at the Gandak barrage (Raudkivi, 1993)

With the sluice gate closed, the pocket serves as a settling pond, and abstracting water from the clearer top flows reduces the amount of diverted sediment. With the sluice gate open, the velocity through the pocket must entrain and transport the sediment through the sluice gate.

Vanoni (1975) uses a ratio of the flow velocity in the river and the velocity in the pocket, to describe the resulting effects:

During flushing, the effect of the flow curvature is dependent on the velocity in the pocket (u_p) in relation to the velocity in the rest of the river (u_{riv}). A ratio u_{riv}/u_p of greater than unity means the flow curvature is towards the river, and thus the sediment is moved by the lateral flow towards the convex side, out of the dividing pocket. If u_{riv}/u_p is less than unity, the flow tends to curve towards the dividing pocket, which increases the sediment that moves towards the intake. The velocity in the pocket is dependent on the pocket width and the sluice gate opening.

A method of determining the pocket width could be with regime theory (equation 3.3), as Avery (1989) showed with the design of an initial division width. If the width is too narrow, the flow curvature is towards the pocket, increasing the transport of sediment towards the pocket and the intake. If the pocket is too wide, circulation within the pocket reduces the settling pond effect of the pocket (Raudkivi, 1993). Vanoni (1975) recommends a slightly converging pocket, rather than a straight one, to improve the scouring in the pocket.

The dividing wall usually extends upstream 2/3 of the pocket width, but it depends on the

diversion size and should be modelled (physically) to find an optimum diversion wall length. The wall can be extended downstream to prevent cross flows. The top of the wall is above flood level, to prevent spillover. (Vanoni, 1975)

Guide Vanes: Guide Vanes induce lateral flow, which either push sediment laden flow away from the intake or push clearer top flows towards the intake. Vanoni (1975) classifies the two types of guide vanes as *bottom vanes* and *surface vanes*.

Bottom vanes are fixed to the bed and angled in the manner seen in Figure 3.18. The clearer top flows are allowed to pass over the vanes, towards the intake, while sediment laden bottom flows are diverted away.

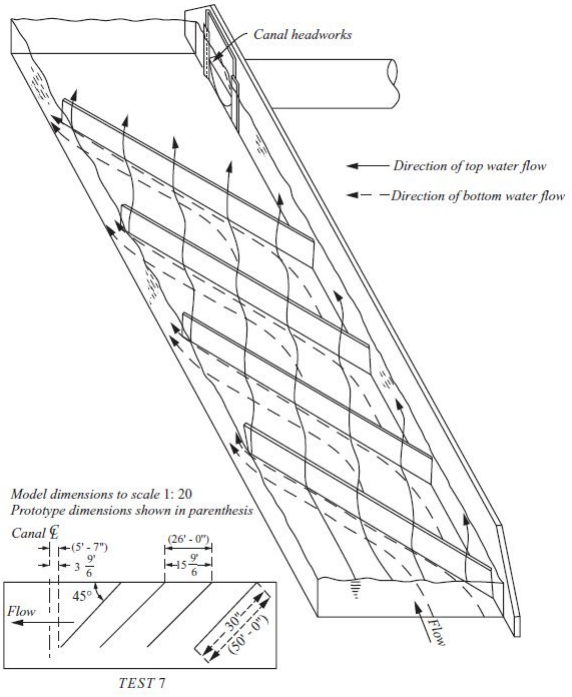

FIGURE 3.18: Bottom Guide Vanes (Vanoni, 1975)

The studies by Odgaard and Spoljaric (1986) and Odgaard and Wang (1991) resulted in the following guidelines for bottom vanes:

- The vane height should be 0.2 to 0.4 times the bankfull flow depth.
- The vane length should be 2 to 3 times the vane height.
- Vanes should be placed in arrays along the bank.
- Vanes on an array are spaced a distance 2 to 3 times the vane height.

- The distance between arrays were still uncertain, but range from 15 to 30 times the vane height.

Surface vanes are supported by a raft-type structure, allowing vanes to protrude a depth into the water, without touching the bed. Sediment laden flows are passed underneath the vanes and clearer top flows are diverted towards the intake as seen in Figure 3.19.

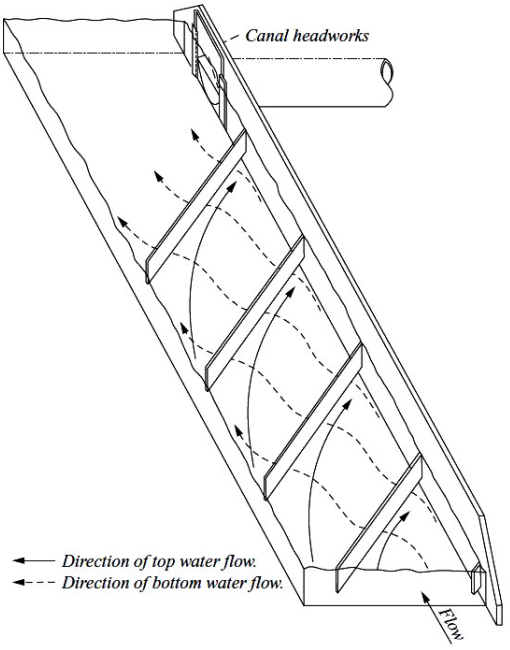

FIGURE 3.19: Surface Guide Vanes (Vanoni, 1975)

Approach Flow Control Most sediment control features control the approaching flow in a way, but groynes, a central island (for abstraction at both banks) and the intake angle are features that only induce or amplify the lateral flow by means of the curvature effect.

Chapter 3.3.2.2 discusses the intake angle, but in summary:

- Figure 3.5 shows the desired effect.
- Bouvard (1992) recommends an angle between 15^0 and 20^0 to promote lateral flow at a bank intake with a weir.
- Van Heerden (2012) found an optimum intake angle of 30^0 for a bank intake without a weir.

For the case where water diversion is necessary at both banks of a river at the same location, a central island is often used to establish curved flow (with the intake on the concave side) at

both banks. Figure 3.20 shows an example at the Kotri barrage in Pakistan. Upstream of the island, guide banks or groynes are used to stabilise the flow.

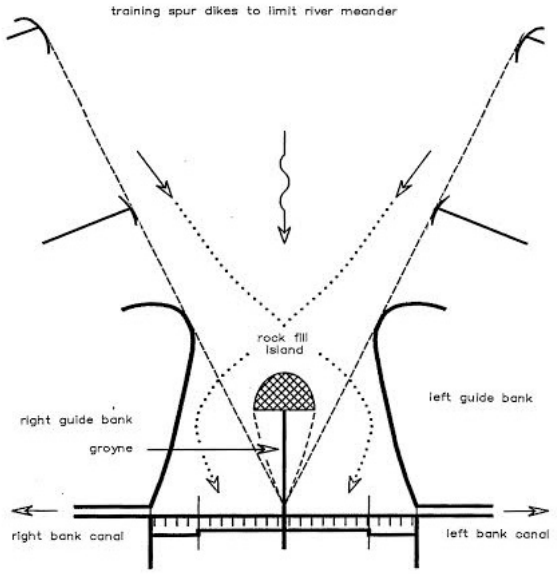

FIGURE 3.20: Central island type diversion works (Kotri barrage, Pakistan) (Raudkivi, 1993)

3.3.3.6 Intake Opening and Trashrack Design

It is a general design feature to lift the bottom of the intake opening above the bed of the channel from which water is abstracted, whether this channel is a concrete lined gravel sluice or whether water is abstracted directly from the river (i.e. designs with dividing walls). It is also custom to place a trashrack (grid) over the opening to prevent floating debris from continuing to the downstream abstraction works. Debris is cleaned from the grids to prevent clogging and thus unwanted flow velocities through the intake.

Intake Opening: Vertical Position and Dimensioning The vertical position (above the bed) should be high enough to allow a reasonable amount of sediment deposition, before the sediment reaches the bottom of the opening. This height is referred to as the *sill height*. If a gravel sluice is connected to the intake wall, the amount of sediment that can be deposited before flushing needs to occur is often called the *capacity* of the gravel sluice. The height (h) from the invert level at the sluice gate to the MOL is used as reference, as seen in Figure 3.21. Bouvard (1992) gave minimum bed clearances of h/4 between the invert levels at the sluice gate and the opening, as well a clearance of h/5 to h/6 over the length of a gravel sluice.

The size (area) of the opening should be determined by the allowable velocities, through the intake opening (calculated with equation 3.4), taking into account the grid and blockage. For

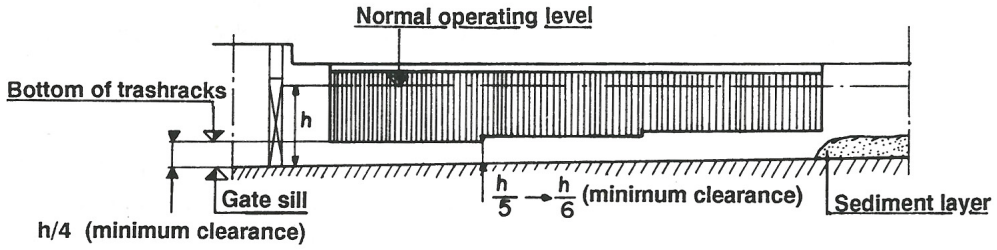

FIGURE 3.21: Required clearance below trashracks (Bouvard, 1992)

normal river intakes (where the intake grid is accessible for cleaning), Bouvard (1992) recommends mean inlet velocities as high as 0.3 m/s (with trashrack bar spacing of 2.5 cm). At higher abstractions (>10 m^3/s) mechanical rack cleaning systems become cost effective and inlet velocities of 0.6 to 1 m/s are acceptable.

$$V = \frac{Q_d}{F.A_{eff}} \tag{3.4}$$

where:

F is the blockage factor

A_{eff} is the area of the opening taking into account the area of the bars

With the reservoir at MOL the intake should be at least completely submerged, but vortex formation should be considered. The intake opening can thus be determined, leaving only the length of the intake opening as variable, to yield the required area, for a given design discharge (Q_d). Bouvard (1992) states that inlet opening lengths longer than $h \times 5$ to $h \times 6$ could result in flushing difficulties.

Trashrack Considerations The trashrack traditionally consists of vertical (or slightly tilted) bars with a certain clearance and centre-to-centre spacing. Basic designs are represented in Figure 3.22. The trashrack deals with floating debris, and are spaced according to the allowable material size that will be passed through. The racks also stop fish from entering the downstream abstraction works.

The trashracks need to be cleaned to prevent head loss at the intake. This is achieved either through installed power rakes or manual cleaning.

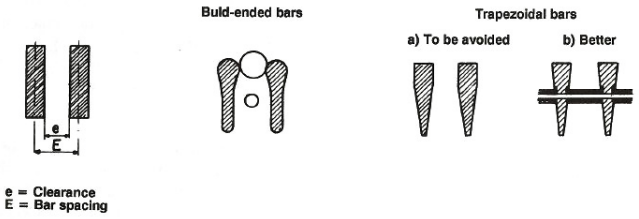

FIGURE 3.22: Trashrack bar designs (Bouvard, 1992)

Chapter 4

Physical Model Design and Tests

4.1 Introduction

This study required physical model tests on a river diversion scenario, with diverted flows typically large enough for run-of-river hydropower plants and large irrigation demands, in terms of South African conditions.

The hydraulic model could be classified as a *design model* by the definition of Ettema (2000), which "simulate actual complex prototype situations to provide specific information for design use or in retrospective study of failures". The experimental model applied in this study is however not one of an existing diversion works design, but rather a generic design that is typically used in South Africa. The features were designed according to empirical guidelines and/or features from case studies.

The river was modelled as a straight rectangular channel in the Hydraulics Lab of the University of Stellenbosch. The concrete lined channel had a loose bed surface and sediment was fed into the system. A straight channel was modelled to asses the effect of the intake angle without the effect of a river bend, which would induce secondary flow.

The diversion structures were designed (on prototype scale) with a basic weir and a graveltrap combination, as shown in Figure 4.1, which is commonly used on larger rivers in South Africa. The graveltrap is situated in front of the intakes, with a downstream sluice gate to flush the graveltrap clean. Three diversion structures, each with a different weir height (2.5, 3.5 and 4.5 m), were designed to abstract prototype flows of 1, 5 and 10 m^3/s. The structures were tested at three increasing intake angles (30^0, 45^0 and 60^0) to determine the angles' effect on sediment diversion and graveltrap flushing.

The prototype was scaled with Froude similarities criteria, as prescribed by Ettema (2000) for free-surface flow modelling. To account for the scaling effect on fluid viscosity, Reynolds similarity can be applied, but Ettema (2000) states that if the flow is rough-turbulent at full scale, the effect is negligible and Reynolds similarity unnecessary. The scaling effects on surface tension is negligible if the model flow depth is larger than 20mm, which is the case of this study.

The prime concern when modelling flow over a loose boundary surface is the initiation of sediment transport. Exact similitude of sediment movement was not considered important for the purpose of this study; it was rather ensured that the model sediment will be entrained at a point (flow) similar to that of the prototype, as discussed in Chapter 4.5.

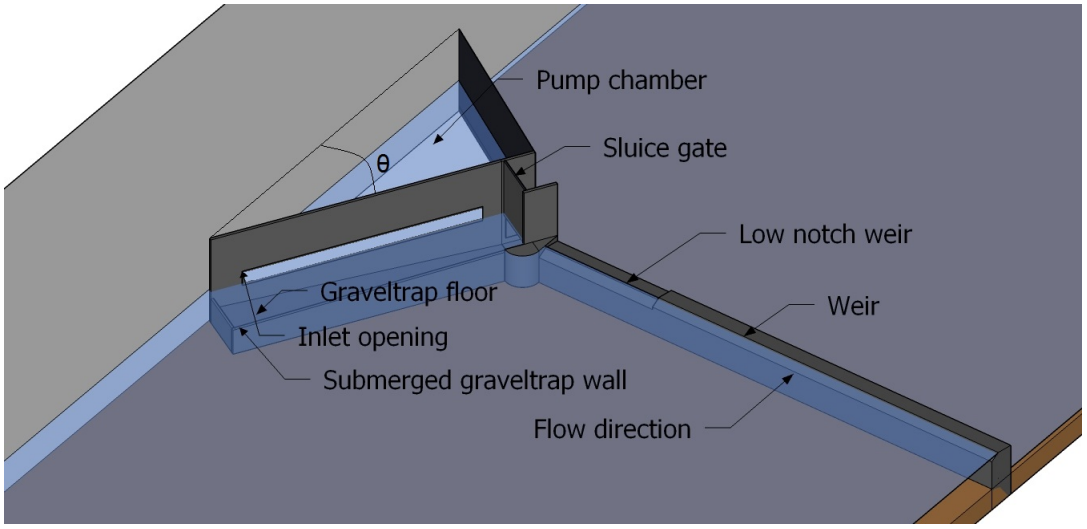

FIGURE 4.1: Diversion works designed for physical model tests

The plan was to apply the tests on all three structures at all three intake angles, resulting in 9 orientations. The three main tests were:

- Sediment diversion tests were conducted, with two objectives. Firstly, the sediment diversion of each orientation (structure and intake angle combination) are compared to comment on the effect of the intake angle and the diversion works size. Secondly, sediment diversion tests were applied at increasing inlet heights at each structure to determine the effect of vertical sediment distribution on sediment rejection.
- Sediment flushing through the graveltrap was analysed for flows ranging from low flows to flood flows. Starting with low flows and increasing, firstly the point of effective flushing with the sluice gate open and secondly the point where flushing with the sluice gate open is no longer effective was determined. Effective sediment flushing was determined visually and the time of flushing was recorded.

- The range where enough sediment is scoured (with the sluice gate closed) from the graveltrap to clear the intake opening. It was determined by surveying the sediment level in the graveltrap along its length, after each flow. This indicated which size flow cleaned the graveltrap sufficiently. The results of each structure were compared and the optimum intake angle determined.

Besides the main tests, the first test that was conducted for each structure, was to determine the sediment transport capacity upstream of the diversion works. The sediment feed was calibrated by measuring the transport whilst sediment was fed into the system.

4.2 Channel Design

The straight rectangular channel was designed keeping in mind that the prototype river width had to be as large as possible to simulate a larger river in South Africa. The flow under flood conditions is limited by the lab capacity, which is a maximum of 700 l/s. The channel was designed to handle typical flood flows and the following assumptions were made for a river in flood: (1) the velocity is $3m/s$; (2) the depth of flow is 8 to 10 m and the river can be assumed to be rectangular. Equation 4.1 was used to determine the prototype flood flow (Q_p), for a chosen width (B_p) and depth (D_p). This was scaled with the froude similarities equations 4.2, 4.3, 4.4 and 4.5 (Ettema, 2000) to determine whether the model flow (Q_m) is within the limits of the labs flow capacity. The scale affects the model size and flows, but it was finally decided to have the scale at 1:25.

$$Q_p = u_p A_p = u_p(B_p D_p) \tag{4.1}$$

$$\frac{L_p}{L_m} = \Theta \tag{4.2}$$

$$\frac{u_p}{u_m} = \Theta^{0.5} \tag{4.3}$$

$$\frac{t_p}{t_m} = \Theta^{0.5} \tag{4.4}$$

$$\frac{Q_p}{Q_m} = \Theta^{2.5} \tag{4.5}$$

where:

L_p and L_m are prototype and model lengths, respectively.
u_p and u_m are prototype and model velocities, respectively.
t_p and t_m is prototype and model time, respectively.
Q_p and Q_m are prototype and model flows, respectively.
Θ is the scale factor

The assumed prototype river model parameters are tabulated in Table 4.1:

TABLE 4.1: Channel Parameters

Parameter	Prototype Dimension
B_p(m)	75
D_p (m)	8
$Q_{p,max}$ (m^3/s)	1800
Scale	1:25
B_m (m)	3
D_m (m)	0.32
$Q_{m,max}$ (m^3/s)	0.576

The channel roughness expressed as Manning n value was assumed to be 0.045, which is a common roughness for river channels (Chadwick *et al.*, 2004). The slope of the river in the scenario tabulated in 4.1 was determined from the Manning equation (4.6) to be 1:678. In the model channel this slope is negligible and sediment was placed at a constant level before initiation of the tests.

$$Q = \frac{1}{n}\frac{A^{5/3}}{P^{2/3}}S^{1/2} \tag{4.6}$$

where:

A is the cross-sectional area of the river channel.
P is the wetted perimeter of the river channel.

The prototype flow depth downstream of the diversion structure was determined with the Manning equation (4.6), after which it was scaled to model depth, for the range of flows tested. This depth was controlled by downstream sluice gates and a downstream water level gauge.

4.3 Layout

As seen in the layout (Figure 4.2), the flow was supplied through one of two pipes. A 200 mm pipe released flow into a box fixed with a V-notch weir and a level gauge (Figure 4.4), to measure the flows below 12.8 l/s. Above 12.8 l/s the flow could be measured with a electronic flow gauge. The 200 mm pipe delivers a maximum flow of 70 l/s. The second pipe is a 600 mm pipe that could deliver the 600 l/s flow capacity available. Downstream of the supply pipes, a brick wall with four open valves let the flow into the channel. Downstream of the valves, a converging section leads to the model channel. Figure 4.3 follows on Figure 4.2, with more detail of the model channel and a detail view of the structure in the channel.

Also seen on the layout (Figure 4.2) are:

- Stilling bricks to reduce turbulence
- The upstream and downstream water level gauge (Figure 4.5)
- Position of the sediment feed conveyor belt system (Figure 4.6)
- Diversion works structure and base (Figure 4.7)
- Position of the abstraction pump(s) (Figure 4.8)
- Stilling basin (constructed for a previous project)
- Downstream sluice gates, which controlled the downstream water level

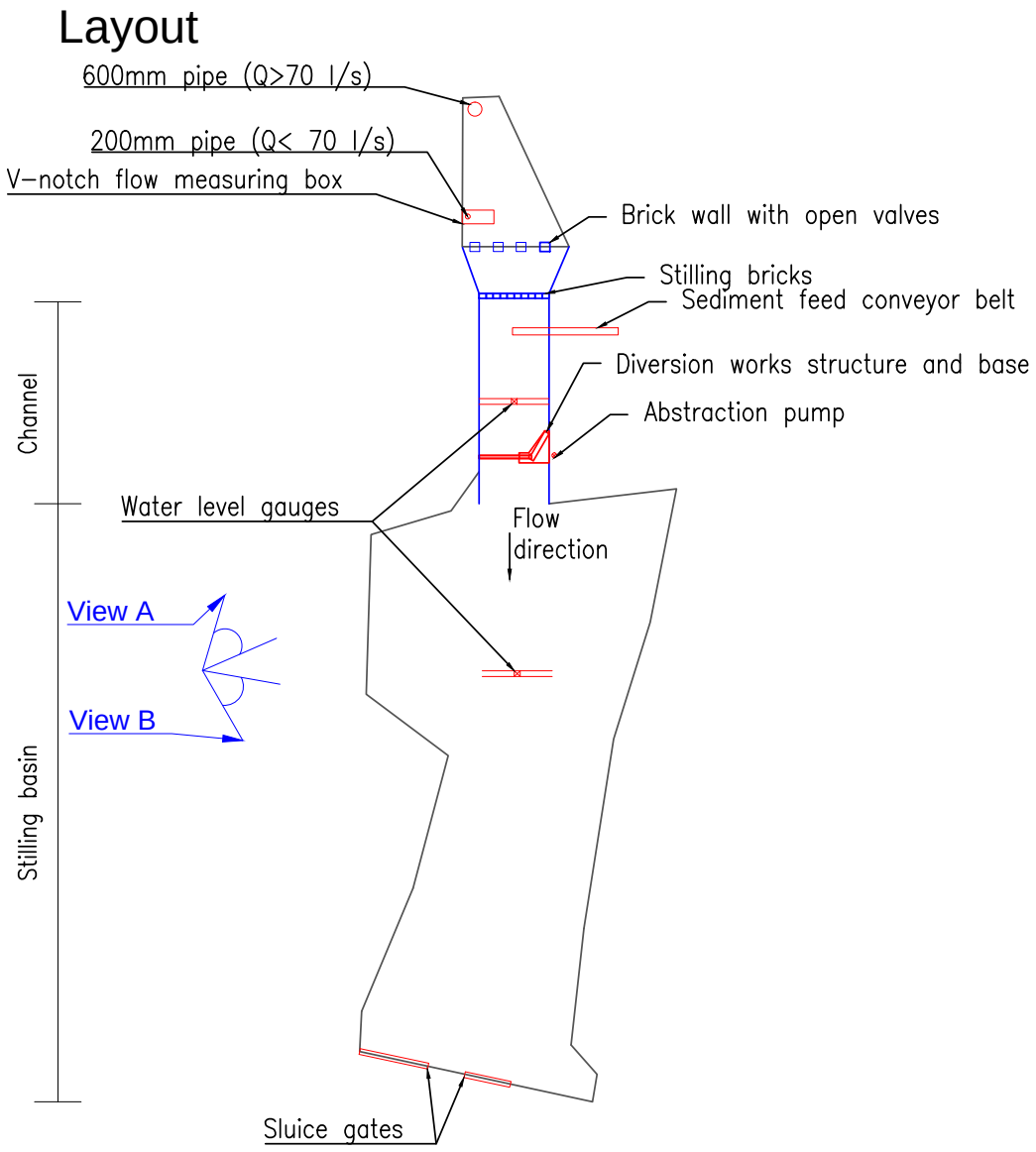

View A

View B

FIGURE 4.2: Complete Model Layout

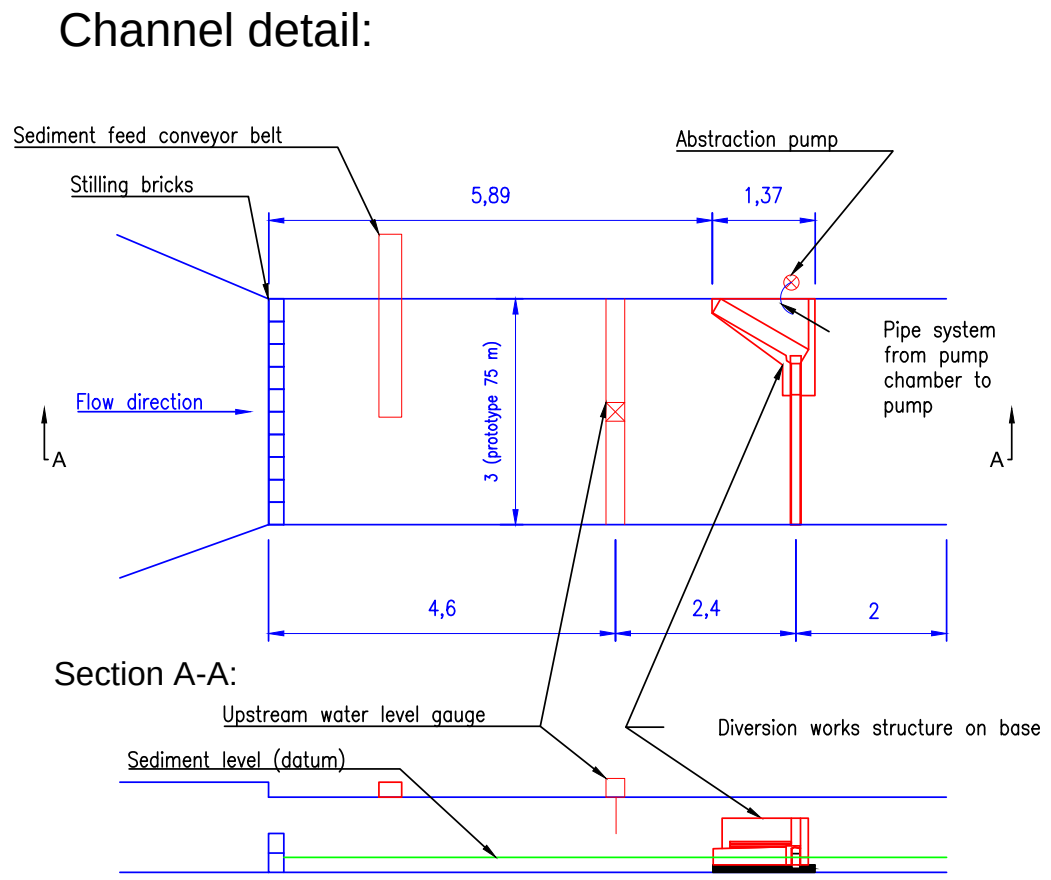

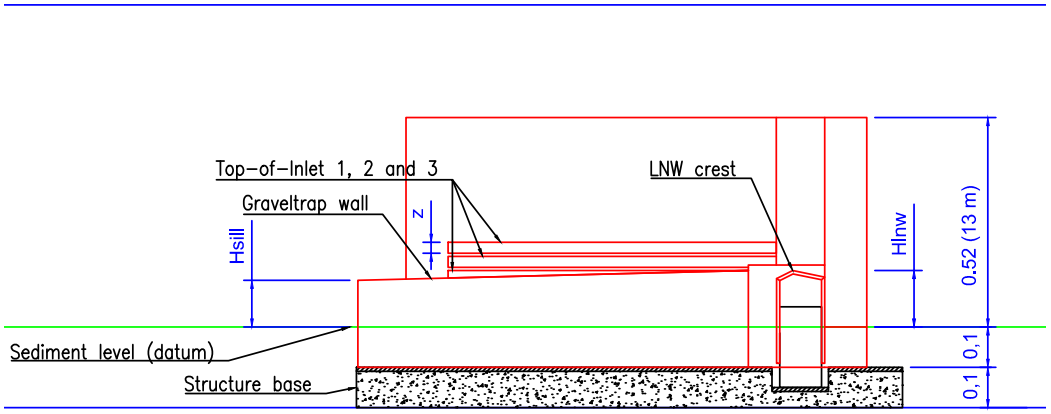

FIGURE 4.3: Detail of components in the model channel and detail view of the structure

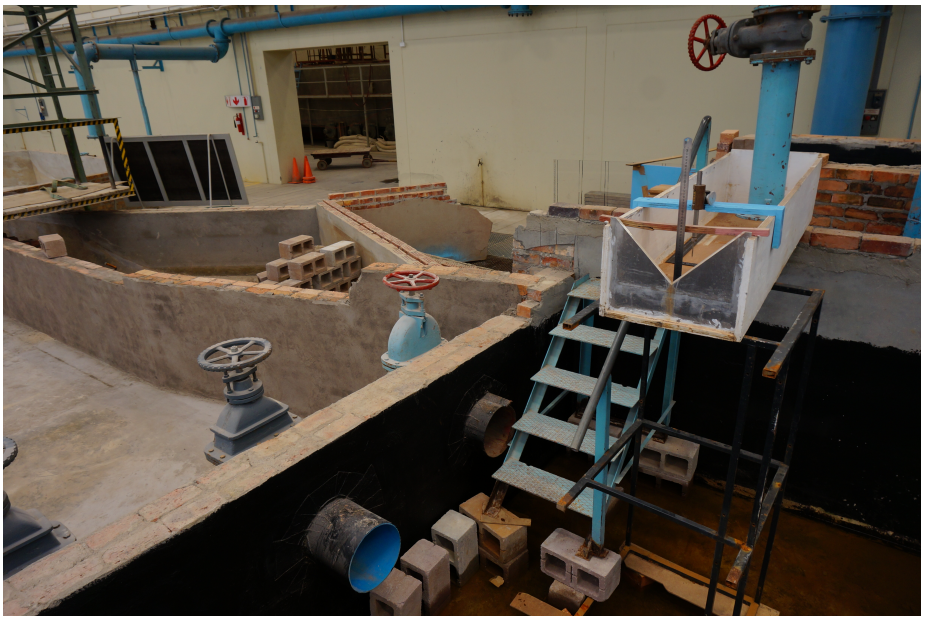

FIGURE 4.4: V-notch flow measuring box and 200 mm supply pipe

(a) (b)

FIGURE 4.5: (a) Upstream and (b) downstream water level gauge

FIGURE 4.6: Sediment feed conveyor belt system

FIGURE 4.7: Diversion structure on base

(a)

(b)

FIGURE 4.8: (a) Pump A used at structure A and B and (b) Pump B used at structure C

4.4 Diversion Works Design — Dynamics of Weir Height, Graveltrap Length and Intake Opening Dimensions

The structure tested (presented in Figure 4.1 and with detail in Figure 4.9) is a widely used design that consists of a weir and a submerged graveltrap. The weir dams the flow, to allow for abstraction at lower flows and the graveltrap prevents sediment from blocking the intake, through intermittent settling and flushing periods.

Diversion works and especially those with a weir are extremely dynamic designs and most components are interdependent. From literature and case studies, it was attempted to find design guidelines for certain components.

With certain aspects of the design fixed by lab constraints or trusted guidelines, the effects of other parameters (specifically the intake angle, weir height and intake opening level) on the total design could be analysed. The structure was designed in prototype dimensions and scaled to model size.

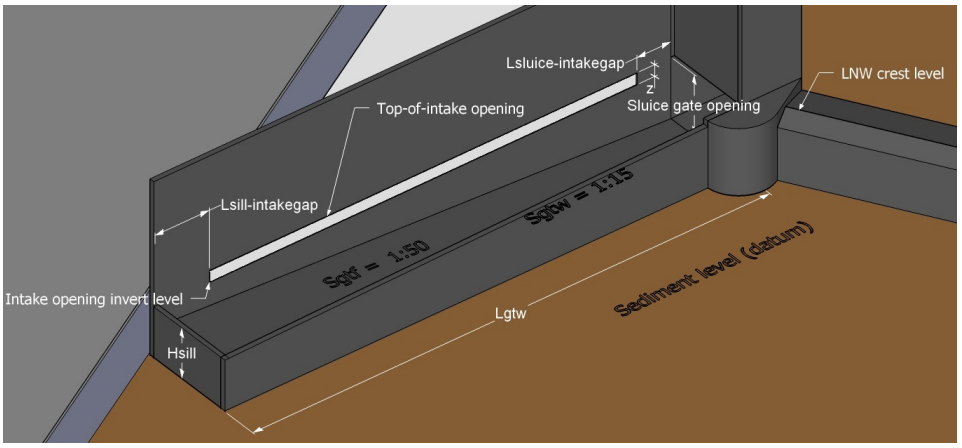

FIGURE 4.9: Detail sketch of diversion works designed for physical model tests

4.4.1 Lab Constraints

As discussed above, the lab flow capacity limited the width of the channel, $B_p = 75$ m ($B_m = 3$ m). The largest intake angle was 60^0 (refer to Figure 3.4) and the structure length (submerged graveltrap wall length) could not be more than 30 m, to prevent too large flow contraction. The 30 m structure at a 60^0 intake angle would block 40 % of the river.

4.4.2 Design Guidelines

Summarised in Table 4.2 are the guidelines taken from various sources. Some dimensions were based on case studies in the source mentioned.

TABLE 4.2: Diversion works design guidelines from literature

Component	Guideline	Source
Graveltrap width	5 m	Basson (2006); Basson (2012)
Submerged gravel trap wall slope	negative 1 : 50	Basson (2006)
Graveltrap floor slope	1:15	Basson (2006); Basson (2012)
Height between the inlet and the graveltrap floor	$\geq$ h/5 (Chapter 3.3.3.6)	Bouvard (1992)
Gap between the sluice gate and inlet	2 m	Basson (2006); Basson (2012)
Velocity through the inlet	0.6 m/s, with 50% blockage	Basson (2006)
Low notch weir length	0.25 $\times$ (Total Weir Length)	Basson (2012)

4.4.3 Design Process

H_{lnw} was incrementally increased (from 2.5 m to 4.5 m) to decide which weir heights were to be tested. For a specific H_{lnw}, it was attempted to have a large as possible graveltrap length (governed by equation 4.7). Due to the negative slope of the graveltrap wall and the steep positive slope of the gravel trap floor, it was necessary to ensure the H_{sill} is higher than the graveltrap floor level (governed by equation 4.8) at the position of the sill (x = L_{gtw}). The relationships are graphically represented in Figure 4.10.

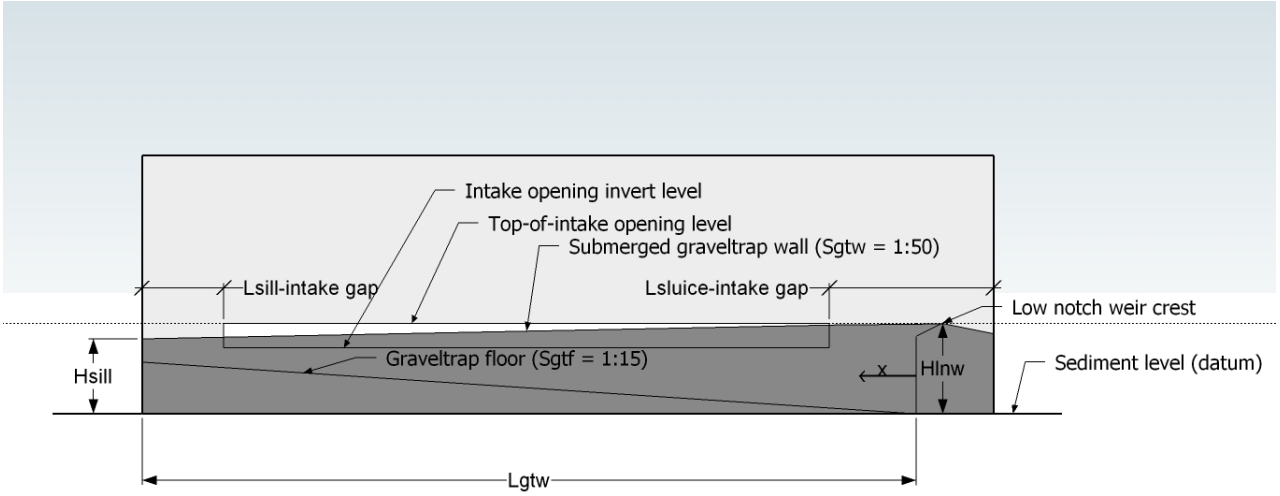

FIGURE 4.10: Diversion Structure Components Relationships

$$L_{gtw} = (H_{lnw} - H_{sill})/S_{gtw} \tag{4.7}$$

$$Graveltrap\ floor\ level = x \times S_{gtf} \tag{4.8}$$

where:

L_{gtw} is the length of the submerged graveltrap wall.
H_{lnw} is the height of the low notch weir.
H_{sill} is the height of the sill.
S_{gtw} is the slope of the submerged graveltrap wall.
S_{gtf} is the slope of the graveltrap floor.

Once an accepted graveltrap length and sill height was established, the intake opening could be designed. The first intake must be fully submerged with the water level at the LNW level, further the invert level of the intake opening is constrained as in Table 4.2. Two factors played a role on the intake opening dimension, (1) the allowable velocity through the intake opening, which is dependent on the abstracted flow (Q_d) (equation 4.9), and (2) the length of the intake opening, which is controlled by the horizontal gap between the sill and the intake.

$$A = L_{intake} * z = Q_d / V_{intake} \tag{4.9}$$

where:

$L_{intake} = L_{gtw} - L_{sill-intakegap} - L_{sluice-intakegap}$

A is the size of the inlet opening.
L_{intake} is the length of the intake opening.
$L_{sill-intakegap}$ is the length of the gap between the sill and the intake opening.
$L_{sill-intakegap}$ is the length of the gap between the sluice gate and the intake opening.
z is the height dimension of the inlet opening.
V_{intake} = 0.3 m/s is the unblocked flow velocity through the intake opening.

For a specific sill-intake gap length, the position where the intake starts was calculated as a distance x from the sluice gate (x = $L_{gtw} - L_{sill-intakegap}$). At this position (x) the graveltrap floor level was determined with equation 4.8 and the intake opening invert level with equation 4.10. It was ensured that at least a 1 m gap is available between the intake opening invert and the graveltrap floor at position x for all structures, which is acceptable according to the h/5 requirement of Bouvard (1992), bearing in mind that for the largest structure tested h = 4.5 m. The h/5 requirement is thoroughly discussed in Chapter 3.3.3.6.

$$Intake\ Opening\ Invert\ Level = LNW - z \tag{4.10}$$

The invert level of the second and third intake were both set 0.3 m above the top of the previous intake, for all three structures. Thus, the top of intake 1 is at MOL, the top of inlet 2 at (0.3 m + z) above MOL and the top of inlet 3 at (0.6 m + 2z) above MOL.

4.4.4 Crump Weir Design

The crump weir is an effective and popularly used flow measuring structure, due to its stable and constant coefficient of discharge in the modular flow range and its relative insensitivity to drowned flow conditions. Figure 4.11 shows the shape and parameters of a crump weir, where H is the design head. According to Wessels (2013), the design head also determines the width of the crump weir. To simplify the design the design head and thus the width of the weir was kept constant at H = 1m and thus L = 3m, respectively for all the structures analysed.

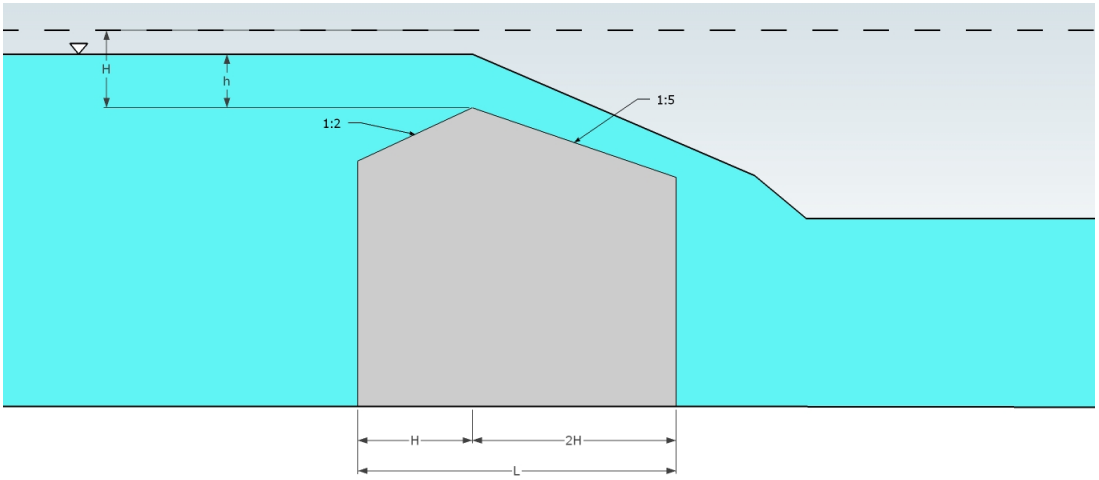

FIGURE 4.11: Crump Weir Design

The weir consisted of a low notch weir and a second weir at a level 0.3 m above the LNW. The length of the LNW was designed to be a portion (0.25) of the total weir length. This means that for each intake angle, the total weir length and thus the LNW length would change. It was decided, to simplify the model by designing the LNW length for the 30^0 intake angle and then merely shorten the remaining weir length for the 45^0 and $60\ ^0$ intake angles. It was decided to further simplify and keep the low-notch weir length equal for all the structures, which was designed according the first structure tested, structure A at a 30^0 intake angle. The final low-notch weir length was 13.5 m for all the structures. The flow over the weir or the water level above the crest is calculated with equation 4.11 (Wessels, 2013).

$$Q = C_{de}\frac{2}{3}\sqrt{\frac{2}{3}}gbH^{2/3} \tag{4.11}$$

where:

$C_{de} = 1.163$
b is the length of the weir
$H = h + v^2/2g$, where v is the oncoming velocity.

4.4.5 Graveltrap Design

The graveltrap width was set to 5 m, based on the design of the Berg River Abstraction Works at Voëlvlei Dam and the Berg River Supplement Scheme abstraction works (Basson, 2006), of which both had similar sized graveltraps. The graveltrap floor slope was set as steep as the steepest example found, to enhance the flushing capabilities of the graveltrap. The lower sill level is governed by two operational guidelines: (1) The sill must be high enough to exclude bedload and a portion of the suspended sediment and (2) the sill must create sufficient velocities in the graveltrap to flush the sediment through the sluice gate during low river flows Avery (1989). The sill was chosen to be at a normal direction to the flow, which means sediment will deposit against the sill, but it should create a better flushing flow in the graveltrap.

The flow over the submerged graveltrap wall and the sill was assumed to be the same as flow over a sharp-crested weir due to the model wall thickness of 8 mm, which equals the 200 mm thickness (b) at prototype scale. During most flows, the head (H) above the wall and sill is much larger than the submerged wall (weir) height (P), reinforcing the sharp-crested weir flow assumption. The shape and design are as seen in Chadwick *et al.* (2004) and Wessels (2013), shown in Figure 4.12. Figure 4.13 shows an example of the flow over the submerged graveltrap wall of the model.

The sluice gate was designed to open up to the LNW level of each structure and without any contractions along the graveltrap, the gate was equal to the graveltrap width of 5 m for all structures tested.

As seen on Figure 4.14, a hydraulic jump should occur downstream of the sluice gate between positions 2 and 3. As mentioned, the downstream depth (y_3) is controlled by the geometric properties of the river as well as the river flow. The stability of the hydraulic jump depends on the relation between the actual downstream depth (y_3) and the downstream depth (y_3') necessary for the hydraulic jump to form. The momentum equation (4.12) which is simplified for a rectangular channel by Chadwick *et al.* (2004) can be used to determine y_3'. The depth, y_2 is a function (equation 4.13) of a contraction coefficient, C_c and the gate opening, y_G. Chadwick *et al.* (2004) assumes a value of $C_c = 0.61$ for vertical sluice gates, like the one used in the model.

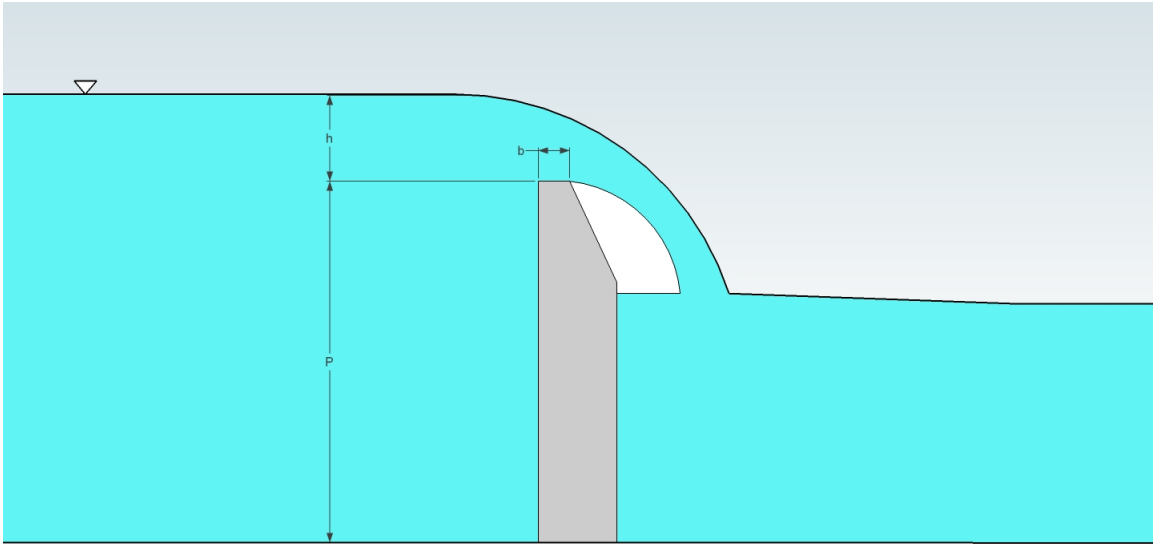

FIGURE 4.12: Sharp Crested Weir

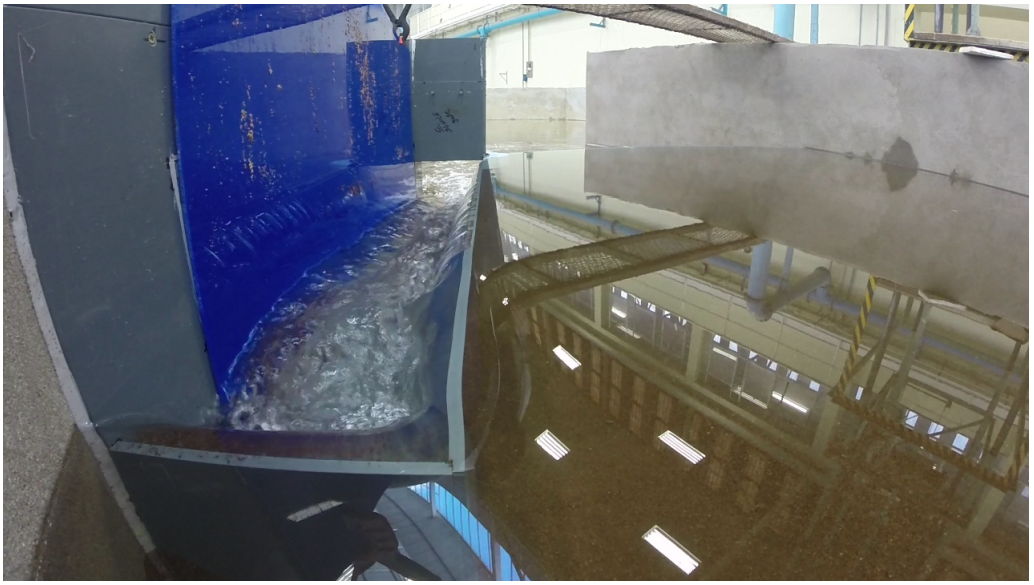

FIGURE 4.13: Photo of flow over model graveltrap

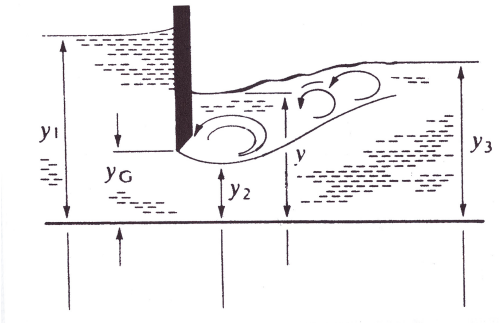

FIGURE 4.14: Flow through sluice gate, showing the downstream hydraulic jump (Chadwick *et al.*, 2004)

$$y_3' = (y_2/2)(\sqrt{1 + 8Fr_2^2} - 1) \tag{4.12}$$

where:

Fr is the Froude number at position 2

$$y_2 = C_c y_G \tag{4.13}$$

Chadwick *et al.* (2004) states the following about the stability of the hydraulic jump:

- If $y_3 = y_3'$, a stable jump forms.
- If $y_3 > y_3'$, the jump moves upstream and possibly into the graveltrap.
- If If $y_3 < y_3'$, the jump moves downstream and away from the graveltrap.

If the hydraulic jump moves upstream, into the graveltrap, the velocity in the graveltrap will slow down and the flushing ability compromised.

4.4.6 Summary of Diversion Works Designed (Prototype Scale)

Three structures (A, B and C) were designed with prototype weir heights of 4.5 m, 3.5 m and 2.5 m respectively. Figures 4.1 and 4.9 present the parameters that were varied, namely the weir height (and resulting intake opening level and graveltrap sill height) and intake angle (θ).

Structure A was designed to be able to abstract flows of 10 m^3/s through an intake opening of 25×1.333 m, with the top-of-intake opening level of the first inlet at 4.5 m. The rectangular graveltrap has a length of 30 m and sill height of 3.9 m.

Structure B was designed to be able to abstract flows of 5 m^3/s through an intake opening of 25×0.667 m, with the top-of-intake opening level of the first inlet at 3.5 m. The rectangular graveltrap has a length of 30 m and sill height of 2.9 m.

Structure C was designed to be able to abstract flows of 1 m^3/s through an intake opening of 17×0.196 m, with the top-of-intake opening level of the first inlet at 2.5 m. The rectangular graveltrap has a length of 25 m and sill height of 2 m.

All the structures have graveltrap floor slopes of 1:15 and submerged wall slope of 1:50 as discussed in Chapter 4.4.5. Table 4.3 summarises the main parameters of each structure, both in model and prototype dimensions.

TABLE 4.3: Designed Diversion Structures Parameter Summary

Parameter*	Prototype scale	Model scale	Prototype scale	Model scale	Prototype scale	Model scale
Structure	**A**		**B**		**C**	
Weir (H_{lnw})	4.5 m	0.180 m	3.5 m	0.140 m	2.5 m	0.100 m
Sluice gate opening	4.5 m	0.180 m	3.5 m	0.140 m	2.5 m	0.100 m
L_{gtw}	30 m	1.200 m	30 m	1.200 m	25 m	1.000 m
H_{sill}	3.9 m	0.156 m	2.9 m	0.116 m	2 m	0.080 m
Graveltrap width	5 m	0.200	5	0.200	5	0.200
$L_{sill-intakegap}$	3 m	0.120 m	3 m	0.120 m	6 m	0.240 m
$L_{sluice-intakegap}$	2 m	0.080 m	2 m	0.080 m	2 m	0.080 m
L_{intake}	20 m	0.800 m	20 m	0.800 m	17 m	0.680 m
z	1.333 m	0.053 m	0.667 m	0.027 m	0.196 m	0.008 m
Inlet 1 invert level	3.167 m	0.127 m	2.833 m	0.113 m	2.304 m	0.092 m
Inlet 1 top level	4.5 m	0.180 m	3.5 m	0.140 m	2.5 m	0.100 m
Inlet 2 invert level	4.8 m	0.192 m	3.8 m	0.152 m	2.8 m	0.112 m
Inlet 2 top level	6.133 m	0.245 m	4.467 m	0.179 m	2.996 m	0.120 m
Inlet 3 invert level	6.433 m	0.257 m	4.767 m	0.191 m	3.296 m	0.132 m
Inlet 3 top level	7.766 m	0.311 m	5.433 m	0.217 m	3.492 m	0.140 m

* All levels are measured from the datum shown in Figures 4.3, 4.9 and 4.10

4.5 Model Sediment

Crushed peach pips were used as the model sediment. The sediment available were two batches with d_{50} particle sizes of 0.4 mm and 0.8 mm and d_{90} of 0.6 mm and 1.28 mm, respectively. Both batches had a relative density of 1.3. Equal volumes of each batch were mixed to yield a sediment mixture with a d_{50} of 0.56 mm.

The modified Lui diagram was used to determine what size of sediment the model sediment represent. The river parameters, as summarised in Table 4.1, yielded a bed slope of 1:678, calculated with equation 4.6.

The calculation and modified Lui diagram in Appendix C concluded that the model sediment mixture represents a prototype sediment size of 1.4 mm, which is very coarse sand in the field.

4.6 Experimental Procedures

The conducted tests are categorised as Diverted Sediment (DS) tests, Self-Scour (SS) of the graveltrap tests and Sediment Flushing (SF) tests. The configurations are labelled, e.g. A30, which means: structure A at a 30^0 intake angle. The test applied at a certain configuration are labelled, e.g. DSA30, which means: the diverted sediment test of structure A at a 30^0 intake angle. The tests that were conducted are summarised in Tables:

- The DS tests and test conditions in Table 4.4
- The SS tests and test conditions in Table 4.5
- The SF tests and test conditions in Table 4.6

TABLE 4.4: Summary of diverted sediment (DS) test conditions

Test	Q_{riv} (l/s)	DDR	Downstream depth (mm)
DSA30 : Diverted Sediment Test of structure A at a 30^0 intake angle, Q_d = 2.4 l/s			
DSA301	128	1.88%	124
DSA302	192	1.25%	160
DSA303	256	0.94%	191
DSA304	320	0.75%	220
DSA305	384	0.63%	247
DSA306	576	0.42%	320
DSA45 : Diverted Sediment Test of structure A at a 45^0 intake angle, Q_d = 2.4 l/s			
DSA451	128	1.88%	124
DSA452	192	1.25%	160
DSA453	256	0.94%	191
DSA454	320	0.75%	220
DSA455	384	0.63%	247
DSA456	576	0.42%	320
DSA60 : Diverted Sediment Test of structure A at a 60^0 intake angle, Q_d = 2.4 l/s			
DSA601	128	1.88%	124
DSA602	192	1.25%	160
DSA603	256	0.94%	191
DSA604	320	0.75%	220
DSA605	384	0.63%	247
DSA606	576	0.42%	320
DSB30 : Diverted Sediment Test of structure B at a 30^0 intake angle, Q_d = 1.1 l/s			
DSB301	128	0.87%	124
DSB302	192	0.58%	160
DSB303	256	0.43%	191
DSB304	320	0.35%	220
DSB305	384	0.29%	247
DSB306	528	0.21%	302
DSB45 : Diverted Sediment Test of structure B at a 45^0 intake angle, Q_d = 1.1 l/s			
DSB451	128	0.87%	124
DSB452	192	0.58%	160
DSB453	256	0.43%	191
DSB454	320	0.35%	220
DSB455	384	0.29%	247
DSB456	528	0.21%	302
DSB60 : Diverted Sediment Test of structure B at a 60^0 intake angle, Q_d = 1.1 l/s			
DSB601	128	0.87%	124
DSB602	192	0.58%	160
DSB603	256	0.43%	191
DSB604	320	0.35%	220
DSB605	384	0.29%	247
DSB606	528	0.21%	302
DSC45 : Diverted Sediment Test of structure C at a 45^0 intake angle, Q_d = 0.41 l/s			
DSC451	64	0.64%	81
DSC452	128	0.32%	124
DSC453	192	0.21%	160
DSC454	256	0.16%	191
DSC455	320	0.13%	220
DSC456	384	0.11%	247
DSC457	528	0.08%	302
DSC60 : Diverted Sediment Test of structure C at a 60^0 intake angle, Q_d = 0.41 l/s			
DSC601	64	0.64%	81
DSC602	128	0.32%	124
DSC603	192	0.21%	160
DSC604	256	0.16%	191
DSC605	320	0.13%	220
DSC606	384	0.11%	247
DSC607	528	0.08%	302

TABLE 4.5: Summary of self scour (SS) of the graveltrap test conditions

Test	Q*riv* (l/s)	Downstream depth (mm)	Test	Q*riv* (l/s)	Downstream depth (mm)
SSA30 : Self Scour of graveltrap test, of structure A at a 30^0 intake angle			**SSB45 :** Self Scour of graveltrap test, of structure B at a 45^0 intake angle		
SSA301	128	124	SSB451	128	124
SSA302	192	160	SSB452	192	160
SSA303	256	191	SSB453	256	191
SSA304	320	220	SSB454	320	220
SSA305	384	247	SSB455	384	247
SSA306	480	285	SSB456	480	285
SSA307	576	320	SSB457	528	302
SSA45 : Self Scour of graveltrap test, of structure A at a 45^0 intake angle			**SSB60 :** Self Scour of graveltrap test, of structure B at a 60^0 intake angle		
SSA451	128	124	SSB601	128	124
SSA452	192	160	SSB602	192	160
SSA453	256	191	SSB603	256	191
SSA454	320	220	SSB604	320	220
SSA455	384	247	SSB605	384	247
SSA456	480	285	SSB606	480	285
SSA457	576	320	SSB607	528	302
SSA60 : Self Scour of graveltrap test, of structure A at a 60^0 intake angle			**SSC45 :** Self Scour of graveltrap test, of structure C at a 45^0 intake angle		
SSA601	128	124	SSC451	128	124
SSA602	192	160	SSC452	192	160
SSA603	256	191	SSC453	256	191
SSA604	320	220	SSC454	320	220
SSA605	384	247	SSC455	384	247
SSA606	480	285	SSC456	480	285
SSA607	576	320	SSC457	528	302
SSB30 : Self Scour of graveltrap test, of structure B at a 30^0 intake angle			**SSC45 :** Self Scour of graveltrap test, of structure C at a 45^0 intake angle		
SSB301	128	124	SSC601	128	124
SSB302	192	160	SSC602	192	160
SSB303	256	191	SSC603	256	191
SSB304	320	220	SSC604	320	220
SSB305	384	247	SSC605	384	247
SSB306	480	285	SSC606	480	285
SSB307	528	302	SSC607	528	302

TABLE 4.6: Summary of sediment flushing (SF) test conditions

Test	Q_{riv} (l/s)	Downstream depth (mm)	Test	Q_{riv} (l/s)	Downstream depth (mm)
SFA30 : Sediment flushing test of structure A at a 30^0 intake angle			**SFB45 :** Sediment flushing test of structure B at a 45^0 intake angle		
SFA301	4	15	SFB451	4	15
SFA302	25.6	46	SFB452	25.6	46
SFA303	38.2	59	SFB453	38.4	59
SFA304	64	81	SFB454	64	81
SFA305	128	124	SFB455	128	124
SFA306	192	160			
SFA45 : Sediment flushing test of structure A at a 45^0 intake angle			**SFB60 :** Sediment flushing test of structure B at a 60^0 intake angle		
SFA451	4	15	SFB601	4	15
SFA452	25.6	46	SFB602	25.6	46
SFA453	38.2	59	SFB603	38.4	59
SFA454	64	81	SFB604	64	81
SFA455	128	124	SFB605	128	124
SFA456	192	160			
SFA60 : Sediment flushing test of structure A at a 60^0 intake angle			**SFC45 :** Sediment flushing test of structure C at a 45^0 intake angle		
SFA601	4	15	SFC451	4	15
SFA602	25.6	46	SFC452	12.8	30
SFA603	38.2	59	SFC453	25.6	46
SFA604	64	81			
SFA605	128	124			
SFA606	192	160			
SFB30 : Sediment flushing test of structure B at a 30^0 intake angle			**SFC60 :** Sediment flushing test of structure C at a 60^0 intake angle		
SFB301	4	15	SFC451	4	15
SFB302	25.6	46	SFC452	12.8	30
SFB303	38.4	59	SFC453	25.6	46
SFB304	64	81			
SFB305	128	124			

4.6.1 Sediment Transport Determination and Feed Calibration

The sediment feed and sediment transport for the range of flows tested were determined and calibrated once for each structure, with the structure at the 30^0 diversion angle, and was kept constant for the 45^0 and 60^0 intake angles.

Without sediment feed, the sediment transport upstream of the weir was measured with the measuring net seen in Figure 4.15. The 100×100 mm measuring net was used to catch sediment to be weighed. The time of catching was recorded and used to relate the mass caught to a width averaged transport capacity (G_{riv}) with equation 4.14. The point of measurement was in the centre of the channel, 500 mm upstream of the upstream water level gauge (Figure 4.2).

$$G_{riv} = \frac{weight\ of\ sediment\ caught}{time} \times \frac{channel\ width}{net\ width} \tag{4.14}$$

FIGURE 4.15: Survey ruler, sediment transport measuring net and the internal net of pump A (from left to right)

The measured G_{riv} was then used as the first feed estimate (G_{feed}). With sediment fed, the G_{riv} was measured again and the sediment feed increased accordingly. It was attempted to have G_{riv} and G_{feed} values as close as possible, but accepted if the G_{feed} was more than the G_{riv} or not more than 5% less. It was assumed that the excess sediment would settle upstream of the

structure. The position of the sediment feed was set far enough upstream of the structure to ensure that the sediment distributes across the width of the channel. The distribution of the sediment was eavaluated during the tests and found acceptable.

4.6.2 Diverted Sediment Test

The amount of sediment abstracted was evaluated at various flows, at 8 configurations (e.g. A30) but also for varying (three) intake opening levels for 5 configurations. Thus, 18 scenarios were tested for a minimum of 6 flows each, adding up to more than 108 tests. Sediment was fed during all the tests where any sediment transport in the river was measured. The Q_d was scaled with equation 4.5 from the prototype values 1, 5 and 10 m^3/s, resulting in 3.2, 1.6 and 0.32 l/s for structures A, B and C respectively. However, the Q_d was constrained by the ability of the pump used.

The time-averaged flow achieved by the pump (Figure 4.8) used to achieve the Q_d, was determined by 10 or more tests which consisted of pumping, for a measured amount of time from the pump chamber into a container of which the contained volume could be determined. The values achieved and tested with each structure were 2.4, 1.1 and 0.41 l/s for structures A, B and C respectively. The pump calibrations are tabulated in Appendix B.

The diverted flow is pumped from the pump chamber during the tests. Different pumps were used to to achieve the different Q_d values. Pump A (Figure 4.8) was used with structure A and B, to pump 2.4 and 1.1 l/s , respectively. Pump B (Figure 4.8) was used with structure C to pump 0.41 l/s.

During abstraction with Pump A, the sediment was caught with the net situated in the pump (Figure 4.15) and transferred to marked plastic bags which could be weighed. The accuracy of the method was tested by adding a known amount (weight) of sediment to a water filled container clean of sediment and weighing the amount of sediment caught after abstraction from the container. This test is tabulated in Appendix B and the average accuracy of the method found to be 93 %.

Pump B had no internal net and the sediment was caught with the net in Figure (Figure 4.15) at its downstream end. There was thus no point in the system where sediment could be lost.

All sediment samples were weighed whilst wet, but traditionally the sediment transport indicators (i.e. G_{riv} and G_d) are dry weight values. A factor of wet to dry weight was established for a range of sample sizes. The factor, $F_{dry/wet}$ was determined equal to 58 % and applied to the wetted sample weights to determine the dry weight. Samples of various sizes were used to determine $F_{dry/wet}$, shown in Table B.2 in Appendix B

The procedure of each diverted sediment test was as follow:

1. Set the downstream water level gauge, according to the flow.
2. Initiate the flow (e.g. Test DSA301)
3. Force the downstream water level to the gauge level (by adjusting the downstream sluice gates).
4. Start sediment feed (correct G_{feed} for the specific flow).
5. Open intake opening and initiate abstraction (start pump) while recording the abstraction time.
6. Close the intake opening.
7. Abstract the remaining water in the pump chamber ensuring all deposited sediment is abstracted with the water.
8. Transfer the abstracted sediment from the pump to be weighed.

4.6.3 Self Scour of the Graveltrap at the Intake Opening

The tests were conducted to determine the optimum intake angle, as well as the *clearance flow*. The *clearance flow* is the minimum river flow which scours enough sediment from the graveltrap to clear the intake opening of sediment along its complete length. Ultimately only 8 configurations were necessary to test. For each configuration, the graveltrap was filled up to the invert of the first (lowest) intake opening before initiation of the tests. It was determined at which flow sediment movement is initiated, which was set as the lowest flow tested.

After each flow the sediment level in the graveltrap was surveyed at six points along its length, with the survey ruler (Figure 4.15), modified to have a base piece that covers the width of the graveltrap. The base piece also ensured that the ruler did not penetrate the surface. The test procedure of each configuration was as follow:

1. Fill the graveltrap to the invert level of the lowest intake.
2. Set the downstream water level gauge, according to the flow.
3. Initiate the first flow (e.g. SSA301).
4. Force the downstream water level to the gauge level (by adjusting the downstream sluice gates).

5. Read the upstream water level gauge.
6. Survey points 1 to 6.
7. Repeat steps 2 to 6 for the next flow (e.g. SSA302)

4.6.4 Sediment Flushing Test

The efficiency of the sediment flushing through an open sluice gate with water level draw down was evaluated in terms of time taken to clean the graveltrap. The graveltrap was filled to the top of the graveltrap sill level before each test. The purpose is to determine the largest river flow at which the sluice gate can still be opened with the desired effect. Per configuration and for all the river flows (e.g. SFA301 to SFA306), the graveltrap was filled with the sediment mixture and the time to flush the graveltrap sufficiently clean was recorded. It was observed that some residue remained at the upstream end against the graveltrap sill wall, in which case the timer was stopped when no more significant sediment movement is observed. Camera (GoPro) footage was used to review the timing results. The test procedure of each configuration was as follow:

1. Fill the graveltrap with wetted sediment.
2. Set the downstream water level gauge, according to the flow.
3. Initiate the first flow (e.g. SFA301).
4. Force the downstream water level to the gauge level (by adjusting the downstream sluice gates).
5. Read the upstream water level gauge.
6. Open the sluice gate, set timer and GoPro
7. Stop timer (when the graveltrap is clean or flushing seems to cease to have effect).
8. Repeat from step 1, for the next flow (e.g. SFA302).

Chapter 5

Results

5.1 River Sediment Transport and Feed Calibration

It was necessary to determine the sediment transport in the channel, G_{riv}, as well as the calibrated sediment feed, G_{feed}), once for each structure at each flow rate tested. Note that the calibration was done at a 30^0 intake angle for structures A and B, but at 45^0 for structure C, because the 30^0 was eliminated by the first two structures tested. The calibration was done as described in Chapter 4.6.1. Table 5.1 summarises the measured and calibrated G_{riv} and G_{feed} for each structure and the range of flow rates tested during the diverted sediment tests. It was observed that of the flows tested, sediment entrainment was initiated at Q_{riv} = 192 l/s for structure A and B and at Q_{riv} = 128 l/s for structure C.

TABLE 5.1: Measured sediment transport and calibrated sediment feed

Structure A			Structure B			Structure C		
Flow (l/s)	G_{riv} (g/s)	G_{feed} (g/s)	Flow (l/s)	G_{riv} (g/s)	G_{feed} (g/s)	Flow (l/s)	G_{riv} (g/s)	G_{feed} (g/s)
64	0	0	64	0	0	64	0	0
128	0	0	128	0	0	128	5	6
192	2	6	192	11	12	192	70	88
256	11	12	256	29	29	256	115	175
320	60	58	320	70	70	320	234	234
384	64	76	384	174	175	384	251	263
576	110	105	528	254	380	528	323	409

5.2 Diverted Sediment (DS) Tests - Varying Intake Angle

Tests were conducted as described in Chapter 4.6.2 and the results of the diverted sediment tests are expressed as graphs, where the diverted sediment ratio (DSR) is plotted against the diverted discharge ratio (DDR). For each structure, the smallest Q_{riv} tested is a flow smaller than the

smallest flow capable of sediment entrainment in the channel. This flow rate was tested as a precaution and to evaluate whether the Q_d entrained local sediment close to the intake. The DSR values were only plotted from the flow rate which first yielded diverted sediment ($G_d > 0$) and upwards.

The abstracted flow (Q_d) was kept constant for each structure and thus the DDR decreased as Q_{riv} increased. Refer to Table 4.4, which summarises the test conditions (Q_{riv}, DDR and downstream depth) of each test series.

The effect of the intake angle is evaluated per structure with the intake opening at the lowest height (with the top at LNW level).

5.2.1 Tests on Structure A (DSA tests, Q_d = 2.4 l/s)

A flow range of Q_{riv} = 128 to 576 l/s was tested and the resulting DDR ranged from 1.88 % to 0.42 %.

The results are shown in Figure 5.1. Test series DSA30 yielded higher DSR values than DSA45 and DSA60 over the complete range of DDR tested. The DSR values of DSA45 and DSA60 are closer related with average DSR values of 0.48 % and 0.44 %. At the lowest DDR tested, 0.41 %, the DSR of test DSA60 was higher than that of DSA45 (0.83 % vs 0.44 %). For the rest of the range tested the DSA45 test yielded higher DSR values than DSA60.

Test series DSA30 and DSA60 yielded the lowest DSR (0.37 % and 0.12 %, respectively) at DDR = 0.63 % (Q_{riv} = 384 l/s). The test series DSA45 yielded its lowest DSR (0.23 %) at DDR = 0.75 % (Q_{riv} = 320 l/s).

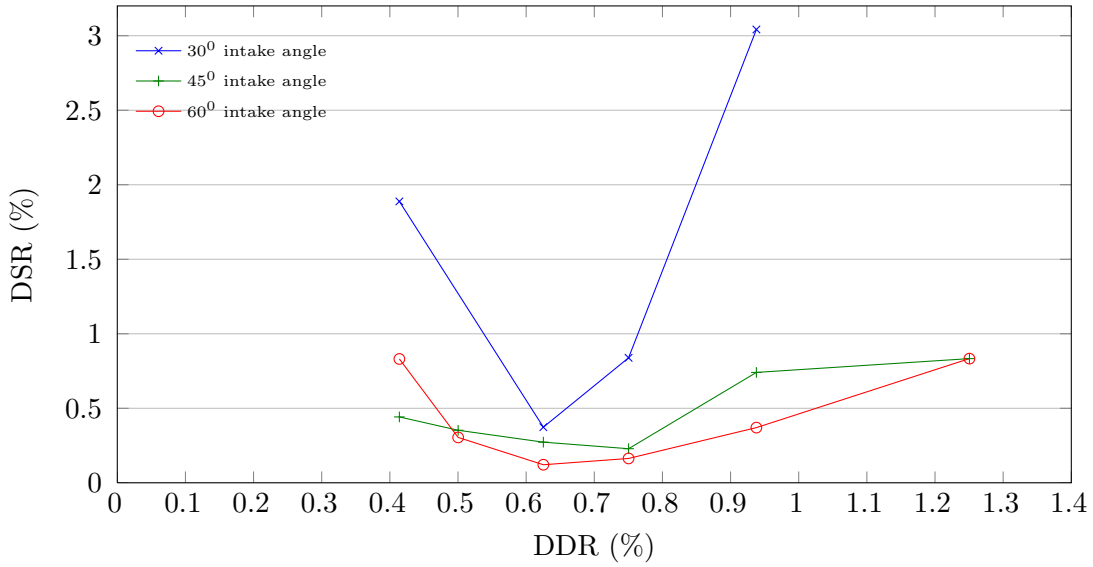

FIGURE 5.1: Test DSA: Diverted sediment tests of structure A at varying intake angles

5.2.2 Tests on Structure B (DSB tests, Q_d = 1.1 l/s)

A flow range of Q_{riv} = 128 to 576 l/s was tested the and thus the DDR ranged from 0.87 % to 0.21 %.

As seen in Figure 5.2, the results of test series DSB30, DSB45 and DSB60 showed a consistent trend. The 60^0 intake angle yielded the lowest DSR and the 30^0 intake angle the highest. The maximum DSR of structure B was recorded during test series DSB30 at DDR = 0.58 %, DSR = 1.05 %. During test series DSB45 and DSB60 no sediment was abstracted with DDR = 0.58 % (Q_{riv} = 192 l/s) and thus no DSR is plotted.

The lowest DSR values recorded are equal to 0.18 %, 0.15 % and 0.02 % at intake angles 30^0, 45^0 and 60^0, respectively. The lowest DSR values were all recorded at DDR = 0.29 % (Q_{riv} = 384 l/s).

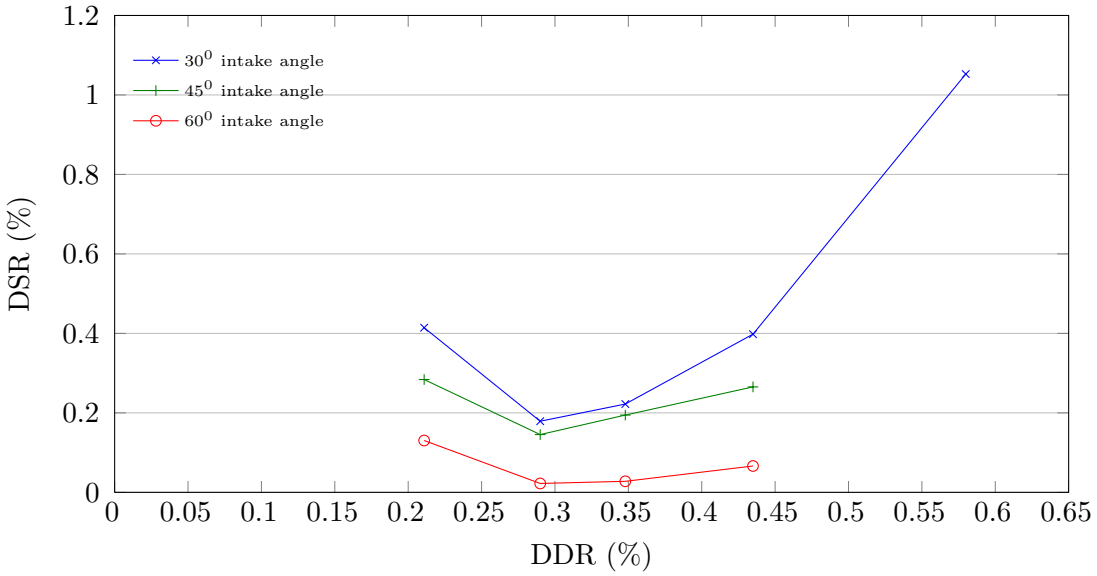

FIGURE 5.2: Test DSB: Diverted sediment tests of structure B at varying intake angles

5.2.3 Tests on Strucure C (DSC tests, Q_d = 0.41 l/s)

The flow range tested was Q_{riv} = 64 l/s to 528 l/s, resulting in a DDR range of 0.64 % to 0.08 %.

The results of test series DSC45 and DSC60, shown in Figure 5.3, do not reflect the clear distinction between intake angles. The trend is also not clear. It was observed during the test that more local sediment from around the graveltrap was transported into the graveltrap and was abstracted through the lower (compared to structure A and B) intake openings of the structure. It is believed that this influenced the results, but correctly so, as this would occur at a diversion works of the same size.

The lowest DSR values were recorded as 0.042 % and 0.056 % at DDR values 0.13 % (Q_{riv} = 320 l/s) and 0.21 % (Q_{riv} = 192 l/s) for DSC45 and DSC60, respectively.

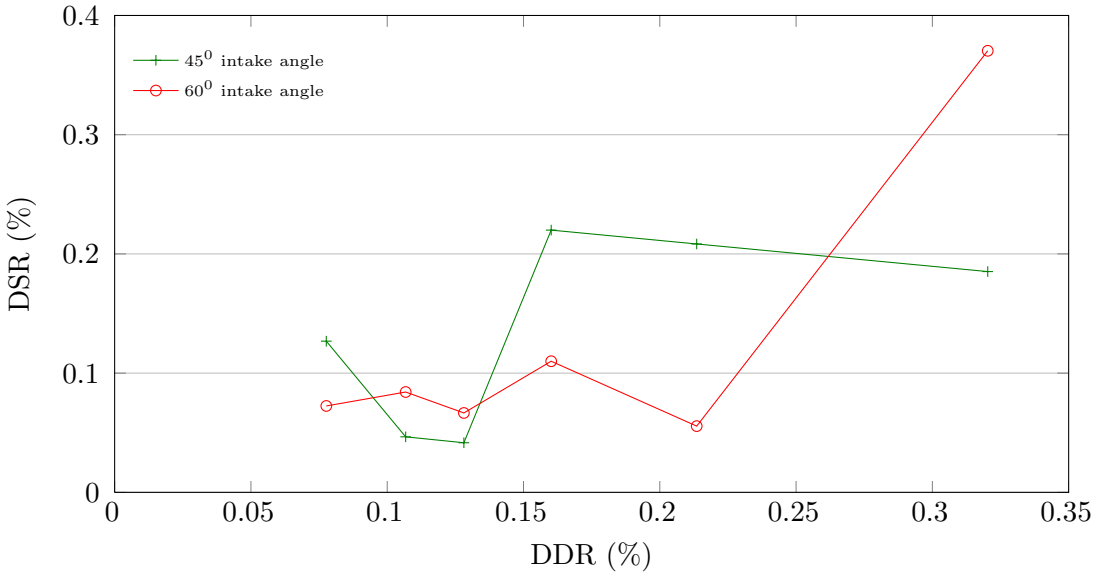

FIGURE 5.3: Test DSC: Diverted sediment tests of structure C at varying intake angles

5.2.4 Analysis of DS Tests and the effect of the intake Angle

If DSR can be considered to give an indication of the ratio of sediment concentration in the abstracted water to that in the river, it is possible to determine an intake angle which could be more effective to develop spiral flow adjacent it in the river and therefore cause less sediment concentration in the diverted flow.

It is attempted to determine the optimum intake angle for each structure. Further, correlations are drawn between the structures (test series DSA, DSB and DSC).

From the DS tests it is also possible to comment on the effect of the weir height and the size of the abstracted flow (Q_d) on the diverted sediment.

The DDR and DSR values of the study is in general very low, with a maximum DSR of 3.04 % observed with structure A at a 30^0 intake angle. The maximum DDR tested is 1.88 %. This can be attributed to the size of the prototype river (B_p = 75 m), with larger river flows and sediment loads compared to the diverted flow and sediment load. Table 4.4 summarises the test conditions, showing the diverted flow and river flow of each test.

The results of test series DSA showed the 60^0 intake angle yields the lowest average DSR value over the range of flows tested and also the lowest overall value, with DSR = 0.12 % at a DDR = 0.63 % (Q_{riv} = 384 l/s). Note that even though the 60^0 angle resulted as the optimum angle, the improvement from the 45^0 angle is slight.

The tests on structure B also showed the 60^0 intake angle to be the optimum angle, yielding the

lowest DSR across the range of flows tested. The lowest DSR (0.02 %) recorded was at DDR = 0.29 % (Q_{riv} = 384 l/s).

From the results of tests on structure A and B, the 30^0 intake angle could be identified as the least effective angle in terms of minimising diverted sediment and was excluded in the tests on structure C.

The results at structure C did not yield a clear distinction between the 45^0 and 60^0 intake angle. The variability in results could be attributed to the influence of local sediment which was abstracted by the lower (compared to structure A and B) intake opening.

With DSR as basis of analysis, it must be considered that the 60^0 intake angle could be more effective than the 30^0 and 45^0 intake angles to develop spiral flow which is effective in minimising the DSR.

The DSR-DDR curve of each test yielded an **optimum operating point**, where the DSR is at a minimum for the flow range tested. The results of each structure shows the optimum operating point can be related to a DDR, regardless of the intake angle. The optimum DDR differed however between structures. It was observed that the optimum operating point occurred at similar Q_{riv} flows for all three structures, as seen in Figure 5.4, showing the results of tests DSA45, DSB45 and DSC45.

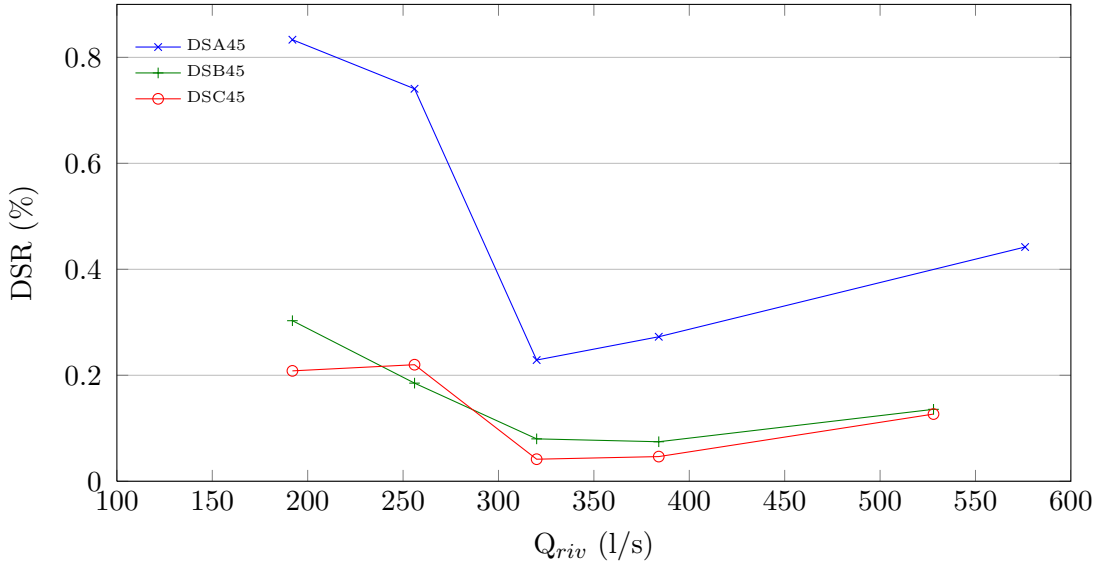

FIGURE 5.4: DSR vs Q_{riv} of structure A, B and C at a 45 ^{0} intake angle

When comparing the results of the structures in terms of DDR and DSR as a conglomerate, the known effect of increasing DSR with increasing DDR is seen at all three intake angles (Figures 5.5 5.6 and 5.7). Bare in mind that each structure was designed to abstract a range of DDR

and the effects of the design features like the weir height and intake opening level must be taken into account.

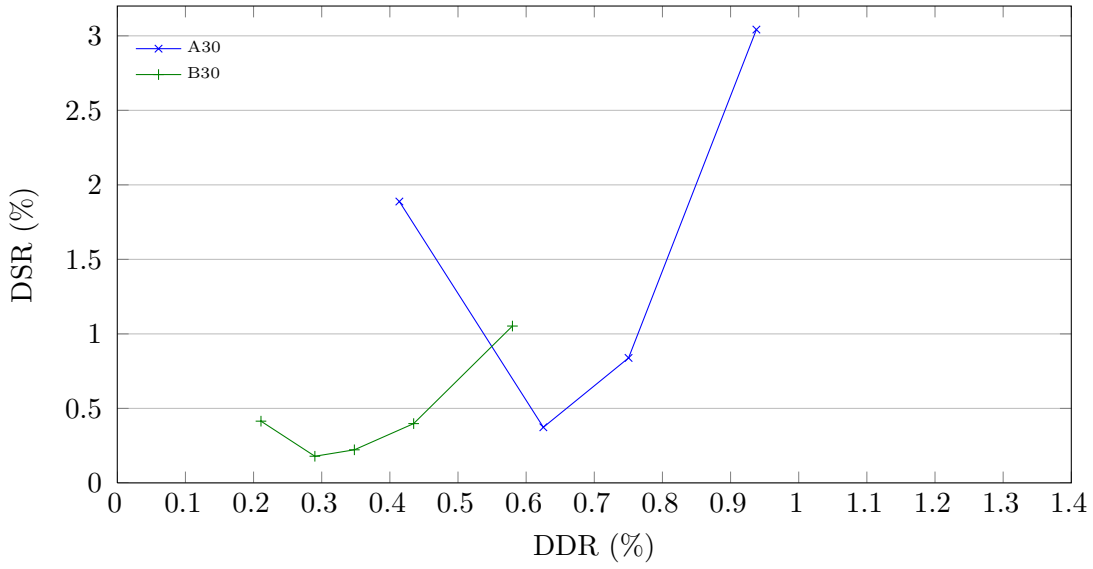

FIGURE 5.5: Combined diverted sediment results of structures A and B at a 30 ^{0} intake angle

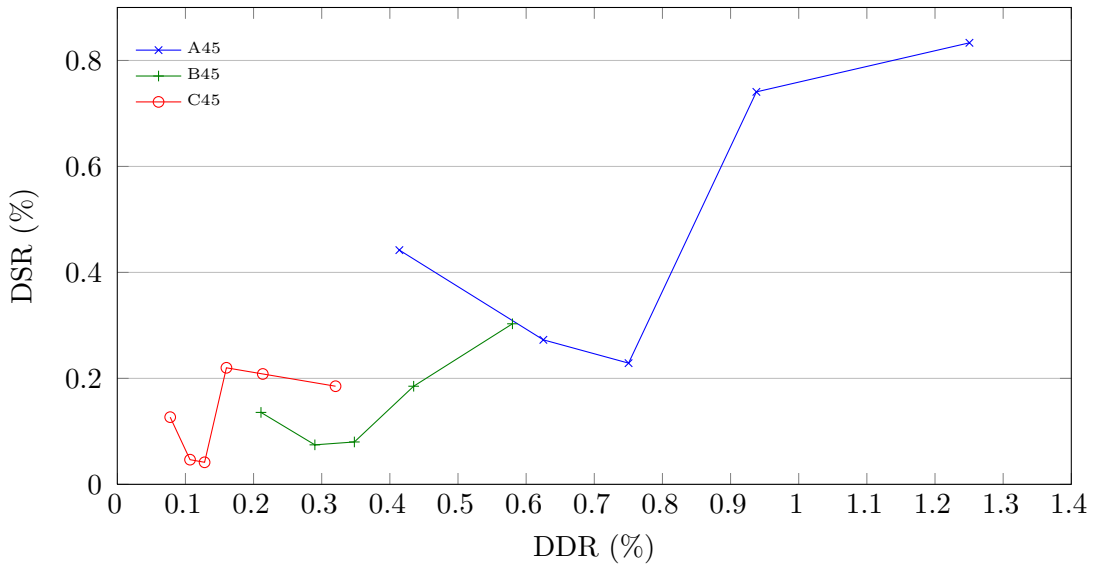

FIGURE 5.6: Combined diverted sediment results of structures A, B and C at a 45 ^{0} intake angle

Figure 5.8 shows lines through the optimum operating points (minimum DSR) of each structure, per intake angle. It is clear from this representation that the 30^0 intake angle is the least effective in minimising the DSR, whilst the 60^0 intake angle is the most effective. The irregularity seen at structure C with a 60^0 intake angle is attributed to local sediment entrained through the lower (compared to structure A and B) intake opening.

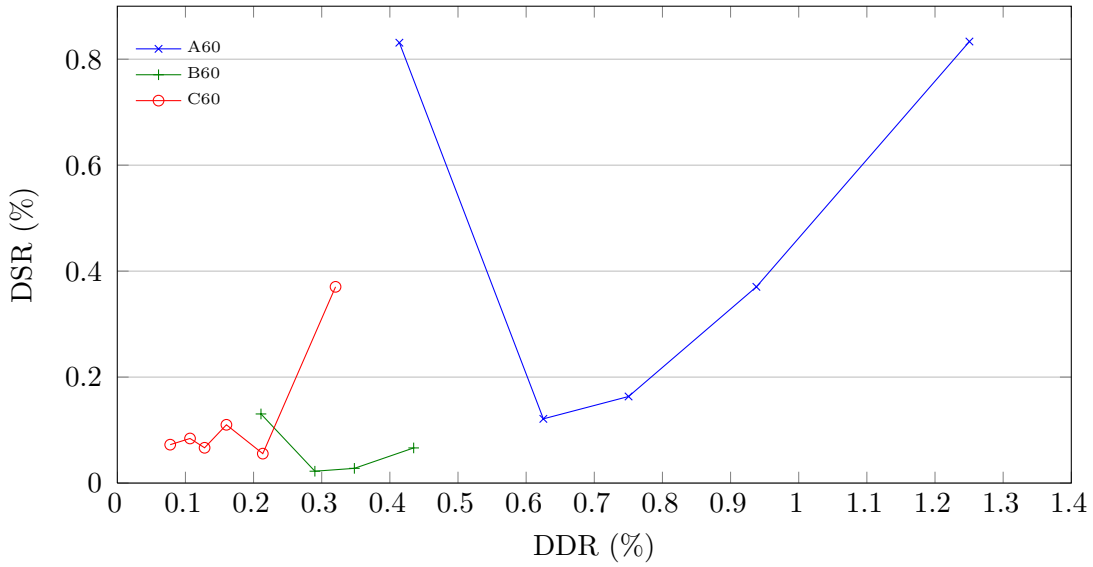

FIGURE 5.7: Combined diverted sediment results of structures A, B and C at a 60 ^{0} intake angle

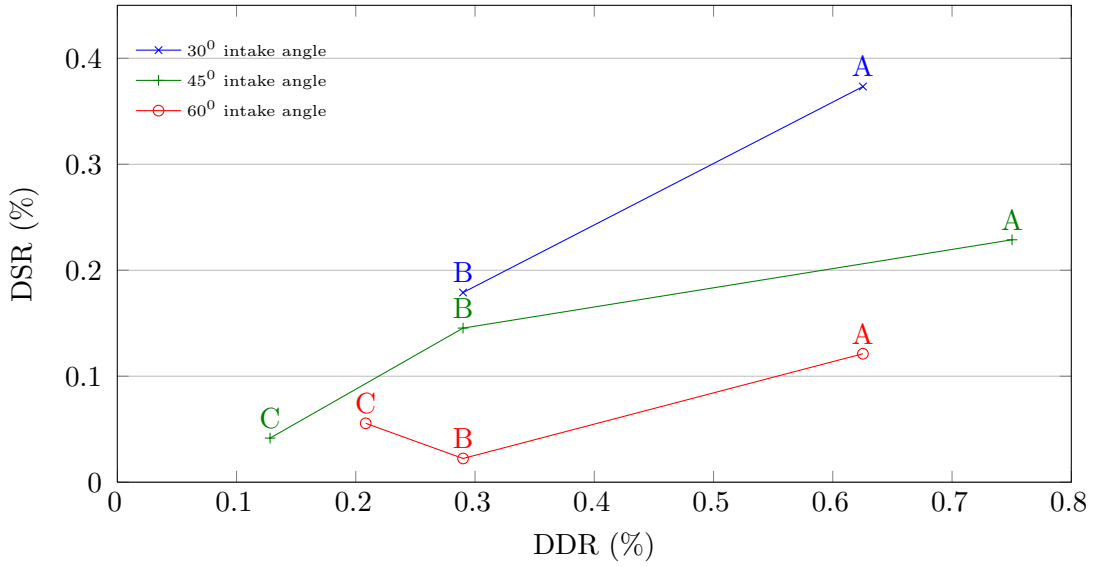

FIGURE 5.8: Lines through minimum operating points of each structure, per intake angle

It is important to note that the tests were evaluated with a initial bed level that consisted of a constant level, as one would expect a river without a weir would have. A weir affects the upstream profile of the river, by creating a pool with slower velocities. The sediment transport capacity decreases and as a result sediment deposits against the weir. This will continue until the sediment reaches the top of the weir, after which a new equilibrium slope of the river will establish.

During the diverted sediment tests, the bed was thus placed as a scenario before weir sedimentation took place. The equilibrium state of sedimentation should occur if the model flow (Q_{riv}) is allowed to flow for a long enough time. As described in Chapter 4.6, the tests were done consecutively, starting with the lowest flow. Thus, it is certain that during the larger flows tested the equilibrium state is reached, but at which point this occurred for each structure is uncertain.

The only test where local sediment seemed to have an influence on the results is that of structure C, which has the lowest weir and would reach equilibrium state at the lowest Q_{riv}. The bulk of the tests only diverted already entrained sediment.

5.3 Diverted Sediment (DS) Tests - Varying Inlet Height

The intake height was evaluated at some of the configurations namely, DSA30, DSA45, DSA60, DSB45 and DSC45, at which the diverted sediment tests were repeated for inlets 2 and 3 as well as inlet 1.

The results are expressed as graphs plotting the diverted sediment (G_d) against the channel flow (Q_{riv}), both in model scale. Inlet 1 is the lowest intake opening designed as described in Chapter 4.4.3, with the top of inlet 1 at MOL. The top of inlet 2 is (0.3 m + z) above MOL and the top of inlet 3 is (0.6 m + 2z) above MOL. The result of a specific flow is plotted if the flow yielded a $G_d > 0$, for any of the three inlets.

Figure 5.9 shows the results of test series **DSA30**. With Q_{riv} = 192 l/s inlet 1 diverted no sediment, whilst inlet 2 and 3 resulted in G_d values equal to 0.058 and 0.037 g/s, respectively. The data showed inlet 1 diverted more sediment than inlet 2 for the complete range of flows. The diverted sediment of inlet 3 shows unexpected results, with the G_d larger than that of inlet 1 and/or 2 at $Q_{riv} \geq$ 384 l/s.

The average G_d diverted through inlet 1, 2 and 3 for the range of flows tested are 0.63, 0.22 and 0.34 g/s.

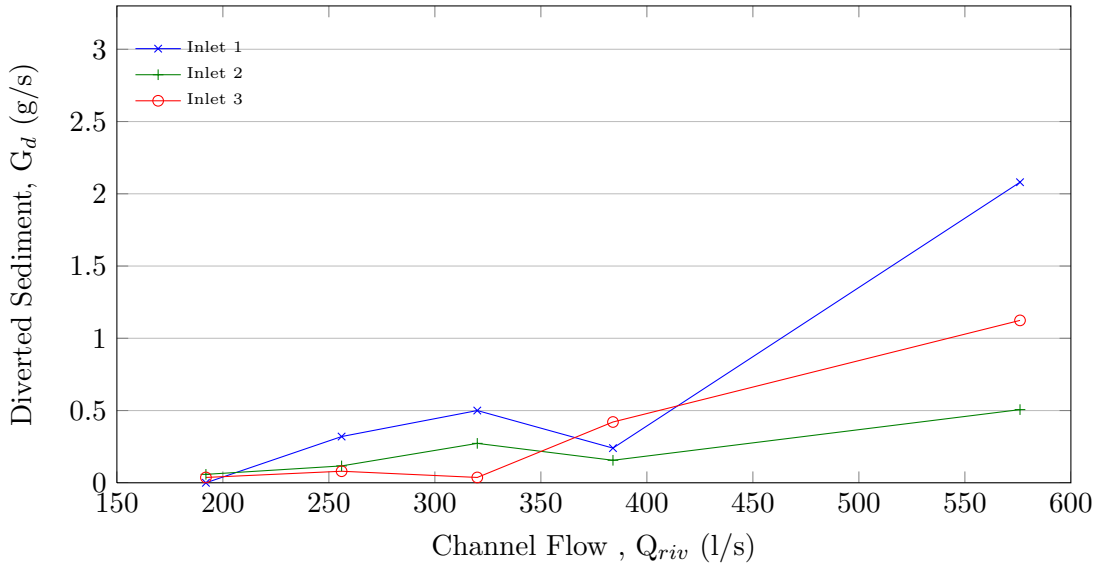

FIGURE 5.9: Test DSA30: Diverted sediment tests of structure A at a 30^0 intake angle, at varying inlet heights

The results of test series **DSA45** at all three inlets are shown in Figure 5.10. The results show reasonable trends. Inlet 3 diverted the least sediment for the whole range of flows tested. With Q_{riv} = 192-384 l/s, similar G_d values were observed for inlet 1 and 2. The result of Q_{riv} = 256 l/s yielded a possible outlier, where inlet 2 diverted drastically more sediment than inlet 1. With Q_{riv} = 576 l/s, the results are as expected, where inlet 1 diverted the most sediment and inlet 2 and 3 incrementally less.

The average G_d diverted through inlet 1, 2 and 3 for the range of flows tested are 0.18, 0.17 and 0.08 g/s.

The results of test series **DSA60** at all three inlets are shown in Figure 5.11. The data of inlet 1, 2 and 3 varies very little. Inlet 1 diverted more sediment than inlet 2 and 3 for all the flows tested, excluding Q_{riv} = 192 and 576 l/s. The data of inlet 2 and 3 are closely related with minor fluctuations in trend. The result of inlet 3 with Q_{riv} = 576 l/s varies from the trend observed during the rest of the flows tested. Note that the DSA60 test series yielded diverted sediment at inlet heights 1 and 2 with Q_{riv} = 128 l/s, at which no sediment transport in the channel was measured ($G_{riv} = 0$). This means local sediment around the intake was abstracted.

The maximum flow Q_{riv} = 576 l/s could not be tested for inlet 2 due to water supply difficulties in the laboratory, but a maximum of 528 l/s was achieved. The data of the maximum flow tested is excluded in the averages for all three inlets and can thus not be compared to the averages of the other configurations.

The only configuration of structure B used to test the effect of the inlet heights is **DSB45**, of

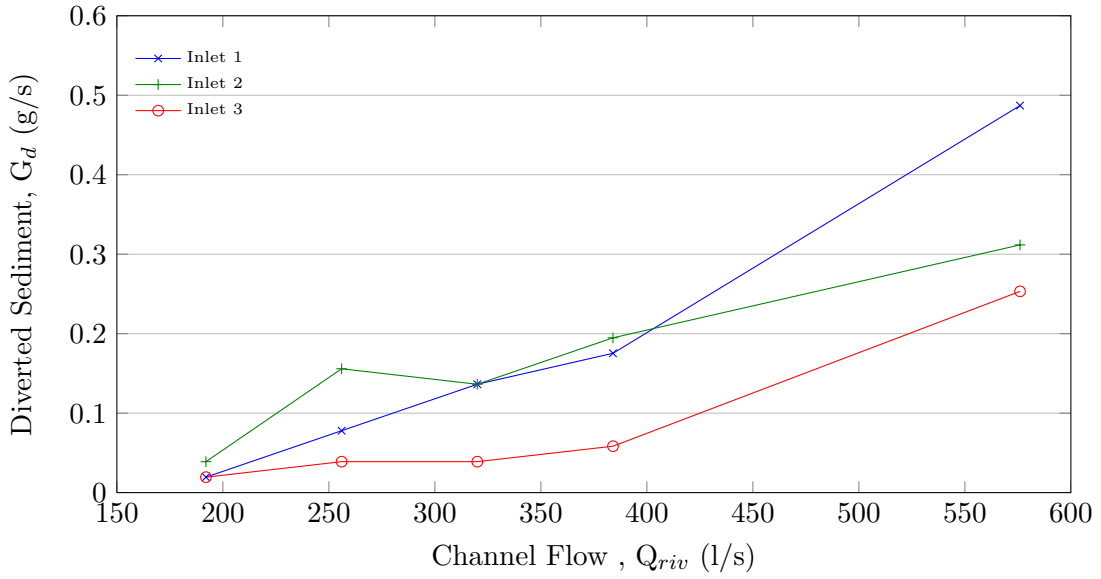

FIGURE 5.10: Test DSA45: Diverted sediment tests of structure A at a 45^0 intake angle, at varying inlet heights

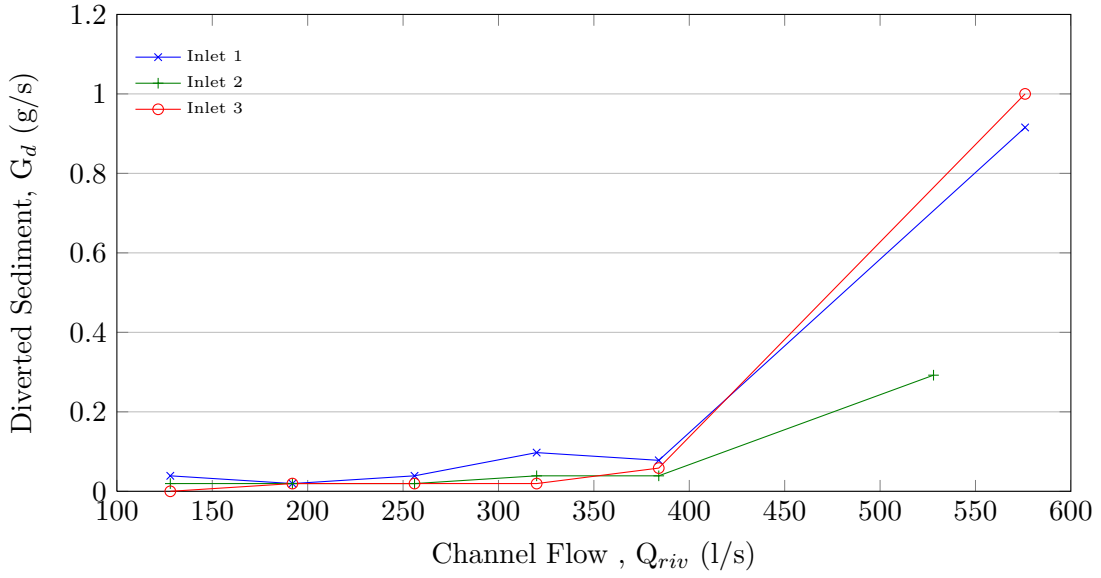

FIGURE 5.11: Test DSA60: Diverted sediment tests of structure A at a 60^0 intake angle, at varying inlet heights

which the results are shown in Figure 5.12. The results show a reasonable distribution of data, where inlet 1, 2 and 3 yielded the highest to lowest G_d for all the flows tested, excluding Q_{riv} = 192 l/s. With Q_{riv} = 192 l/s inlet 2 and 3 diverted sediment and inlet 1 did not, implicating the result of inlet 1 at this flow as incorrect.

The average G_d diverted through inlet 1, 2 and 3 for the range of flows tested are 0.24, 0.11 and 0.05 g/s.

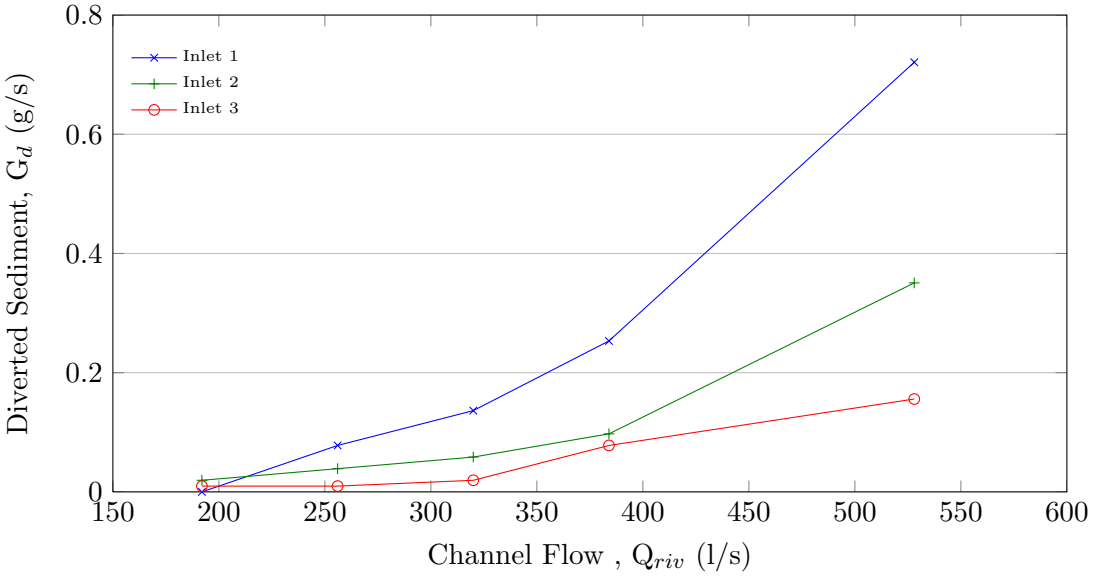

FIGURE 5.12: Test DSB45: Diverted sediment tests of structure B at a 45^0 intake angle, at varying inlet heights

Structure C was also only tested at a 45 ^{0} intake angle. The results in Figure 5.13 do not present a clear distinction in diverted sediment between inlet 1, 2 and 3, as expected, except at the maximum flow Q_{riv} = 528 l/s. During the test on inlet 1, it was clearly seen that local sediment was abstracted during Q_{riv} = 192 and 256 l/s, explaining the variation in the results.

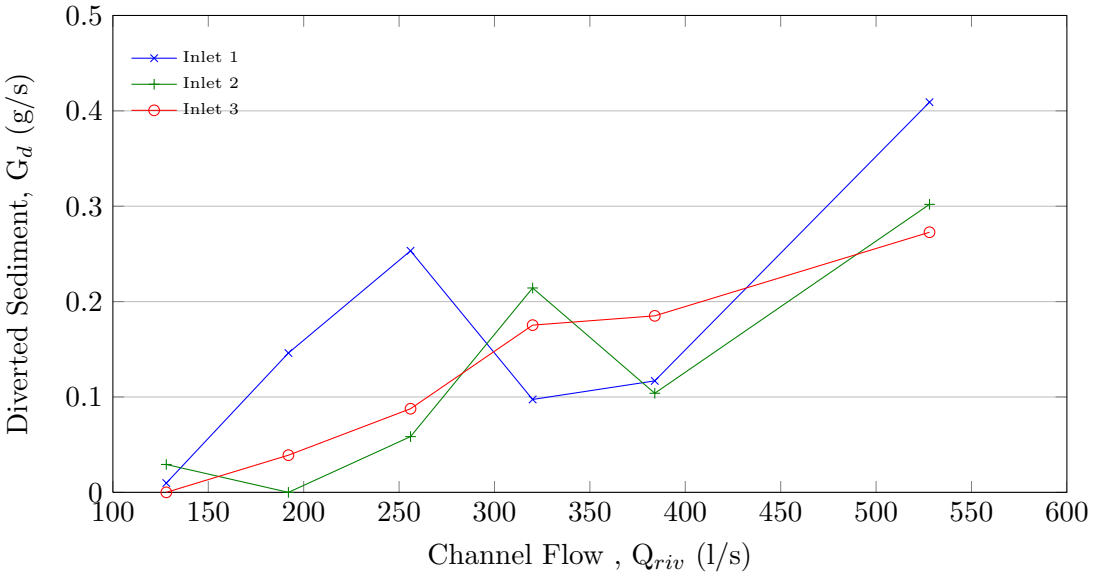

FIGURE 5.13: Test DSC45: Diverted sediment tests of structure C at a 45^0 intake angle, at varying inlet heights

5.3.1 Analysis on DS Tests and the effect of the inlet height

The tests were conducted to determine the extent of the improvement in sediment rejection of consecutive higher inlets. Tests series DSA30, DSA45, DSA60, DSB45 and DSC45 showed the expected results, with inlet 1, 2 and 3 abstracting decreasing amounts of sediment at most tests (i.e. Figure 5.12). Rearranging the data to plot G_d against the top-of-inlet level (measured from the datum in Figures 4.9 and 4.10) for each test series shows the difference in G_d over the range of river flow tested. The steepness of the decrease in G_d for a specific Q_{riv} indicates the extent of the improvement in sediment rejection. The improvement between inlets over the range of river flows tested can be expressed as a percentage improvement, calculated with equation 5.1.

$$\%Improvement = \frac{(G_{d,max\ inlet\ a} - G_{d,min\ inlet\ a}) - (G_{d,max\ inlet\ b} - G_{d,min\ inlet\ b})}{(G_{d,max\ inlet\ a} - G_{d,min\ inlet\ a})} \tag{5.1}$$

where:

Inlet a is either inlet 1 or 2
Inlet b is either inlet 2/3 or 3
$G_{d,max}$ is the maximum G_d at the specific inlet over the complete range of Q_{riv} tested.
$G_{d,min}$ is the minimum G_d at the specific inlet over the complete range of Q_{riv} tested.

Figures 5.14, 5.15 and 5.16 show the diverted sediment flow recorded at inlet 1, 2 and 3 for the range of flows tested at structures A, B and C all at a 45^0 intake angle. Table 5.2 summarises

the percentage improvement of sediment rejection between the inlets, calculated with equation 5.1. The % Improvement at structure B yields higher values compared to structures A and C, which can be attributed to the much higher G_d observed with Q_{riv} = 576 l/s. In general, the most drastic % Improvement is seen between inlets 1-2 and inlets 1-3. This indicates that it might be feasible to only have two consecutive inlets, with either a 0.3 or 0.6 m (full scale) gap between them. The decision should depend on the flood frequency, which will determine if an inlet (0.6 m + 2z) above MOL will be in operation frequently or not.

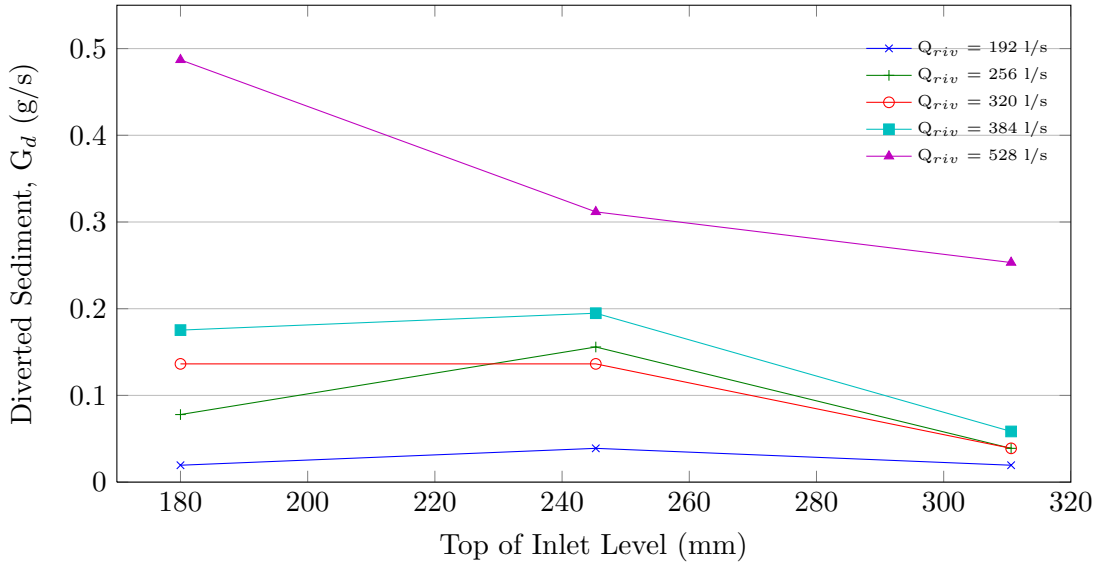

FIGURE 5.14: Test DSA45: Diverted sediment tests of structure A at a 45^0 intake angle, plotted against top-of-inlet level

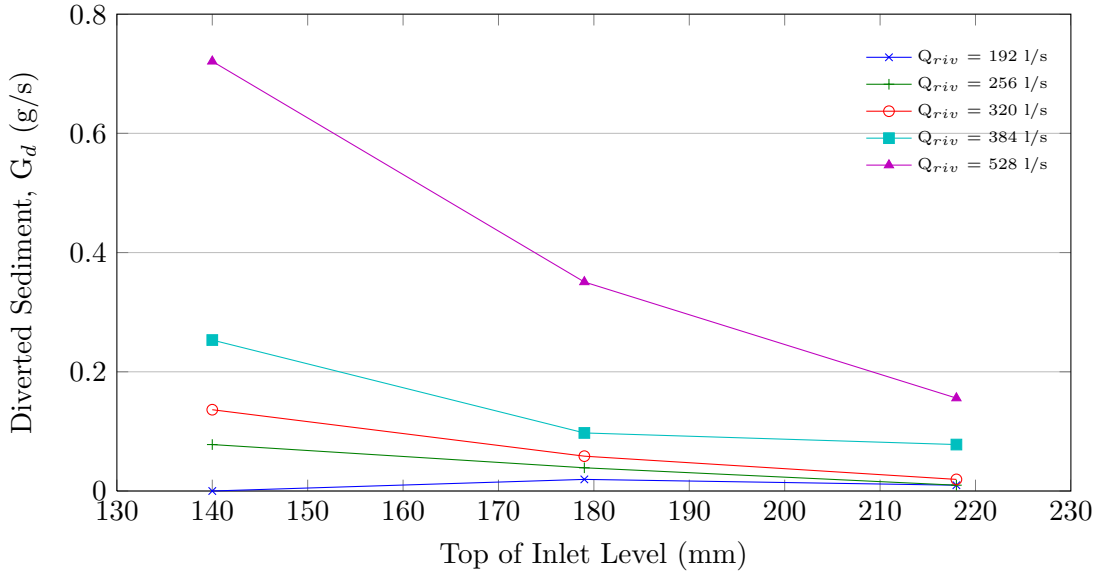

FIGURE 5.15: Test DSB45: Diverted sediment tests of structure B at a 45^0 intake angle, plotted against top-of-inlet level

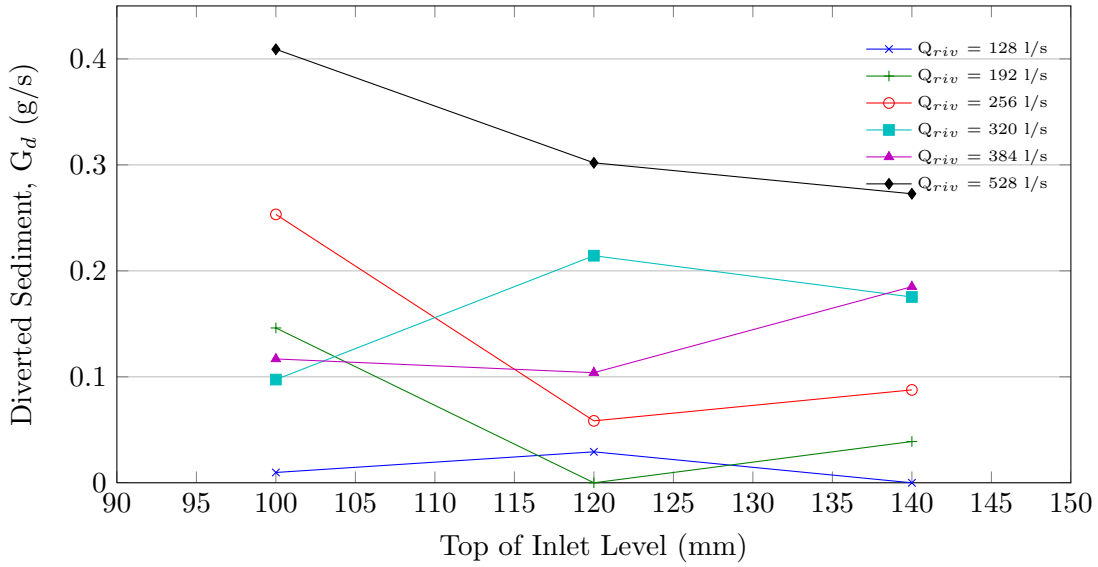

FIGURE 5.16: Test DSC45: Diverted sediment tests of structure C at a 45^0 intake angle, plotted against top-of-inlet level

TABLE 5.2: % Improvement observed between inlets at all three structures

	% Improvement over range of flows tested		
	Inlet 1 — 2	Inlet 2 — 3	Inlet 1 — 3
A45	36%	19%	48%
B45	54%	56%	80%
C45	32%	14%	41%
Average	41%	30%	56%

To evaluate the results of the tests on structures A, B and C as a whole, the effect of the varied diverted flow should be eliminated by converting the diverted sediment (Gd) to the concentration, C_d. C_d is measured in mg/l and calculated with equation 5.2. The C_d versus inlet level plot is shown in Figure 5.17. The results of all three structures at a 45^0 intake angle are used to compare. Note that the different weir heights yield increased sediment load in the channel (G_{riv}) for lower weirs. This explains the shift seen between the results of different structures at similar inlet heights.

Practically the results can be compared, realising that the structures were designed for a specific diverted flow and weir height. For each structure the river sediment transport would be characteristic. For example, the lowest intake tested can only be achieved at structure C due to the lower weir and decreased Q_d. If Q_d is increased, the intake opening size would have to increase to accommodate the allowable velocity through the inlet. Recalling that the top of the lowest intake opening of a structure must be at the minimum operating level or lower, which means the increased opening size would disagree with the guideline on the clearance between the intake opening and the graveltrap floor. Refer to Chapter 4.4, which discusses the design

process and specifically Table 4.2 summarises the guidelines on the flow velocity through the intake and the clearance below the intake opening.

$$C_d = \frac{G_d}{Q_d} \tag{5.2}$$

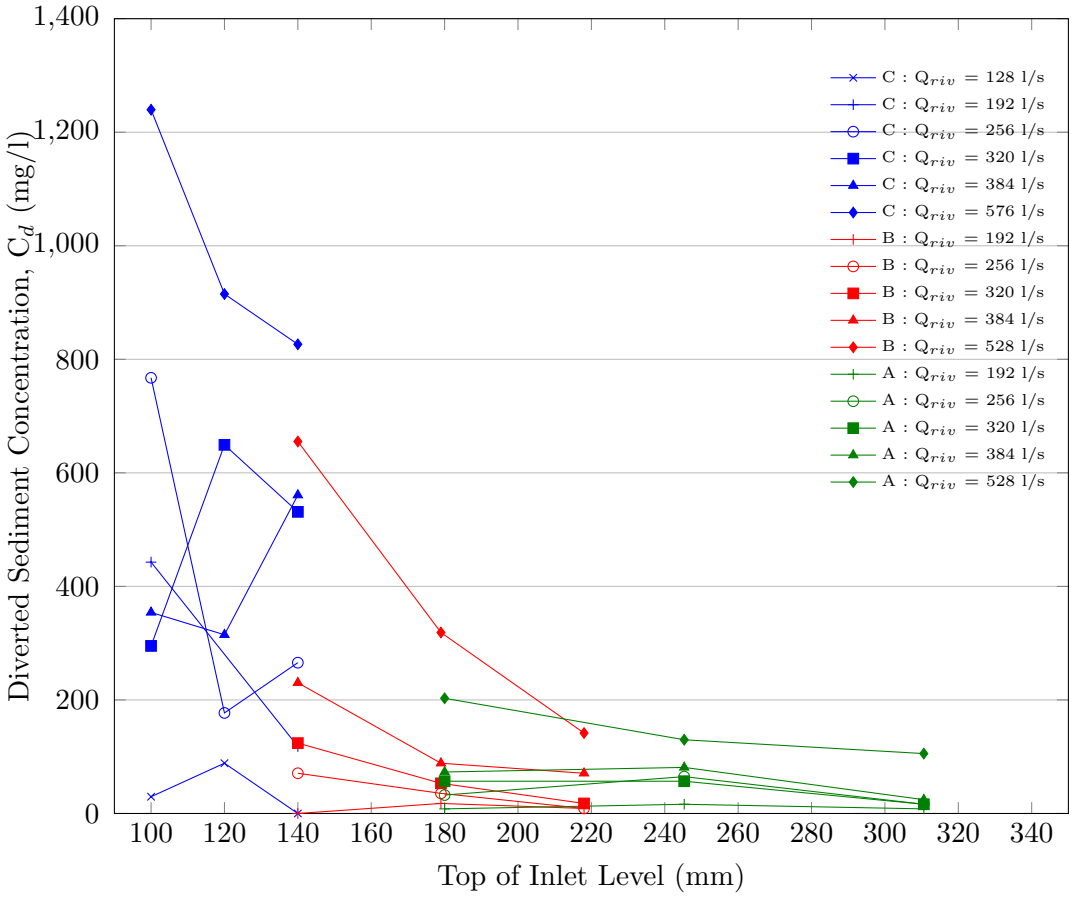

FIGURE 5.17: Diverted sediment concentration of structure A, B and C at a 45^0 intake angle, plotted against top-of-inlet level

The results in Figure 5.17 shows that the concentration of the diverted flow decreases rapidly at the lower inlets between 180 to 100 mm above the datum and mildly for inlets 180 to 310.6 mm above the datum. It is important to note that the inlets lower than 140 mm (of structure C) did not yield improvement between inlets, except at the maximum river flow.

The decision to design consecutive higher inlets at diversion structures with lower weirs (i.e. 2.5 m) is thus very dependent on the flood frequency of the river. It would be feasible to operate only two inlets, one top-of-inlet level at MOL and the second 1 m (at prototype scale) above MOL, if the water level of the river reaches the top of the second inlet frequently.

Inlet heights from 140 mm to 179 mm and from 179 to 218 mm showed reasonable improvement over the complete range of river flows tested. It could be feasible to design two consecutive higher inlets at a diversion structure with full scale weir height of 3.5 m. In other words, for a diversion works with a 3.5 m weir height, three inlets can be designed with the top-of-inlet levels at MOL, 1 m above MOL and 1.9 m above MOL.

The highest two inlet heights tested, from 245.3 mm to 310.6 mm above the datum, showed little improvement. If consecutive inlets are to be designed at a diversion structure with a prototype weir height of 4.5 m it would be better to have only two inlets, with the top of the second inlet at 3.3 m (at prototype scale) above MOL, if the flood frequency allows it.

5.4 Diverted Sediment Tests Accuracy

Five spot checks were done to determine the accuracy of the diverted sediment tests. Table 5.3 presents the checks, and shows the results to be acceptably accurate.

Table 5.3: Diverted Sediment Tests Accuracy

Test	Original test (g/60s)	Check (g/60s)
DSA602 (inlet 1)	2	2
DSA602 (inlet 3)	2	2
DSA604 (inlet 2)	4	2
DSA605 (inlet 2)	4	6
DSA606 (inlet 2)	28	24

5.5 Self Scour (SS) of Graveltrap Tests

The SS tests were conducted as described in Chapter 4.6.3. The results of test series SSA30, SSA45, SSA60, SSB30, SSB45, SSB60, SSA45 and SSA60 are presented in the form of graphs depicting the long section of the graveltrap with surveyed sediment levels. The graphs indicate the sediment level in the graveltrap, as measured at points along the length of the graveltrap. Six points were surveyed for structures A and B and only five points at structure C due to its shorter graveltrap length. The origin of the x-axis (as seen in Figure 5.18) is at the upstream end of the graveltrap and indicates the distance downstream along the graveltrap. The y-axis datum is at the initial river bed level (shown in Figure 5.18). The initial sediment level in the graveltrap is at the invert of the intake opening level, which is also shown on the long section. The survey was conducted at a range of river flows. The first test in a series (e.g. SSA301) is at the flow rate that initiates movement in the graveltrap.

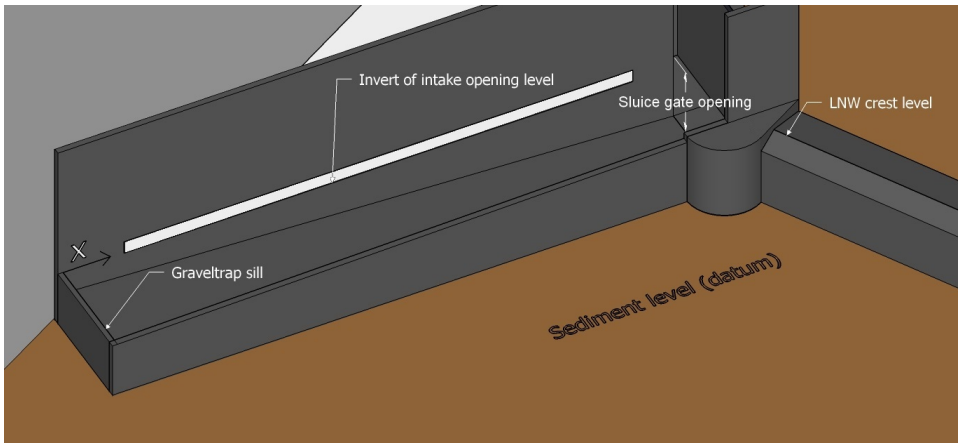

FIGURE 5.18: SS Tests: Graveltrap with position of x-origin of graveltrap survey

Comment is made on the smallest flow (so-called *clearance flow*) that scours enough sediment, such that the sediment level in the graveltrap is below the invert of the intake opening along the complete length of the opening. The remaining sediment level (profile) in the graveltrap, after the maximum flow tested, is observed and the average and minimum clearance between the intake opening and the sediment level is mentioned as points of discussion.

5.5.1 Tests on Structure A (SSA tests)

The results of **SSA30** (Figure 5.19) shows that sediment was displaced forward during the lowest flow (Q_{riv} = 128 l/s), causing the intake opening to be blocked from x = 500 - 1200 mm. No major change in sediment level occurred during Q_{riv} = 256 and 320 l/s. Q_{riv} = 384 l/s displaced even more sediment, causing extensive blockage at x = 900 - 1100 mm. Q_{riv} = 480 l/s caused enough displacement of sediment to clear the intake opening along the complete length of the graveltrap. The maximum flow tested (Q_{riv} = 576 l/s) increased the clearance between the intake opening and the sediment level to an average of 71 mm and a minimum clearance of 49 mm at x = 900 mm. Figure 5.20 shows the sediment remaining in the graveltrap after the completed test.

Figure 5.21 shows the results of test series **SSA45**. It is observed that the sediment was displaced forward during Q_{riv} = 128 and 192 l/s, blocking the intake opening. Q_{riv} = 384 l/s cleared the intake opening completely along the length of the graveltrap. The sediment level was further decreased by the increased flows. The maximum flow tested (Q_{riv} = 576 l/s) yielded an average clearance of 52 mm and a minimum clearance of 27 mm at x = 300 mm. Figure 5.22 shows the sediment remaining in the graveltrap after the completed test.

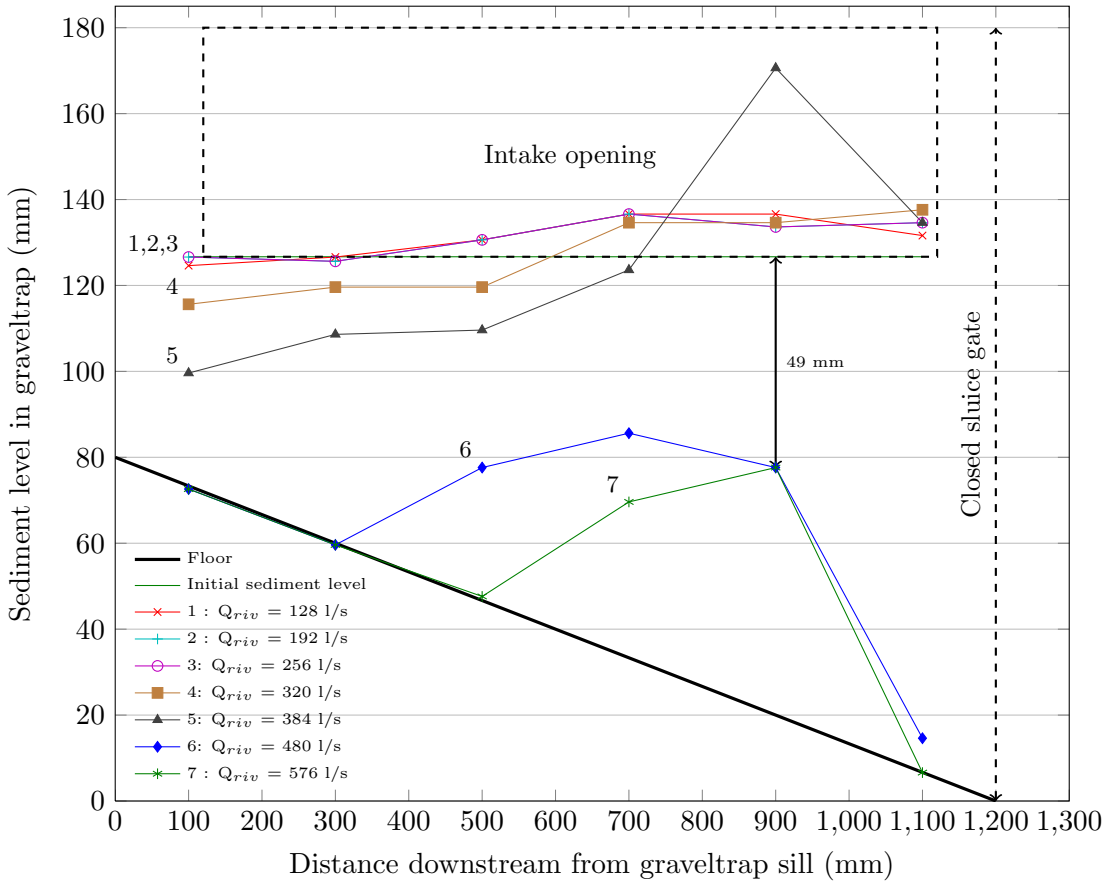

FIGURE 5.19: Long section of the graveltrap at the intake, showing the sediment levels during test SSA30

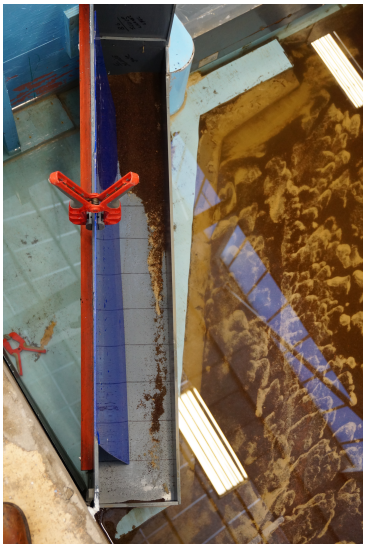

FIGURE 5.20: Sediment in the graveltrap post test SSA30

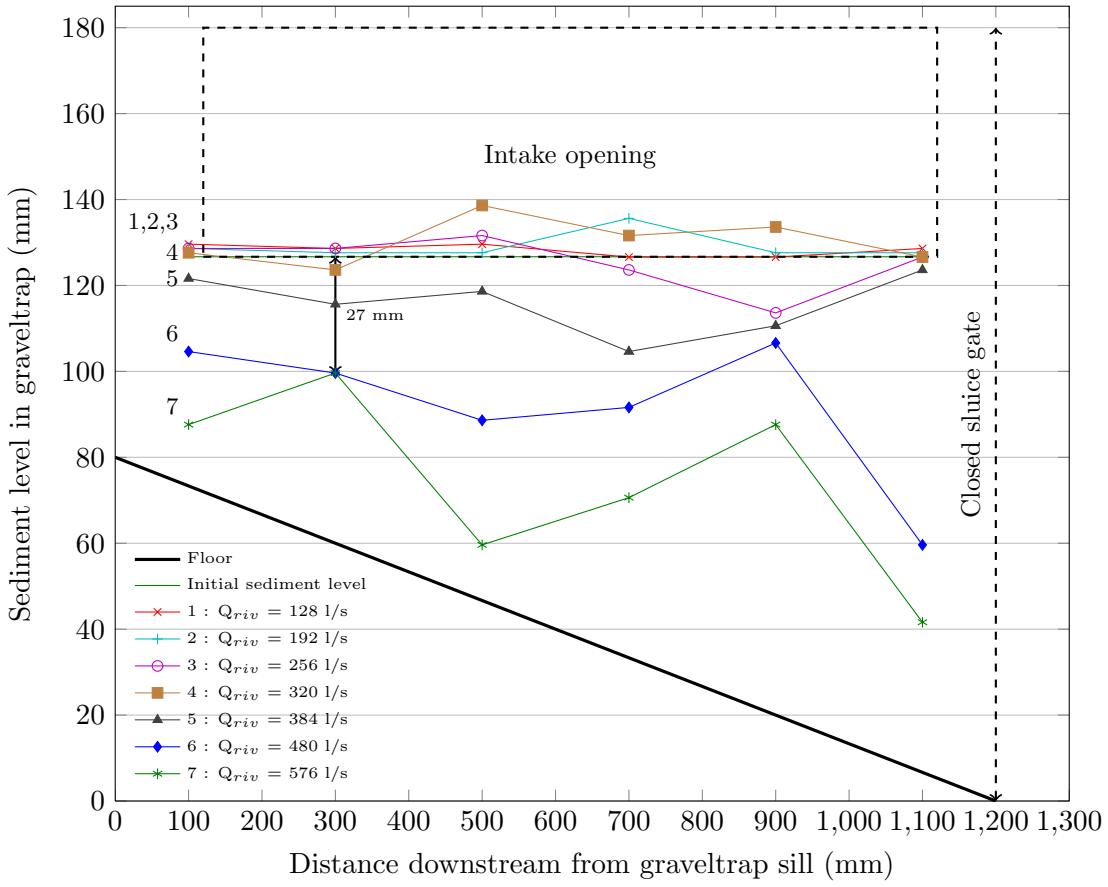

FIGURE 5.21: Long section of the graveltrap at the intake, showing the sediment levels during test SSA45

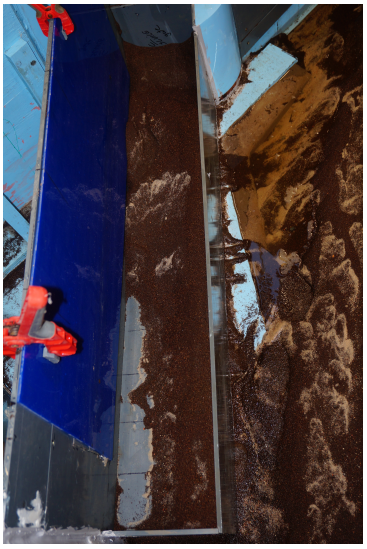

FIGURE 5.22: Sediment in the graveltrap post test SSA45

As seen in Figure 5.23 minor displacement took place during most of test **SSA60**. Q_{riv} flows of 128 to 480 l/s did not sufficiently flush the graveltrap, leaving sediment above and close to the intake opening invert. The maximum flow (Q_{riv} = 576 l/s) did flush enough sediment to increase the clearance between the sediment level and the intake opening to an average of 35 mm and a minimum clearance of 24 mm at x = 100 mm. Figure 5.24 shows the sediment remaining in the graveltrap after the completed test.

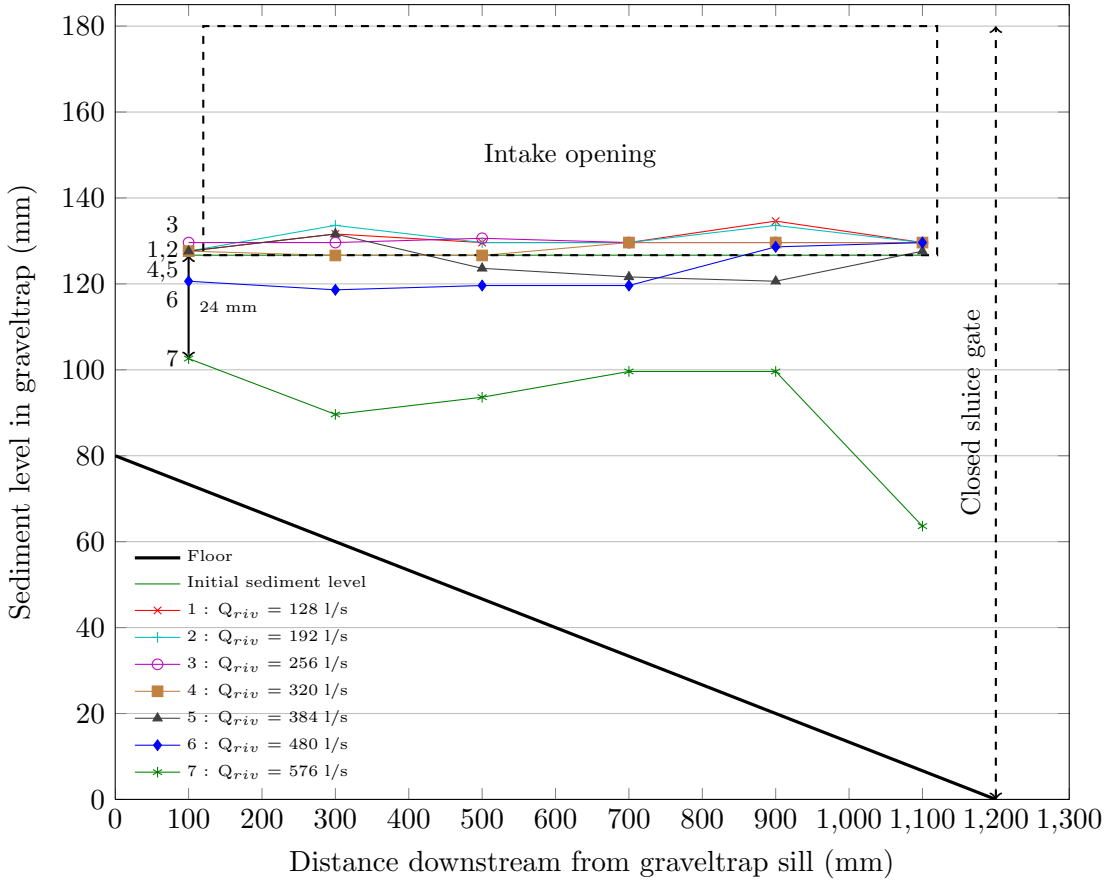

FIGURE 5.23: Long section of the graveltrap at the intake, showing the sediment levels during test SSA60

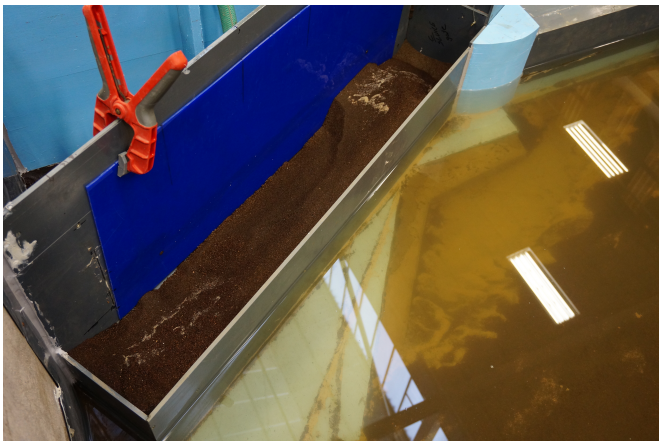

FIGURE 5.24: Sediment in the graveltrap post test SSA60

5.5.2 Tests on Structure B (SSB tests)

The results of test **SSB30** are shown in Figure 5.25. It is observed that the the first three flows tested, Q_{riv} = 128 to 256 l/s caused minor fluctuations of the sediment level, but the first flow that was able to clear the inlet is Q_{riv} = 320 l/s. The sediment level decreased with increasing flows and the maximum flow (Q_{riv} = 528 l/s) cleared the entire graveltrap except for a 4 mm residue (89 mm clearance) at x = 900 mm, as seen in Figure 5.26.

Figure 5.27 shows test **SSB45** had constant sediment displacement for flows larger than Q_{riv} = 192 l/s. Q_{riv} = 192 l/s merely displaced sediment downstream within the graveltrap, blocking the intake opening at x = 900 mm. Q_{riv} = 256 l/s is the smallest flow to sufficiently clear the intake opening and increasing flows increases the clearance further as expected. After the maximum flow (Q_{riv} = 528 l/s) was tested, the average clearance was 33 mm and the minimum clearance 17 mm at x = 900 mm. Figure 5.28 shows the sediment remaining in the graveltrap after the completed test.

The results of test **SSB60** (Figure 5.29) shows that flows of Q_{riv} = 256 l/s and smaller did not displace enough sediment to clear the intake opening. A larger amount of sediment was scoured on the upstream section (x = 700 to 1100 mm) by Q_{riv} = 320 l/s, but downstream the sediment level remained above the intake invert level. The smallest flow to completely clear the intake opening is Q_{riv} = 480 l/s. After the maximum flow of Q_{riv} = 528 l/s, the sediment level left an average clearance of 39 mm and minimum clearance of 26 mm at x = 100 mm. The remaining sediment is seen in Figure 5.30.

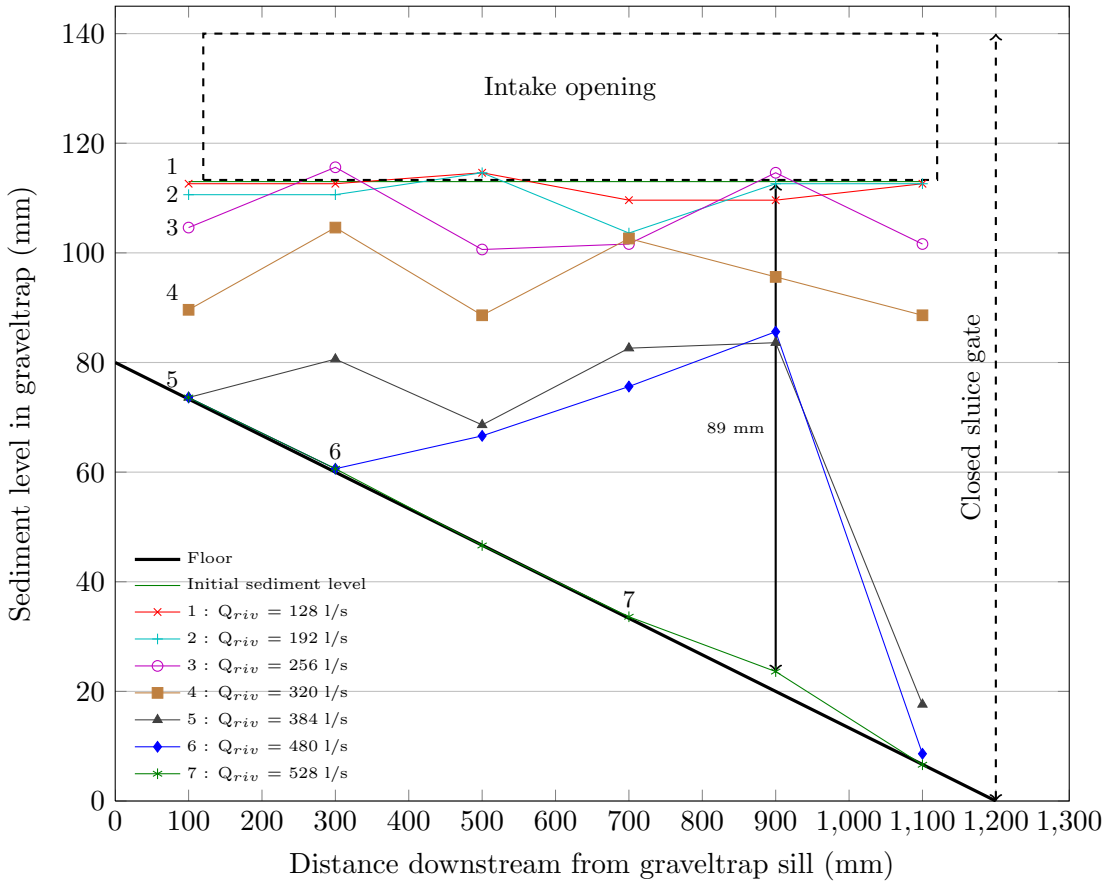

FIGURE 5.25: Long section of the graveltrap at the intake, showing the sediment levels during test SSB30

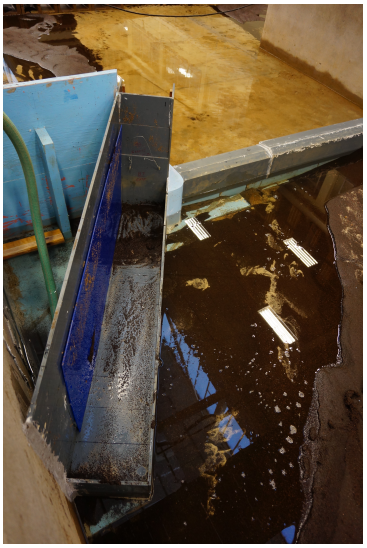

FIGURE 5.26: Sediment in the graveltrap post test SSB30

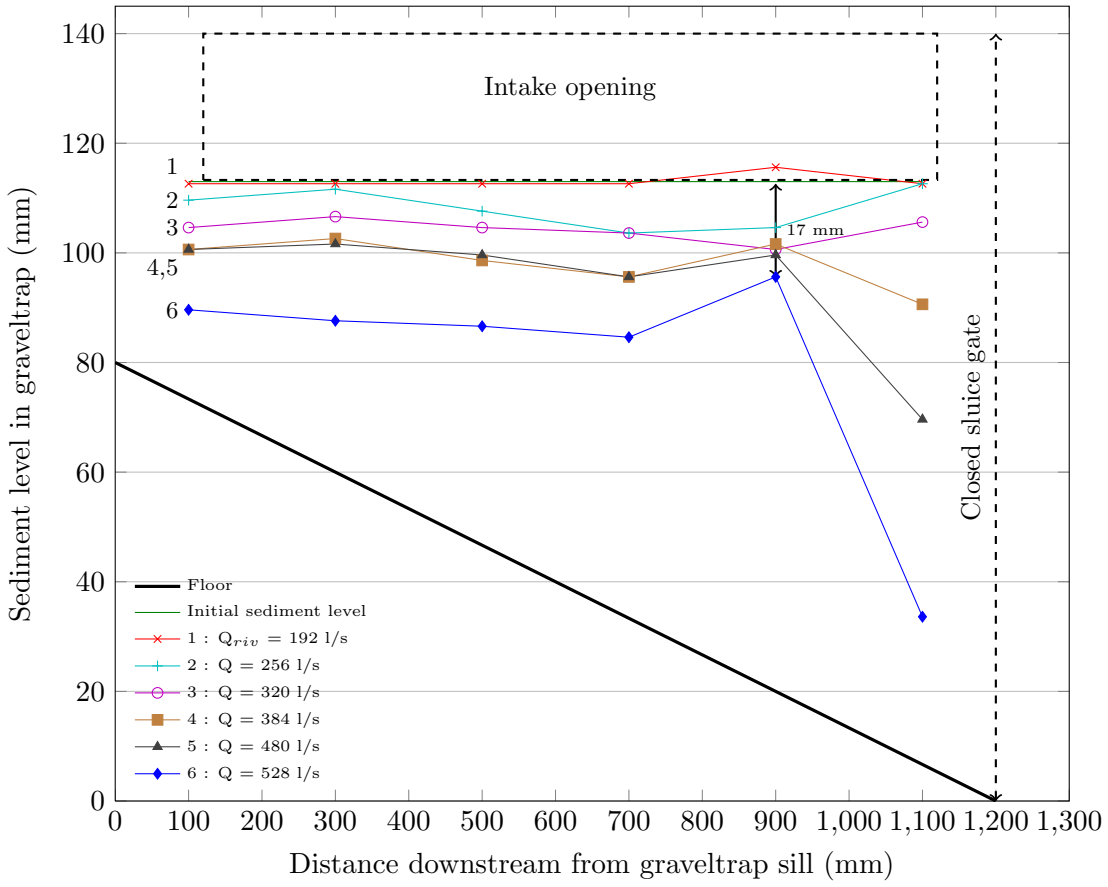

FIGURE 5.27: Long section of the graveltrap at the intake, showing the sediment levels during test SSB45

FIGURE 5.28: Sediment in the graveltrap post test SSB45

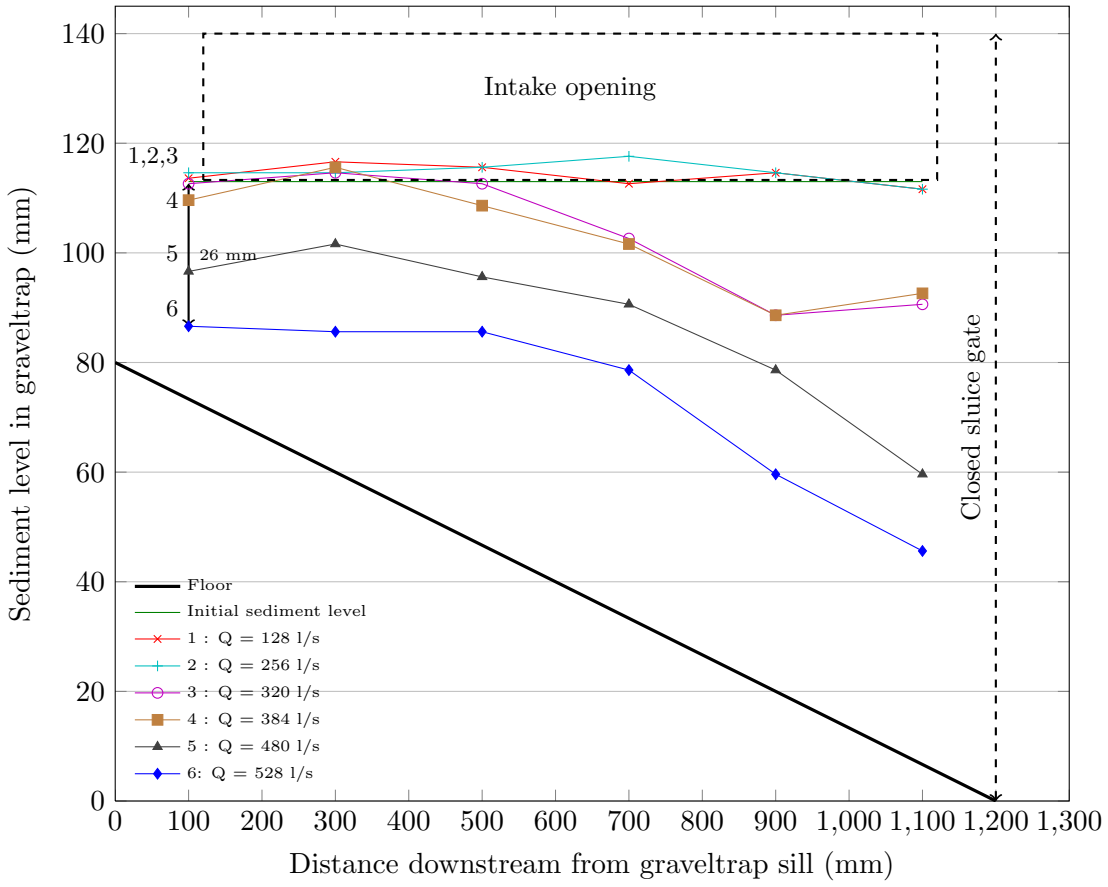

FIGURE 5.29: Long section of the graveltrap at the intake, showing the sediment levels during test SSB60

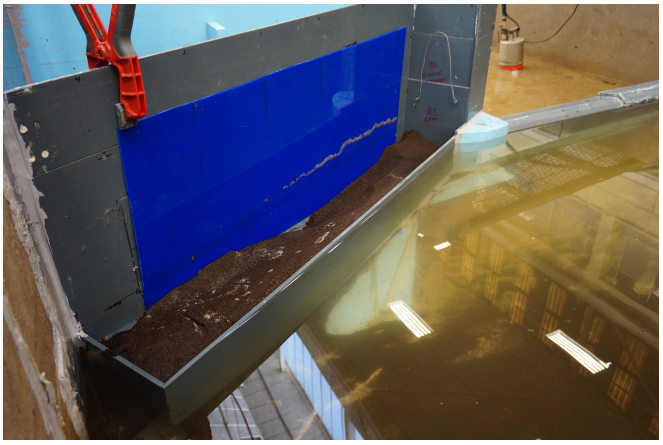

FIGURE 5.30: Sediment in the graveltrap post test SSB60

5.5.3 Tests on Structure C (SSC tests)

The results of test series **SSC45** are shown in Figure 5.31. With Q_{riv} = 128 l/s, enough sediment scoured away to clear the intake opening. However, the minimum clearance was 1 mm and the sequential flow blocked the intake again. The clearance flow is identified as Q_{riv} = 256 l/s. Increasing flows further increased the clearance and the maximum flow (Q_{riv} = 528 l/s) completely cleaned the graveltrap, leaving no significant residue.

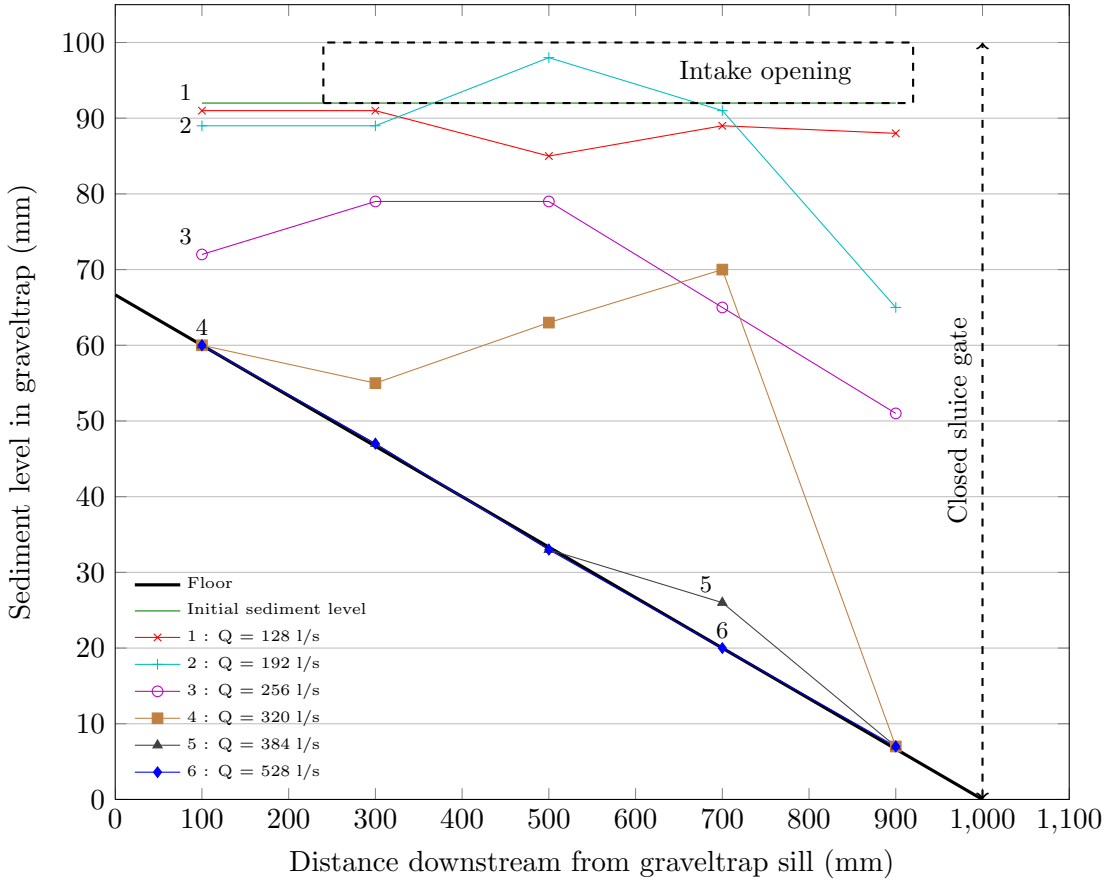

FIGURE 5.31: Long section of the graveltrap at the intake, showing the sediment levels during test SSC45

Test series **SSC60** yielded the same clearance flow as test SSC45 (Q_{riv} = 256 l/s), but the clearance is to a much lesser extent as seen in Figure 5.32. The maximum flow tested (Q_{riv} = 528 l/s) left a fair amount of sediment in the graveltrap, with an average clearance of only 46 mm and a minimum clearance of 30 mm at x = 100 mm. The remaining sediment is shown Figure 5.33.

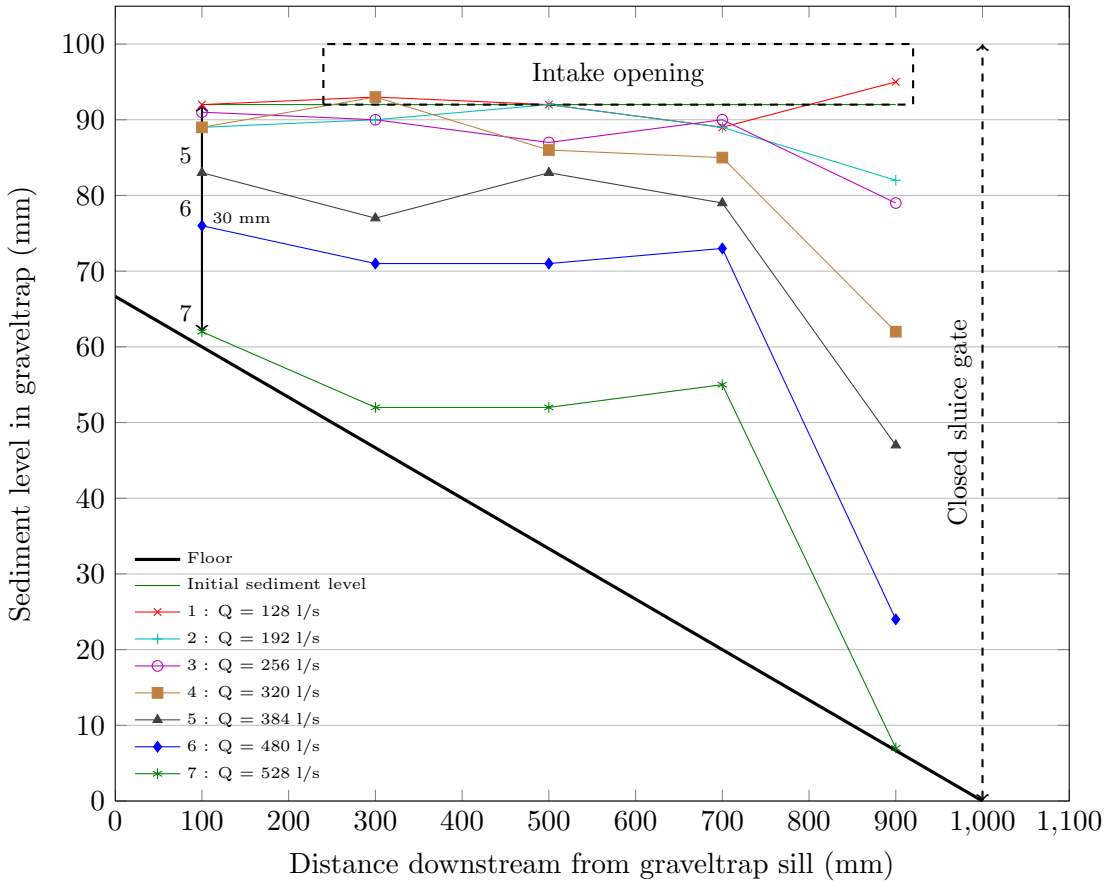

FIGURE 5.32: Long section of the graveltrap at the intake, showing the sediment levels during test SSC60

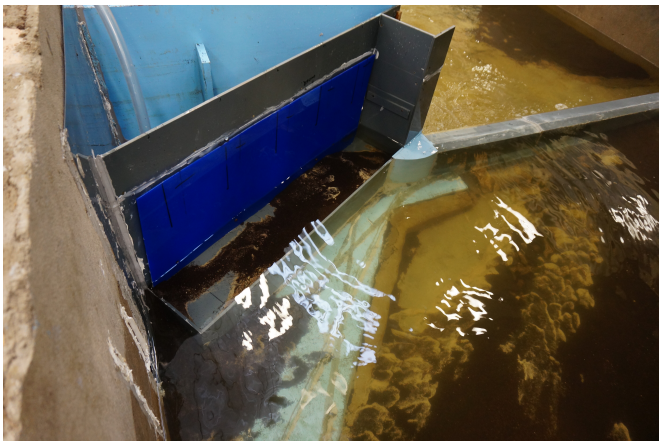

FIGURE 5.33: Sediment in the graveltrap post test SSC60

5.5.4 Analysis of SS Tests

The analysis aims to comment on the effect of the intake angle on the self scouring of the graveltrap of each structure separately. Further, correlations are drawn between the test series. The intake angle causes flow constriction and induces lateral flow as discussed in Chapter 3.3.2.2 and seen in Figure 3.5. The effect of weir height on the self scouring ability of the graveltrap is analysed and discussed.

The SS tests yielded clearance flows of varying size, summarised in Table 5.4. The point of minimum clearance (observed after the maximum river flow in a test series) is also included in Table 5.4.

If the clearance flow is considered an indication of the effectiveness of the induced spiral flow to scour the graveltrap, it is possible to identify the intake angle (per structure) that induces the most effective spiral flow.

For structure A and B the smallest clearance flow occurred at a 45^0 intake angle, whilst at structure C no distinction could be made between intake angles 45^0 and 60^0 in terms of clearance flow. However, the difference in the extent of scouring between test series SSC45 and SSC60 (Figures 5.31 and 5.32) is clear. The graveltrap was completely cleared after test series SSC45, but with remaining sediment post test series SSC60.

TABLE 5.4: Automatic flushing clearance flow and point of minimum scour of each configuration tested

Test	Clearance Flow (l/s)	Point of Min Scour (mm)
SSA30	480	900
SSA45	384	900
SSA60	576	300
SSB30	320	900
SSB45	256	900
SSB60	480	100
SSC45	256	clear graveltrap
SSC60	256	100

It is observed that for both test series SSA and SSB, the point of minimum clearance was similar for intake angles of 30^0 and 45^0, with x = 900 mm. The 60^0 intake angle on the other hand showed minimum points of clearance at x = 300 mm and x = 100 mm for tests SSA60 and SSB60. The lack of scouring at the upstream end of the graveltrap could mean that the point where the lateral flow is strongest moved downstream to where it is not as effective in initiating scouring.

Evaluation of the clearance flow and position of minimum clearance covered a sufficient range to establish that **the 45^0 intake angle is the optimum angle of all three structures**.

Comparing the results of tests on structures A and B it can be seen that the graveltrap of a structure with a lower weir will be flushed sufficiently by lower flows than for structures with higher weirs. Observing the 45^0 intake angle, the clearance flow was 384 and 256 l/s for structure A and B. The clearance flow of structure C at a 45^0 intake angle was 256 l/s.

5.6 Sediment Flushing (SF) of the Graveltrap Tests

The sediment flushing was tested at all 8 configurations, as described in Chapter 4.6.4. The efficiency is measured as a time recorded to flush the graveltrap clean, which is plotted against the specific Q_{riv}, as well as the downstream water depth. The river flows where flushing ceased to move sediment before the graveltrap is sufficiently clean are deemed as inefficient and not shown on the graphs. It was observed during all the tests that some residual sediment remain against the sill of the graveltrap at the maximum efficient flow, which was accepted if the sediment level is lower than the lowest intake opening and does not extend more than 300 mm downstream of the graveltrap sill. The results are first evaluated per structure and then compared between the structures.

5.6.1 Tests on Structure A (SFA tests)

The results of test series SFA30, SFA45 and SFA60 are shown on Figure 5.34. The graph shows an increase in flushing time as Q_{riv} increases. At all three intake angles the results were similar and no definite distinction can be made between the results.

The maximum flow that efficiently cleaned the graveltrap is Q_{riv} 128 l/s, with an average flushing time 109 s. The downstream water depth at Q_{riv} = 128 l/s is 124 mm. Note that the sluice gate of structure A could open to 180 mm above the river bed.

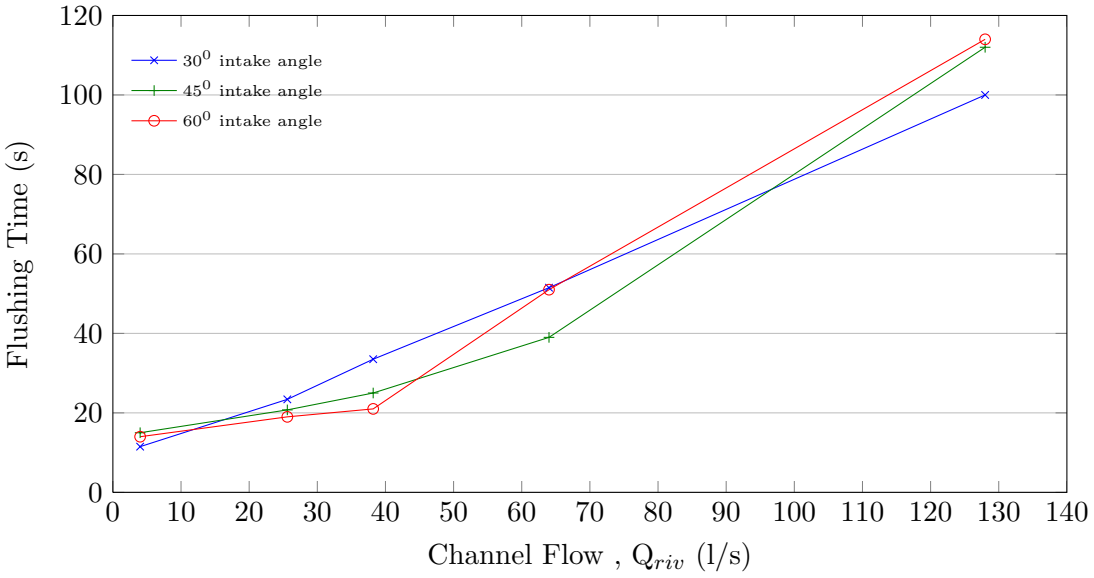

FIGURE 5.34: Test SFA: Sediment flushing test of structure A

5.6.2 Tests on Structure B (SFB tests)

The results of the test series SFB30, SFB45 and SFB60 (Figure 5.35) resulted in increasing flushing time, with increasing Q_{riv}, with no distinction between the results at different intake angles.

$Q_{riv} = 64$ l/s is the maximum flow that efficiently cleaned the graveltrap with an average flushing time of 167 s. The downstream water depth with $Q_{riv} = 64$ l/s is 81 mm and the sluice gate of structure B opens up to 140 mm.

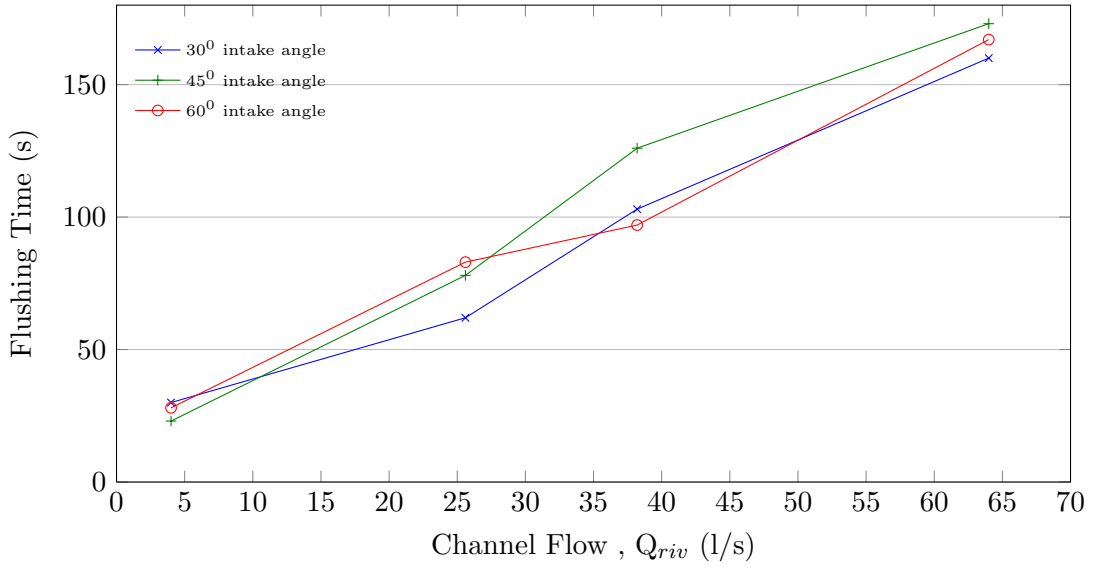

FIGURE 5.35: Test SFB: Sediment flushing test of structure B

5.6.3 Tests on Structure C (SFC tests)

The results of test series SFC45 and SFC60 (Figure 5.36) resulted in a much lower maximum Q_{riv} of 12.8 l/s, which still efficiently flushed the graveltrap. The downstream water depth with Q_{riv} = 12.8 l/s is 30 mm and the sluice gate of structure C opens up to 100 mm above the river bed. The average flushing time with Q_{riv} = 12.8 l/s is 158 seconds.

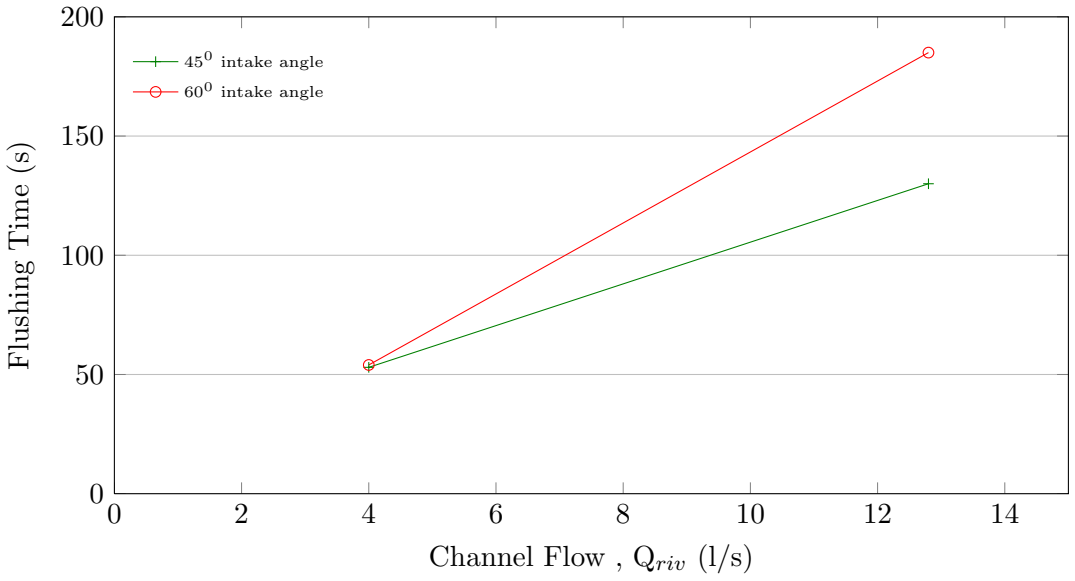

FIGURE 5.36: Test SFC: Sediment flushing test of structure C

5.6.4 Analysis of SF Tests

The average flushing times of structures A, B and C, is plotted against the Q_{riv} flows tested in Figure 5.37. It shows the decreasing flushing efficiency of A to C in terms of flushing time and maximum flow that yielded efficient flushing results.

According to Basson (2006), the velocities in the graveltrap should be 2 to 4 m/s. The velocities in the graveltrap are dependent on the flow that passes through the graveltrap, as well as the upstream and downstream water level. It is difficult to measure the velocity in the graveltrap during flushing, but the following observations concerning the submergence of the graveltrap wall as well as the sluice gate are made.

The upstream water level affects the flow over the submerged graveltrap wall, which should form a separated nappe to allow the impact of the flow to entrain the sediment in the graveltrap (Bouvard, 1992). To observe the effect of the upstream water level, the flow over the submerged graveltrap wall is evaluated with Q_{riv} = 25.6 l/s for all three structures at a 60 ^{0} intake angle as example. The water level above the structure (i.e. the gravletrap sill) should be the same for

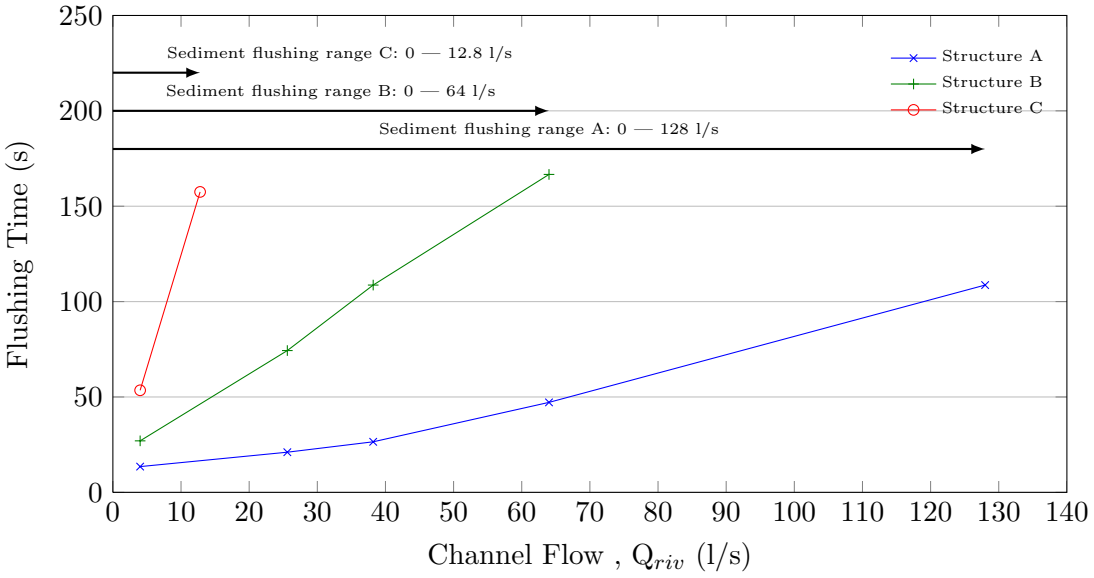

FIGURE 5.37: Average flushing times of structure A, B and C

structures A and B and slightly less for structure C, due to the shorter graveltrap length and resulting longer weir length.

The water levels recorded before the flushing gate was opened should confirm this, as seen in Table 5.5, with reference to Figures 5.38, 5.39 and 5.40, which show the flow over the submerged graveltrap wall for structures A ,B and C respectively.

TABLE 5.5: Upstream water level and graveltrap sill height with Q_{riv} = 25.6 l/s

Structure	Upstream Water level (mm)	Sill height (mm)	Water level above sill (mm)	Reference figure
A	219	156	63	5.38
B	182	116	66	5.39
C	140	80	60	5.40

Note that as the size of the structure decreases (from A to C) the graveltrap floor level remains constant and as a result the submerged weir height (P) decreases, which results in easier submergence of the weir. For a specific Q_{riv}, the extent of submergence should increase from structure A to C, as seen in Figures 5.38, 5.39 and 5.40.

As seen in Figure 5.37, at Q_{riv} = 25.6 l/s the graveltrap of structure A flushed quickly and efficiently, graveltrap B flushed more than three times slower than A but still efficiently. Graveltrap C did not flush with Q_{riv} = 25.6 l/s.

The difference in flushing efficiency cannot purely be due to the upstream water depth and the submergence of the graveltrap wall. The downstream water level affects the submergence of the flow through the sluice gate, as discussed in Chapter 4.4.5. The flow through the sluice gate is

FIGURE 5.38: Flow in graveltrap of structure A, with $Q_{riv} = 25.6$ l/s

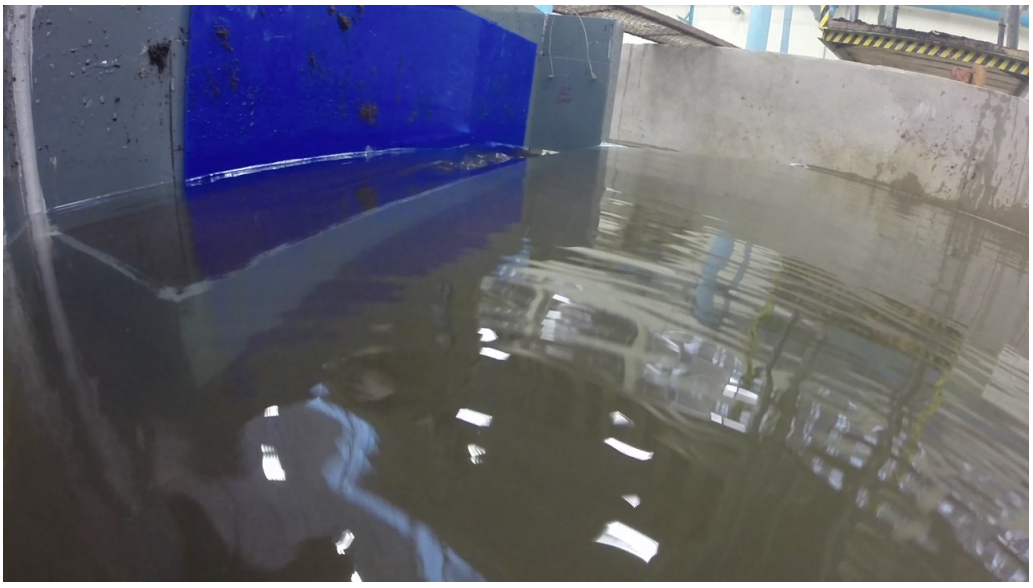

FIGURE 5.39: Flow in graveltrap of structure B, with $Q_{riv} = 25.6$ l/s

submerged if the actual downstream depth (y_3) exceeds the depth (y'_3) necessary for a hydraulic jump to form.

The flow rate passing through the sluice gate is unknown and it is thus not possible to determine y'_3. It is rather attempted to comment on y_3/y_2 and y_3/y_G terms. The calculations follow the annotation of Figure 4.14, with y_G the sluice gate opening size and y_2 as the depth below the sluice gate. The value of $C_c = 0.61$ for a vertical sluice gate as seen in Chadwick *et al.* (2004), is assumed. Bare in mind that y_G is equal to the low-notch weir height (H_{lnw}).

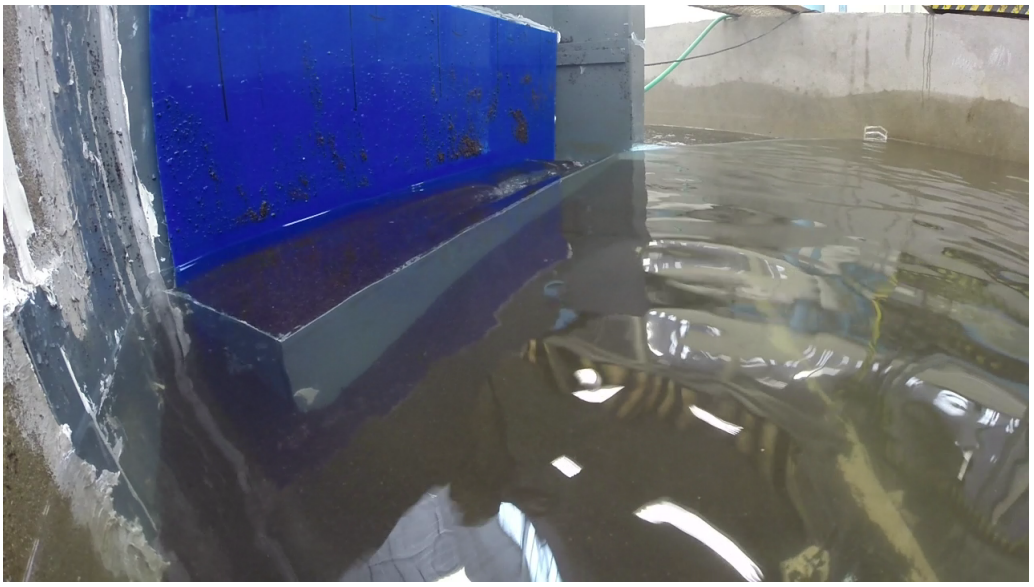

FIGURE 5.40: Flow in graveltrap of structure C, with Q_{riv} = 25.6 l/s

The values of y_3/y_2 for each structure at the flushing and non-flushing flows are shown in Table 5.6.

TABLE 5.6: Submergence of sluice gate calculation

Structure	Q_{riv} (l/s)	y_3 (mm)	y_G (mm)	$y_2 = C_c y_G$ (mm)	$\mathbf{y_3/y_G}$	$\mathbf{y_3/y_2}$
Maxiumum efficient flushing flow per structure						
A	128	124	180	109.8	**0.69**	**1.13**
B	64	81	140	85.4	**0.58**	**0.95**
C	12.8	30	100	61	**0.31**	**0.50**
Minimum non-flushing flow per structure						
A	192	160	180	109.8	**0.89**	**1.46**
B	128	124	140	85.4	**0.88**	**1.45**
C	25.6	46	100	61	**0.46**	**0.75**

It is observed that for the maximum efficient flushing flow of both structures A and B, y_3/y_2 is close to 1. Structure C showed a y_3/y_2 of 0.5 at its maximum efficient flushing flow.

During the minimum non-flushing flow of both structures A and B, y_3/y_2 exceeds 1. At structure C the ratio is less, with $y_3/y_2 = 0.75$.

It is deduced from the results that for structures A and B (with full-scale weir heights of 3.5 and 4.5 m) that it would be a good operational guideline to flush the graveltrap during flows resulting in $y_3/y_2 < 1$.

It is suspected that at structure C (with a full-scale weir height of 2.5m) the graveltrap efficiency is effected negatively by the flow over the graveltrap wall before the $y_3/y_2 < 1$ guideline comes

into effect.

Figure 5.41 gives an indication under which conditions it is safe to apply sediment flushing with water level draw down. The conditions are river flow, downstream depth and structure size, in terms of sluice gate opening size (and thus low-notch weir height).

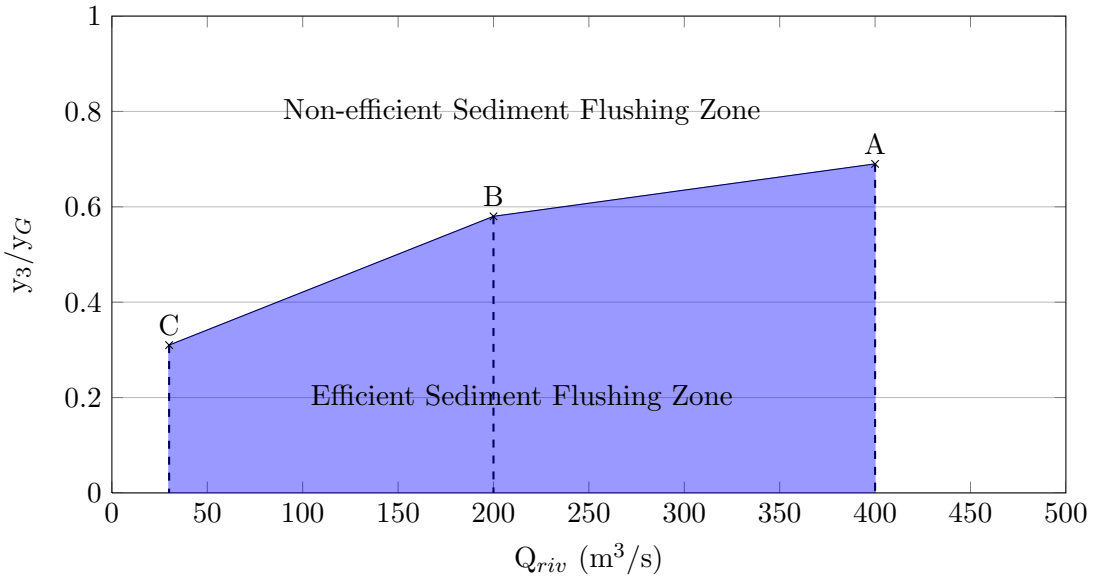

FIGURE 5.41: y_3/y_G VS prototype Q_{riv}, showing efficient sediment flushing zone

5.7 Relating the Results to Prototype Scale

The results were presented on model scale, but practically the results should be related to full scale parameters, especially the river flow (Q_{riv}) and the downstream depth. The complete range of all the tests conducted (DS, SS and SF) is Q_{riv} form 4 l/s to 576 l/s, as well as the related downstream depth is scaled to prototype in Table 5.7. Any of the results presented can be related to prototype scale via the Froude similarity equations 4.2, 4.3, 4.4 and 4.5.

The downstream depth and the upstream depth recorded (in model and prototype scale) at each configuration is presented in Table A.13 in Appendix A.

TABLE 5.7: Coversion of model dimensions to prototype dimensions, of flow rates and downstream water depths

Model scale		Prototype scale		
Q_{riv} (l/s)	Downstream depth (mm)	Q_{riv} (m^3/s)	Unit Discharge (m^3/m.s)	Downstream depth (m)
4	15	12.5	0.2	0.377
12.8	30	40	0.5	0.760
25.6	46	80	1.1	1.157
38.4	59	120	1.6	1.481
64	81	200	2.7	2.023
128	124	400	5.3	3.099
192	160	600	8.0	3.988
256	191	800	10.7	4.775
320	220	1000	13.3	5.496
384	247	1200	16.0	6.169
480	285	1500	20.0	7.114
528	302	1650	22.0	7.562
576	320	1800	24.0	8

5.8 Sediment Control Guidelines of the Graveltrap at the Intake

It was an objective of the study to determine for the scenario tested the range of river flows where sediment flushing with water level drawdown is applicable. It was also determined what size river flow would induce secondary currents which sufficiently scours sediment from the graveltrap, clearing the intake opening . The results showed that the sediment flushing through the sluice gate is not affected by the intake angle (as discussed in Chapter 5.6.4). The optimum intake angle, which promoted the most effective self scouring of the graveltrap was determined to be a 45^0 intake angle.

Figure 5.42 presents the prototype river flow range where sediment flushing (SF) could be applied, as well as the river flow at which self scouring (SS) initiates. The results are presented for the optimum design, at a 45^0 intake angle. The river flow is applicable to the prototype scenario, but can be applied to other rivers, by making use of the related unit discharge values in Table 5.7. Keep in mind that the downstream depth affects the sediment flushing, and that the ranges could shift if the river flow and downstream depth is not similar to this prototype scenario.

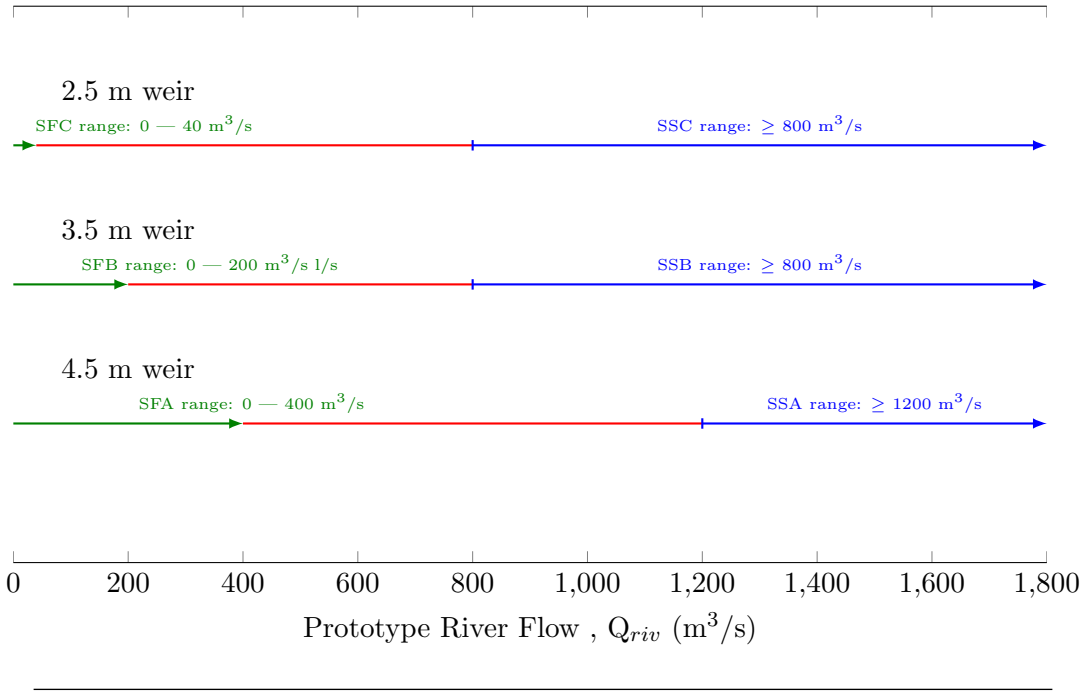

FIGURE 5.42: Sediment flushing and self scour prototype flow ranges of structure A, B and C at a 45^0 intake angle

Chapter 6

Summary and Conclusions

Rivers are the major, readily available source of fresh water. Abstraction from the river is however not without its issues. Firstly, the variability of flow can limit the amount of water that can be abstracted, especially abstraction without damming. Secondly, entrained sediment causes an array of issues at diversion works, but diversion works also impacts the ecology of the river by changing the upstream and downstream flow regime.

Sediment control at diversion works is crucial to prolong the life of the machinery, to ensure efficient operation of the diversion canals and to prevent issues at downstream facilities like water treatment works.

Vanoni (1975) mentions that the most practical principle method of sediment control is by diverting as little sediment as possible and removing deposited sediment with the most cost-effective way.

This study focussed on reducing the diverted sediment of low-weir diversion works, with a graveltrap at the intake. Conclusions based on the findings in this study are made in this chapter on the intake angle, intake opening height, the efficiency and range of sediment flushing at the graveltrap (with water level drawdown) and the self scouring ability of the graveltrap.

The study consisted of a physical model study conducted on a prototype river scenario. The prototype river width was 75 m and was tested for a river flow range of 12.5 m^3/s to 1800 m^3/s. Three diversion structures were designed (as discussed in Chapter 4.4) with respective prototype weir heights equal to 2.5 m, 3.5 m and 4.5 m above the datum (initial sediment level). The experimental procedure of the diverted sediment (DS) tests, the self scouring (SS) of the graveltrap tests and the sediment flushing (SF) tests are described in Chapter 4.6.

6.1 Intake Angle

The intake angle is defined in Figure 3.4. The intake angle should induce secondary currents at the intake which transports sediment away from the intake opening. Therefore, one of the aims of the study was to determine whether a certain intake angle is more effective in inducing secondary currents.

The intake angle was evaluated in terms of diverted sediment, as well as self-scouring, to hopefully find one optimum intake angle for both mechanisms.

In terms of diverted sediment, it was found at that the 60^0 intake angle yielded the lowest diverted sediment ratio (DSR) at structures A (4.5 m weir) and B (3.5 m weir). At structure C (2.5 m weir) no distinction could be made between the 45 ^{0} and 60^0 intake angles. The varying results obtained at structure C are attributed to varying local sediment which was entrained through the lower (compared to structures A and B) intake opening.

The self scour was evaluated in terms of a *clearance flow*, which is the smallest river flow which scoured enough sediment from the graveltrap to clear the intake opening along its complete length. It was found at each structure that the 45 ^{0} intake angle yielded the lowest clearance flow. It could be that the 45 ^{0} intake angle induce secondary currents which are better positioned to scour sediment (especially from the back of the graveltrap).

After each test series the point of minimum scour was evaluated and it was found that at a 60^0 intake angle sediment remains at the upstream end of the graveltrap. This could mean that the point where the secondary currents are at a maximum moved downstream in the graveltrap, to a point where it is less efficient in scouring sediment from the graveltrap. Table 5.4 summarises the clearance flow and point of minimum scour of each test series.

The intake angle had no significant effect on the sediment flushing through the sluice gate and the flushing times were averaged over the three intake angles tested.

The results of the diverted sediment test and the self scouring of the graveltrap resulted in different optimum intake angles (60^0 vs 45^0, respectively). Bouvard (1992) recommended an intake angle as small as 15^0 to 20 ^{0} for diversion works with a weir, but he did mention that larger angles would increase the strength of the secondary current. Bouvard (1992) advised caution on designing intake angles causing large flow constriction, as it may cause the main flow of the river to be directed away from the intake. In the river scenario tested, the 60^0 intake angle constricts more than 40% of the river. In light of the comments of Bouvard (1992) and noting that the 45^0 intake angle already reduced diverted sediment compared to the 30^0 intake angle, the 45^0 intake angle should be used to improve both diverted sediment and self souring.

6.2 The Effect of Diverted Discharge Ratio and the Optimum Operating Point

It was observed that each structure had an optimum operating point where the DSR was at a minimum. This point occurred at similar river flows (model Q_{riv} = 320-384 l/s and prototype Q_{riv} = 1000-1200 m^3/s). It is assumed that the sediment load of the river increases drastically at river flows larger than the one observed at the optimum point. The sediment load is largely dependent on the sediment characteristics in a river and this optimum river flow is thus not applicable to any scenario.

It was also found that as generally known and mentioned by the likes of Avery (1989), Raudkivi (1993) and Bouvard (1992), that the DSR increases with DDR. This result is shown on Figures 5.5 5.6, 5.7 and 5.8.

6.3 Intake Opening Height

As an attempt to further reduce abstracted sediment a second and a third intake opening were tested. The first inlet opening is designed to be submerged with the water level at minimum operating level. During the prototype design of each structure the second inlet was 0.3 m higher than the top of the first inlet and the third inlet was 0.3 m higher than the top of the second inlet. The intake opening size (height, z) influences the ultimate height of inlet 2 and 3. Thus, the top of inlet 1 is at MOL, the top of inlet 2 at (0.3 m + z) above MOL and the top of inlet 3 at (0.6 m + 2z) above MOL. The intake opening size (z) is specific to each structure.

The results showed, as expected, that higher intake opening diverts less sediment. The intake opening height was evaluated as a *percentage improvement* between intake opening height, calculated with equation 5.1.

Table 5.2 shows that the largest improvement is between inlets 1-2 and inlets 1-3. This indicated that it might be feasible to only have two consecutive inlets. Either (0.3 m + z) or (0.6 m +2z) apart, depending on the flood frequency and whether an intake (0.6 m +2z) above MOL will be in operation frequently.

In the case of structure C, the consecutive inlets did not show significant improvement as seen in Figure 5.16. It was observed that at the generally lower inlets of structure C, local sediment in and around the graveltrap was entrained through the inlets, causing the variability in trend.

The effect of inlet height at all three structures was evaluated together by converting the diverted sediment load (G_d) to diverted sediment concentration (C_d), with equation 5.2. Figure 5.17 plots

C_d against the model inlet height.

In the case of structure A (with a prototype weir height of 4.5 m) less improvement was observed between inlets 2-3 than inlets 1-2. At this structure is might be feasible to only design for inlets 1 and 3. The flood frequency must be considered to determine whether inlet 3, of which the top of inlet is 3.3 m above the minimum operating level will be in operation frequently. The analysis revealed in the case of structure B with a prototype weir height of 3.5 m it could be feasible to use any of the three inlets, due to the improvement observed between inlets 1-2 and inlets 2-3.

6.4 Graveltrap Operation: Sediment Flushing and Self Scouring Range

The efficient operation of the graveltrap should result in less sediment deposition at the intake, which would be entrained through the intake opening. Efficient operation of the graveltrap is thus also a method of reducing diverted sediment in the diverted flow.

Sediment flushing with water level drawdown was evaluated at each configuration by recording the time necessary to flush a full graveltrap clean. This was evaluated at increasing river flows and the river flow was determined at which the flushing through the sluice gate ceased to operate efficiently. The recorded average flushing times per structure are presented on Figure 5.37.

The flow over the submerged graveltrap wall and the flow through the sluice gate were analysed to determine the effects on the efficiency of sediment flushing.

Bouvard (1992) stated that the flow over the graveltrap wall must form a separated nappe so that the impact of the flow can entrain sediment. It was observed in this study that flows where the graveltrap wall was obviously submerged, the graveltrap struggled to flush. This confirmed the statement of Bouvard (1992).

Flushing through the sluice gate was evaluated with a y_3/y_2 term, following the annotation of Figure 4.14. y_3/y_2 is the actual downstream depth over the contracted flow depth beneath the sluice gate opening. This term was evaluated at the maximum efficient flushing flow and the minimum non-flushing flow. It was assumed that the flow was sub-critical upstream of the gate at these flows (which was confirmed by the video footage).

In the case of structure A (4.5 m weir) and B (3.5 m weir) it was found that y_3/y_2 was close to 1 during the maximum efficient flushing flow and $y_3/y_2 > 1$ at the minimum non-flushing flow. In the case of structure C (2.5 m weir) y_3/y_2 was smaller than 1 even at the minimum non-flushing flow. The low graveltrap wall of structure C would submerge at lower river flows

than structures A and B. It is assumed that the flushing of the graveltrap of structure C was negatively affected by the flow over the graveltrap wall before the y_3/y_2 guideline had an effect.

A good operational guideline would be to flush the graveltrap at a river flow, resulting in $y_3/y_2 < 1$, but ensuring that the flow over the graveltrap wall is still able to entrain the sediment in the graveltrap.

The sediment flushing was also evaluated as a y_3/y_G term, to serve as a possible operational guideline. y_G is the gate opening size, which was equal to the low notch weir height. Figure 5.41 is a plot of y_3/y_G against prototype river flow, showing zones of effective and ineffective sediment flushing. Table 5.7 can be used to relate model, prototype and unit discharge river flow.

Figure 5.42 presents in prototype dimensions the sediment flushing and self scouring ranges of the three structures tested, all at the optimum intake angle of 45^0. The results give a good indication of the graveltrap operation of structures with different weir heights. The graveltrap of a structure with a 4.5 m weir will have a larger range of river flows where sediment flushing is applicable than a structure with a 3.5 m and 2.5 m weir. On the other hand the graveltrap of structures with lower weirs will be able to scour clean during lower river flows than that of the larger structures.

6.5 Limitations of the Findings and Conclusions

Keep in mind that the river flows and related downstream depths are specific to the scenario tested and that especially the range of sediment flushing, which is greatly affected by the downstream water depth will change according to the size of the river.

It should also be realised that the results of this study was based on a specific sediment characteristic of the sediment used in the physical model of this study and sediment with other characteristics would affect the range of both the sediment flushing and the self scouring of the graveltrap.

Chapter 7

Recommendations

The following recommendations are considered relevant for future research on sediment control features at low-weir diversion works:

- a 3D numerical model study to evaluate the results of the intake angle, focussing on the following:

  The location of the induced secondary currents of each intake angle.

  The effect of varying river sizes (widths)

  Different graveltrap shapes should be evaluated

- a Physical model study dedicated to the flow through the sluice gate and the effect of the downstream water depth on sediment flushing with water level drawdown.

- a Physical model study on the flow over the submerged graveltrap wall, with focus on entrainment of sediment in the graveltrap.

- The following should be kept in mind during future physical model studies on low weir diversion works:

  Determine the equilibrium slope of the river section upstream of the weir

  Place sediment as if the weir has already reached an equilibrium state of sedimentation.

  Repeat tests with varying sediment sizes.

References

Avery, P. (1989). *Sediment Control at Intakes - a Design Guide*. BHRA, The Fluid Engineering Centre.

Bagnold, R. (1966). An approach to the sediment transport problem from general physics. *US Geol. Surv. Prof. Pap., 422*, vol. 1, pp. 231–291.

Basson, G. (2006). *Design guidelines of river abstraction works*, vol. 2. Water Research Commsision.

Basson, G. (2012 May). Hydraulic design of the proposed berg river abstraction works at voëlvlei dam. Tech. Rep., ASP Technology (pty) ltd.

Basson, G. and Rooseboom, A. (1997). *Dealing with Reservoir Sedimentation*. Water Research Commsision.

Beck, J.S., B.G. (2003). Dealing with dam impacts. Tech. Rep., University of Stellenbosch.

Bieri, M., Müller, M., Boillat, J.-L. and Schleiss, A. (2011). Modeling of sediment management for the lavey run-of-river hpp in switzerland. *Journal of Hydraulic Engineering*, vol. 138, no. 4, pp. 340–347.

Bouvard, M. (1992). *Mobile barrages and intakes on sediment transporting rivers*. A.A. Balkema.

Bridge, J. and Jarvis, J. (1982). The dynamics of a river bend: a study in flow and sedimentary processes. *Sedimentology*, vol. 29, no. 4, pp. 499–541.

Brink, C. (2004). *Bend Diversion To Minimise Sediment Intake*. Master's thesis, Stellenbosch University.

Brink, C., Basson, G. and Denys, F. (2006). *Sediment Control At River Abstraction Works In South Africa*, vol. 1. Water Research Commsision.

Bulle, H. (1926). cited in Van Heerden (2012).

Chadwick, A., Morfett, J. and Borthwick, M. (2004). *Hydraulics in Civil and Environmental Engineering*. Fourth edition edn. Spon Press.

Choudhary, U.K. and Narasimhan, S. (1977). Flow in 180 open channel rigid boundary bends. *Journal of the Hydraulics Division*, vol. 103, no. 6, pp. 651–657.

Denys, F. (2006). *Transverse transport of suspended sediment across the main channel–floodplain shear boundary.* Master's thesis, Stellenbosch: University of Stellenbosch.

DWAF (2004 September). National water resource strategy.

Ettema, R. (2000). *Hydraulic modeling: Concepts and practice.* 97. ASCE Publications.

Habermaas, F. (1935). cited in Shen (1971).

Hjulstrom (1935). cited in Raudkivi (1993).

Institution, B.S. (1975). *Methods of Test for Soils for Civil Engineering Purposes: BS 1377, 1975.* British Standards Institution.

Minikin, R. (1920). *Practical river and canal engineering.* C. Griffin.

Moyosi, E. (1965). cited in Shen (1971).

Msadala, V. and Basson, G. (2009). *Sediment yield prediction methodology of South Africa.* Master's thesis, University of Stellenbosch.

Odgaard, A. and Spoljaric, A. (1986). Sediment control by submerged vanes. *Journal of Hydraulic Engineering*, vol. 112, no. 12, pp. 1164–1180.

Odgaard, A.J. and Wang, Y. (1991). Sediment management with submerged vanes. ii: Applications. *Journal of Hydraulic Engineering*, vol. 117, no. 3, pp. 284–302.

Petts, G. and Pratts, J. (1983). Channel changes following reservoir construction on a lowland english river. *Catena*, vol. 10, no. 1, pp. 77–85.

Raudkivi, A. (1993). *Sedimentation: Exclusion and removal of sediment from diverted water.* A.A. Balkema.

Rooseboom, A. (1992a). *Sediment Transport in Rivers and Reservoirs- a Southern African Perspective.* Water Research Commsision.

Rooseboom, A. (2002). The extraction of water from sediment laden streams in southern africa. Tech. Rep., Water Research Commission.

Rooseboom, A. and Mulke, F. (1982). Erosion initiation. *Recent Developments in the Explanation and Prediction of Erosion and Sediment Yield IAHS Publication*, , no. 137.

Rooseboom, A., Verster, E., Zietsman, H. and Lotriet, H. (1992b). *The Development of The New Sediment Yield Map of Southern Africa.* Water Research Commsision.

Rouse, H. (1937). Modern conceptions of the mechanics or fluid turbulence. *Transactions of the American Society of Civil Engineers*, vol. 102, no. 1, pp. 463–505.

Shen, H. (1971). *River Mechanics*, vol. 2. Shen, USA.

Tan, Y. (1996). Design of silt related hydraulic structures'. In: *International Conference on reservoir sedimentation.*

Van Heerden, M. (2012). *Control of sediment diversion in run-of-river hydropower schemes.* Master's thesis, Stellenbosch University.

Vanoni, V.A. (1975). *ASCE Manuals and Reports on Engineering Practice no. 54 : Sedimentation Engineering.* American Society of Civil Engineers.

Wessels, P. (2013). Design of gauging weirs and fishways. pp. 65–73.

Wu, W. (2008). *Computational river dynamics.* London: Taylor & Francis, National Center of Copmutational Hydrosciencs and Engineering, University of Mississippi, MS, USA.

Yang, C.T. (1973). cited in Yang (1996).

Yang, C.T. (1996). *Sediment transport: theory and practice.* McGraw-hill New York.

Appendix A

Test Result Data

Diverted Sediment Tests

Tests on Structure A (DSA)

TABLE A.1: DSA30: Diverted sediment tests of structure A at a 30^0 intake angle

Test	Q_{riv})(l/s)	DDR	G_{riv} (g/s)	$G_{feed,wet}$ (g/s)	Upstream depth (mm)	Downstream depth (mm)
DSA301	128	1.88%	0	0	278	124
DSA302	192	1.25%	2.3	10	306	160
DSA303	256	0.94%	10.5	20	334	191
DSA304	320	0.75%	59.6	100	353	220
DSA305	384	0.63%	64.3	130	373	247
DSA306	576	0.42%	110.2	180	435	320
Test	Q_{riv}	DDR	G_{riv}	G_{feed} (wet)	Upstream depth (mm)	Downstream depth (mm)
			Inlet 1			
DSA301	28	N/A	0	0	0.0000	0
DSA302	27	N/A	0	0	0.0000	0
DSA303	25	N/A	8	0.32	0.0304	0.133
DSA304	20	N/A	10	0.50	0.0084	0.208
DSA305	25	N/A	6	0.24	0.0037	0.1
DSA306	25	N/A	52	2.08	0.0189	0.867
			Inlet 2			
DSA301	60	0	0	0.000	0.0000	0
DSA302	60	6	3.5	0.058	0.0250	0.024
DSA303	60	12	7	0.117	0.0111	0.049
DSA304	60	28	16.4	0.273	0.0046	0.114
DSA305	60	16	9.4	0.156	0.0024	0.065
DSA306	60	34	30.4	0.506	0.0046	0.211
			Inlet 3			
DSA301	0	N/A	0	0	0	0
DSA302	27	N/A	1	0.037	0.01584	0.015
DSA303	25	N/A	2	0.080	0.00760	0.033
DSA304	27	N/A	1	0.037	0.00062	0.015
DSA305	25	18	10.5	0.421	0.00655	0.175
DSA306	26	50	29.2	1.124	0.01020	0.468

TABLE A.2: DSA45: Diverted sediment tests of structure A at a 45^0 intake angle

Test	Q_{riv}	DDR	G_{riv}	G_{feed} (wet)	Upstream depth (mm)	Downstream depth (mm)
DSA451	128	0.0188	0	0	286	124
DSA452	192	0.0125	2	10	314	160
DSA453	256	0.0094	11	20	339	191
DSA454	320	0.0075	60	100	364	220
DSA455	384	0.0063	64	130	385	247
DSA456	576	0.0042	110	180	453	320
Test	Time of abstraction (s)	Abstracted Sediment, wet (g)	Abstracted Sediment, dry (g)	G_d	DSR	C_d
			Inlet 1			
DSA451	60	0	0	0	N/A	0.000
DSA452	60	2	1.2	0.019	0.0083	0.008
DSA453	60	8	4.7	0.078	0.0074	0.032
DSA454	60	14	8.2	0.136	0.0023	0.057
DSA455	60	18	10.5	0.175	0.0027	0.073
DSA456	60	50	29.2	0.487	0.0044	0.203
			Inlet 2			
DSA451	60	4	2.3	0.039	N/A	0.0162
DSA452	60	4	2.3	0.039	0.0167	0.016
DSA453	60	16	9.4	0.156	0.0148	0.065
DSA454	60	14	8.2	0.136	0.0023	0.057
DSA455	60	20	11.7	0.195	0.0030	0.081
DSA456	60	32	18.7	0.312	0.0028	0.130
			Inlet 3			
DSA451	0	0	0	0	N/A	0
DSA452	60	2	1.2	0.019	0.0083	0.008
DSA453	60	4	2.3	0.039	0.0037	0.016
DSA454	60	4	2.3	0.039	0.0007	0.016
DSA455	60	6	3.5	0.058	0.0009	0.024
DSA456	60	26	15.2	0.253	0.0023	0.106

TABLE A.3: DSA60: Diverted sediment tests of structure A at 60^0 intake angle

Test	Q_{riv}	DDR	G_{riv}	G_{feed} (wet)	Upstream depth (mm)	Downstream depth (mm)
DSA601	128	0.0188	0	0	293	124
DSA602	192	0.0125	2	10	325	160
DSA603	256	0.0094	11	20	350	191
DSA604	320	0.0075	60	100	378	220
DSA605	384	0.0063	64	130	408	247
DSA606	576	0.0042	110	180	486	320
Test	Time of abstraction (s)	Abstracted Sediment, wet (g)	Abstracted Sediment, dry (g)	G_d	DSR	C_d
			Inlet 1			
DSA601	60	4	2.3	0.0390	N/A	0.016
DSA602	60	2	1.2	0.0195	0.0083	0.008
DSA603	60	4	2.3	0.0390	0.0037	0.016
DSA604	60	10	5.8	0.0974	0.0016	0.041
DSA605	60	8	4.7	0.0779	0.0012	0.032
DSA606	60	94	54.9	0.9156	0.0083	0.381
			Inlet 2*			
DSA601	60	2	1.2	0.0195	N/A	0.008
DSA602	60	2	1.2	0.0195	0.0083	0.008
DSA603	60	2	1.2	0.0195	0.0019	0.008
DSA604	60	4	2.3	0.0390	0.0007	0.016
DSA605	60	4	2.3	0.0390	0.0006	0.016
DSA606	60	30	17.5	0.2922	0.0027	0.122
*at DSA606-inlet 2 Q_{riv} = 528 l/s and the Downstream depth =. G_{riv} and G_{feed} was assumed to be equal to the values with Q_{riv} = 576 l/s.						
			Inlet 3			
DSA601	0	0	0	0	N/A	0.000
DSA602	60	2	1.2	0.0195	0.0083	0.008
DSA603	60	2	1.2	0.0195	0.0019	0.008
DSA604	60	2	1.2	0.0195	0.0003	0.008
DSA605	60	6	3.5	0.0584	0.0009	0.024
DSA606	60	0	60.0	1	0.0091	0.417

TABLE A.4: DSB30: Diverted sediment tests of structure B at 30^0 intake angle

Test	Q_{riv}	DDR	G_{riv}	G_{feed} (wet)	Upstream depth (mm)	Downstream depth (mm)
DSB301	128	0.0087	0	0	243	124
DSB302	192	0.0058	11	20	274	160
DSB303	256	0.0043	29	50	298	191
DSB304	320	0.0035	70	120	316	220
DSB305	384	0.0029	174	300	343	247
DSB306	528	0.0021	254	650	372	302
Test	Time of abstraction (s)	Abstracted Sediment, wet (g)	Abstracted Sediment, dry (g)	G_d	DSR	C_d
			Inlet 1			
DSB301	60	2	1.2	0.019	N/A	0.018
DSB302	60	12	7.0	0.117	0.0105	0.106
DSB303	60	12	7.0	0.117	0.0040	0.106
DSB304	60	16	9.4	0.156	0.0022	0.142
DSB305	60	32	18.7	0.312	0.0018	0.283
DSB306	60	108	63.1	1.052	0.0041	0.956

TABLE A.5: DSB45: Diverted sediment tests of structure B at 45^0 intake angle

Test	Q_{riv}	DDR	G_{riv}	G_{feed} (wet)	Upstream depth (mm)	Downstream depth (mm)
DSB451	128	0.0087	0	0	242	124
DSB452	192	0.0058	11	20	274	160
DSB453	256	0.0043	29	50	302	191
DSB454	320	0.0035	70	120	326	220
DSB455	384	0.0029	174	300	352	247
DSB456	528	0.0021	254	650	398	302
Test	Time of abstraction (s)	Abstracted Sediment, wet (g)	Abstracted Sediment, dry (g)	G_d	DSR	C_d
			Inlet 1			
DSB451	60	0	0	0	N/A	0.000
DSB452	60	0	0	0	0	0.000
DSB453	60	8	4.7	0.078	0.0027	0.071
DSB454	60	14	8.2	0.136	0.0019	0.124
DSB455	60	26	15.2	0.253	0.0015	0.230
DSB456	60	74	43.2	0.721	0.0028	0.655
			Inlet 2			
DSB451	60	0	0	0	N/A	0.000
DSB452	60	2	1.2	0.019	0.0018	0.018
DSB453	60	4	2.3	0.039	0.0013	0.035
DSB454	60	6	3.5	0.058	0.0008	0.053
DSB455	60	10	5.8	0.097	0.0006	0.089
DSB456	60	36	21.0	0.351	0.0014	0.319
			Inlet 3			
DSB451	60	0	0	0	N/A	0
DSB452	60	1	0.6	0.010	0.0009	0.009
DSB453	60	1	0.6	0.010	0.0003	0.009
DSB454	60	2	1.2	0.019	0.0003	0.018
DSB455	60	8	4.7	0.078	0.0004	0.071
DSB456	60	16	9.4	0.156	0.0006	0.142

TABLE A.6: DSB60: Diverted sediment tests of structure B at 60^0 intake angle

Test	Q_{riv}	DDR	G_{riv}	G_{feed} (wet)	Upstream depth (mm)	Downstream depth (mm)
DSB601	128	0.0087	0	0	248	124
DSB602	192	0.0058	11	20	277	160
DSB603	256	0.0043	29	50	311	191
DSB604	320	0.0035	70	120	337	220
DSB605	384	0.0029	174	300	358	247
DSB606	528	0.0021	254	650	412	302
Test	Time of abstraction (s)	Abstracted Sediment, wet (g)	Abstracted Sediment, dry (g)	G_d	DSR	C_d
			Inlet 1			
DSB601	60	0	0	0	N/A	0.000
DSB602	60	0	0	0	0	0.000
DSB603	60	2	1.2	0.019	0.0007	0.018
DSB604	60	2	1.2	0.019	0.0003	0.018
DSB605	60	4	2.3	0.039	0.0002	0.035
DSB606	60	34	19.9	0.331	0.0013	0.301

TABLE A.7: DSC45: Diverted sediment tests of structure C at 45^0 intake angle

Test	Q_{riv}	DDR	G_{riv}	G_{feed} (wet)	Upstream depth (mm)	Downstream depth (mm)
DSC451	64	0.0064	0	0	163	81
DSC452	128	0.0032	5	10	205	124
DSC453	192	0.0021	70	150	231	160
DSC454	256	0.0016	115	300	256	191
DSC455	320	0.0013	234	400	295	220
DSC456	384	0.0011	251	450	325	247
DSC457	528	0.0008	323	700	400	302
Test	Time of abstraction (s)	Abstracted Sediment, wet (g)	Abstracted Sediment, dry (g)	G_d	DSR	C_d
			Inlet 1			
DSC451	120	0	0	0	N/A	0.000
DSC452	120	2	1.2	0.010	0.0019	0.024
DSC453	120	30	17.5	0.146	0.0021	0.356
DSC454	120	52	30.4	0.253	0.0022	0.618
DSC455	120	20	11.7	0.097	0.0004	0.238
DSC456	120	24	14.0	0.117	0.0005	0.285
DSC457	120	84	49.1	0.409	0.0013	0.998
			Inlet 2			
DSC451	120	0	0	0	N/A	0.000
DSC452	120	6	3.5	0.029	0.0056	0.071
DSC453	0	0	0	0	0	0.000
DSC454	120	12	7.0	0.058	0.0005	0.143
DSC455	60	22	12.9	0.214	0.0009	0.523
DSC456	90	16	9.4	0.104	0.0004	0.253
DSC457	120	62	36.2	0.302	0.0009	0.736
			Inlet 3			
DSC451	120	0	0	0	N/A	0.000
DSC452	120	2	1.2	0.010	0.0019	0.024
DSC453	120	8	4.7	0.039	0.0006	0.095
DSC454	120	18	10.5	0.088	0.0008	0.214
DSC455	120	36	21.0	0.175	0.0007	0.428
DSC456	120	38	22.2	0.185	0.0007	0.451
DSC457	120	56	32.7	0.273	0.0008	0.665

TABLE A.8: DSC60: Diverted sediment tests of structure C at 60^0 intake angle

Test	Q_{riv}	DDR	G_{riv}	G_{feed} (wet)	Upstream depth (mm)	Downstream depth (mm)
DSC601	64	0.0064	0	0	173	81
DSC602	128	0.0032	5	10	205	124
DSC603	192	0.0021	70	150	238	160
DSC604	256	0.0016	115	300	267	191
DSC605	320	0.0013	234	400	294	220
DSC606	384	0.0011	251	450	325	247
DSC607	528	0.0008	323	700	369	302
Test	Time of abstraction (s)	Abstracted Sediment, wet (g)	Abstracted Sediment, dry (g)	G_d	DSR	C_d
			Inlet 1			
DSC601	60	0	0	0	N/A	0.000
DSC602	60	2	1.2	0.019	0.0037	0.018
DSC603	60	4	2.3	0.039	0.0006	0.035
DSC604	120	26	15.2	0.127	0.0011	0.115
DSC605	120	32	18.7	0.156	0.0007	0.142
DSC606	130	47	27.5	0.211	0.0008	0.192
DSC607	120	48	28.1	0.234	0.0007	0.213

TABLE A.9: SSA test: Graveltrap survey of structure A at 30^0 45^0 and 60^0 intake angles

SSA : Self Scour of graveltrap test, of structure A								
Survey points			1	2	3	4	5	6
x			100	300	500	700	900	1100
Floor level (mm above datum)			73.3	60	46.7	33.3	20	6.7
Initial sediment level in graveltrap (mm above datum)			127	127	127	127	127	127
Test	$Qriv$ (l/s)	Downstream depth (mm)	GT survey (mm above datum)					
SSA30 : Self Scour of graveltrap test, of structure A at a 30^0 intake angle								
SSA301	128	124	125	127	131	137	137	132
SSA302	192	160	127	126	131	137	134	135
SSA303	256	191	127	126	131	137	134	135
SSA304	320	220	116	120	120	135	135	138
SSA305	384	247	100	109	110	124	171	135
SSA306	480	285	73	60	78	86	78	15
SSA307	576	320	73	60	48	70	78	7
SSA45 : Self Scour of graveltrap test, of structure A at a 45^0 intake angle								
SSA451	128	124	130	129	130	127	127	129
SSA452	192	160	129	128	128	136	128	128
SSA453	256	191	129	129	132	124	114	127
SSA454	320	220	128	124	139	132	134	127
SSA455	384	247	122	116	119	105	111	124
SSA456	480	285	105	100	89	92	107	60
SSA457	576	320	88	100	60	71	88	42
SSA60 : Self Scour of graveltrap test, of structure A at a 60^0 intake angle								
SSA601	128	124	128	132	130	130	135	130
SSA602	192	160	128	134	130	130	134	130
SSA603	256	191	130	130	131	130	130	130
SSA604	320	220	128	127	127	130	130	130
SSA605	384	247	128	132	124	122	121	128
SSA606	480	285	121	119	120	120	129	130
SSA607	576	320	103	90	94	100	100	64

TABLE A.10: SSB test: Graveltrap survey of structure B at 30^0 45^0 and 60^0 intake angles

SSB : Self Scour of graveltrap test, of structure B								
Survey points			1	2	3	4	5	6
x (mm)			100	300	500	700	900	1100
Floor level (mm above datum)			73.3	60	46.7	33.3	20	6.7
Initial sediment level in graveltrap (mm above datum)			113	113	113	113	113	113
Test	$Qriv$ (l/s)	Downstream depth (mm)	GT survey (mm above datum)					
SSB30 : Self Scour of graveltrap test, of structure B at a 30^0 intake angle								
SSB301	128	124	113	113	115	110	110	113
SSB302	192	160	111	111	115	104	113	113
SSB303	256	191	105	116	101	102	115	102
SSB304	320	220	90	105	89	103	96	89
SSB305	384	247	74	81	69	83	84	18
SSB306	480	285	74	61	67	76	86	9
SSB307	528	302	74	61	47	34	24	7
SSB45 : Self Scour of graveltrap test, of structure B at a 45^0 intake angle								
SSB451	128	124	113	113	113	113	113	113
SSB452	192	160	113	113	113	113	116	113
SSB453	256	191	110	112	108	104	105	113
SSB454	320	220	105	107	105	104	101	106
SSB455	384	247	101	103	99	96	102	91
SSB456	480	285	101	102	100	96	100	70
SSB457	528	302	90	88	87	85	96	34
SSB60 : Self Scour of graveltrap test, of structure B at a 60^0 intake angle								
SSB601	128	124	114	117	116	113	115	112
SSB602	192	160	520	520	520	520	520	520
SSB603	256	191	115	115	116	118	115	112
SSB604	320	220	113	115	113	103	89	91
SSB605	384	247	110	116	109	102	89	93
SSB606	480	285	97	102	96	91	79	60
SSB607	528	302	87	86	86	79	60	46

TABLE A.11: SSC test: Graveltrap survey of structure C at 45^0 and 60^0 intake angles

SSB : Self Scour of graveltrap test, of structure C							
Survey points			1	2	3	4	5
x (mm)			100	300	500	700	900
Floor level (mm above datum)			60	46.7	33.3	20	6.7
Initial sediment level in graveltrap (mm above datum)			92	92	92	92	92
Test	$Qriv$ (l/s)	Downstream depth (mm)	GT survey (mm above datum)				
SSC45 : Self Scour of graveltrap test, of structure C at a 45^0 intake angle							
SSC451	128	124	91	91	85	89	88
SSC452	192	160	89	89	98	91	65
SSC453	256	191	72	79	79	65	51
SSC454	320	220	60	55	63	70	7
SSC455	384	247	60	47	33	26	7
SSC456	480	285	Not tested	Not tested	Not tested	Not tested	Not tested
SSC457	528	302	60	47	33	20	7
SSC60 : Self Scour of graveltrap test, of structure C at a 60^0 intake angle							
SSC601	128	124	92	93	92	89	95
SSC602	192	160	89	90	92	89	82
SSC603	256	191	91	90	87	90	79
SSC604	320	220	89	93	86	85	62
SSC605	384	247	83	77	83	79	47
SSC606	480	285	76	71	71	73	24
SSC607	528	302	62	52	52	55	7

TABLE A.12: Sediment Flushing Test Results

Test	Q_{riv} (l/s)	Downstream depth (mm)	Flushing time (s)
SFA30 : Sediment flushing test of structure A at a 30^0 intake angle			
SFA301	4	15	11.5
SFA302	25.6	46	23.4
SFA303	38.2	59	33.5
SFA304	64	81	51.5
SFA305	128	124	100
SFA306	192	160	ineffective
SFA45 : Sediment flushing test of structure A at a 45^0 intake angle			
SFA451	4	15	15
SFA452	25.6	46	20.75
SFA453	38.2	59	25
SFA454	64	81	39
SFA455	128	124	112
SFA456	192	160	ineffective
SFA60 : Sediment flushing test of structure A at a 60^0 intake angle			
SFA601	4	15	14
SFA602	25.6	46	19
SFA603	38.2	59	21
SFA604	64	81	51
SFA605	128	124	114
SFA606	192	160	ineffective
SFB30 : Sediment flushing test of structure B at a 30^0 intake angle			
SFB301	4	15	30
SFB302	25.6	46	62
SFB303	38.4	59	103
SFB304	64	81	160
SFB305	128	124	ineffective
SFB45 : Sediment flushing test of structure B at a 45^0 intake angle			
SFB451	4	15	23
SFB452	25.6	46	78
SFB453	38.4	59	126
SFB454	64	81	173
SFB455	128	124	ineffective
SFB60 : Sediment flushing test of structure B at a 60^0 intake angle			
SFB601	4	15	28
SFB602	25.6	46	83
SFB603	38.4	59	97
SFB604	64	81	167
SFB605	128	124	ineffective
SFC45 : Sediment flushing test of structure C at a 45^0 intake angle			
SFC451	4	15	53
SFC452	12.8	30	130
SFC453	25.6	46	ineffective
SFC60 : Sediment flushing test of structure C at a 60^0 intake angle			
SFC451	4	15	54
SFC452	12.8	30	185
SFC453	25.6	46	ineffective

TABLE A.13: River flow, downstream depth and upstream depth - in model and prototype scale

Q_{riv}			Downstream depth		Upstream depth	
Model (l/s)	Prototype (m^3/s)	Prototype Unit Discharge (m^3/m.s)	Model (mm)	Prototype (m)	Model (mm)	Prototype (m)
		A30 : Structure A at a 30^0 intake angle				
4	12.5	0.167	15	0.38	194	4.85
25.6	80	1.067	46	1.16	216	5.40
38.2	120	1.600	59	1.48	225	5.63
64	200	2.667	81	2.02	243	6.08
128	400	5.333	124	3.10	278	6.95
192	600	8.000	160	3.99	306	7.65
256	800	10.667	191	4.77	334	8.34
320	1000	13.333	220	5.50	353	8.83
384	1200	16.000	247	6.17	373	9.31
480	1500	20.000	285	7.11	403	10.08
576	1800	24.000	320	8.00	435.25	10.88
		A45 : Structure A at a 45^0 intake angle				
4	12.5	0.167	15	0.38	193	4.83
25.6	80	1.067	46	1.16	219	5.48
38.2	120	1.600	59	1.48	229	5.73
64	200	2.667	81	2.02	249	6.23
128	400	5.333	124	3.10	286	7.15
192	600	8.000	160	3.99	314	7.85
256	800	10.667	191	4.77	339	8.48
320	1000	13.333	220	5.50	364	9.10
384	1200	16.000	247	6.17	385	9.63
480	1500	20.000	285	7.11	413	10.33
576	1800	24.000	320	8.00	453	11.33
		A60 : Structure A at a 60^0 intake angle				
4	12.5	0.167	15	0.38	196	4.90
25.6	80	1.067	46	1.16	219	5.48
38.2	120	1.600	59	1.48	236	5.90
64	200	2.667	81	2.02	283	7.08
128	400	5.333	124	3.10	293	7.31
192	600	8.000	160	3.99	325	8.13
256	800	10.667	191	4.77	350	8.76
320	1000	13.333	220	5.50	378	9.45
384	1200	16.000	247	6.17	408	10.20
480	1500	20.000	285	7.11	459	11.48
576	1800	24.000	320	8.00	486	12.15
		B30 : Structure B at a 30^0 intake angle				
4	12.5	0.167	15	0.38	158	3.95
25.6	80	1.067	46	1.16	179	4.48
38.2	120	1.600	59	1.48	190	4.75
64	200	2.667	81	2.02	210	5.25
128	400	5.333	124	3.10	243	6.08
192	600	8.000	160	3.99	274	6.85
256	800	10.667	191	4.77	298	7.45
320	1000	13.333	220	5.50	316	7.90
384	1200	16.000	247	6.17	343	8.58
480	1500	20.000	285	7.11	372	9.30
576	1800	24.000	320	8.00	386	9.65
		B45 : Structure B at a 45^0 intake angle				
4	12.5	0.167	15	0.38	166	4.15
25.6	80	1.067	46	1.16	182	4.55
38.2	120	1.600	59	1.48	192	4.80
64	200	2.667	81	2.02	210	5.25
128	400	5.333	124	3.10	242	6.05
192	600	8.000	160	3.99	274	6.85
256	800	10.667	191	4.77	302	7.54
320	1000	13.333	220	5.50	326	8.15
384	1200	16.000	247	6.17	352	8.80
480	1500	20.000	285	7.11	398	9.95
576	1800	24.000	320	8.00	418	10.45
		B60 : Structure B at a 60^0 intake angle				
4	12.5	0.167	15	0.38	153	3.83
25.6	80	1.067	46	1.16	182	4.55
38.2	120	1.600	59	1.48	194	4.85
64	200	2.667	81	2.02	211	5.28
128	400	5.333	124	3.10	248	6.20
192	600	8.000	160	3.99	277	6.93
256	800	10.667	191	4.77	311	7.78
320	1000	13.333	220	5.50	337	8.43
384	1200	16.000	247	6.17	358	8.95
480	1500	20.000	285	7.11	412	10.30
528	1650	22.000	302	7.55	419	10.48
		C45 : Structure C at a 45^0 intake angle				
4	12.5	0.167	15	0.38	116	2.90
25.6	80	1.067	47	1.16	138	3.45
38.4	120	1.600	59	1.48	160	4.00
64	200	2.667	81	2.02	163	4.08
128	400	5.333	124	3.10	205	5.13
192	600	8.000	160	3.99	231	5.78
256	800	10.667	191	4.77	256	6.40
320	1000	13.333	220	5.50	295	7.38
384	1200	16.000	247	6.17	325	8.13
480	1500	20.000	285	7.11	N/A	N/A
528	1650	22.000	302	7.56	400	10.00
		C60 : Structure C at a 60^0 intake angle				
4	12.5	0.167	15	0.38	114	2.85
25.6	80	1.067	46	1.16	140	3.50
38.4	120	1.600	59	1.48	160	4.00
64	200	2.667	81	2.02	173	4.33
128	400	5.333	124	3.10	205	5.13
192	600	8.000	160	3.99	238	5.95
256	800	10.667	191	4.77	267	6.68
320	1000	13.333	220	5.50	294	7.35
384	1200	16.000	247	6.17	325	8.11
480	1500	20.000	285	7.11	361	9.03
528	1650	22.000	302	7.56	369	9.21

Appendix B

Pump Calibrations and Dry Weight Factor

Table B.1: Pump A Accuracy

Input weight (g)	Output (weight (g)	Accuracy
56	50	89%
32	30	94%
20	20	100%
12	10	83%
4	4	100%
average accuracy		93%

Table B.2: Samples to determine $F_{dry/wet}$

Wet sample (g)	Dried sample (g)	$F_{dry/wet}$
72	44	61%
186	142	76%
180	142	79%
52	28	54%
128	90	70%
154	66	43%
64	32	50%
56	30	54%
36	20	56%
2	1	50%
14	8	57%
7	4	57%
12	6	50%
Average		58%

Appendix C

Prototype Sediment Size Calculation

Chapter 2.5.4 discusses the modified Lui diagram. The sediment similarity was evaluated without the structure and thus with the parameters as summarised in Table 4.1, which yielded a river bed slope of 1:678.

Table C.1 summarises the river flow, flow depth and energy slope applied. It was observed that the river flow at which the similarity is determined does not affect the result of the prototype sediment size. The Q_{riv} used is in the middle of the test range.

The model sediment settling velocity was determined by Van Heerden (2012) and the prototype sediment settling velocity is determined with equations C.1 or C.2 of Zanke (1977) (cited in Wu (2008)).

The prototype sediment particle size was iterated until it yielded a $\sqrt{gDS}/w$ value close to that of the model sediment. This is graphically shown on Figure C.1. The method yielded a prototype sediment size of 1.4 mm, which is very coarse sand in the field.

Table C.1: Parameters for modified Lui diagram

Parameter	Prototype	Model
Q_{riv}	400 m^3/s	128 l/s
D	3.1 m	0.124 mm
S_f (1/x)	678	678

$$w = 10\frac{\nu}{d}(1 + \frac{0.01(Ss-1)gd^3}{\nu^2})^{0.5} - 1) \tag{C.1}$$

$$w = 1.1((Ss-1)gd)^{1/2} \tag{C.2}$$

where:

ν is the viscosity of water, with an assumed value of 1.14×10^{-6}
d is the particle diameter in meter.
For equation C.1 : 0.1 mm < d < 1 mm
For equation C.2 : d > 1 mm
S_s is the relative sediment density, with an assumed value of 2.65

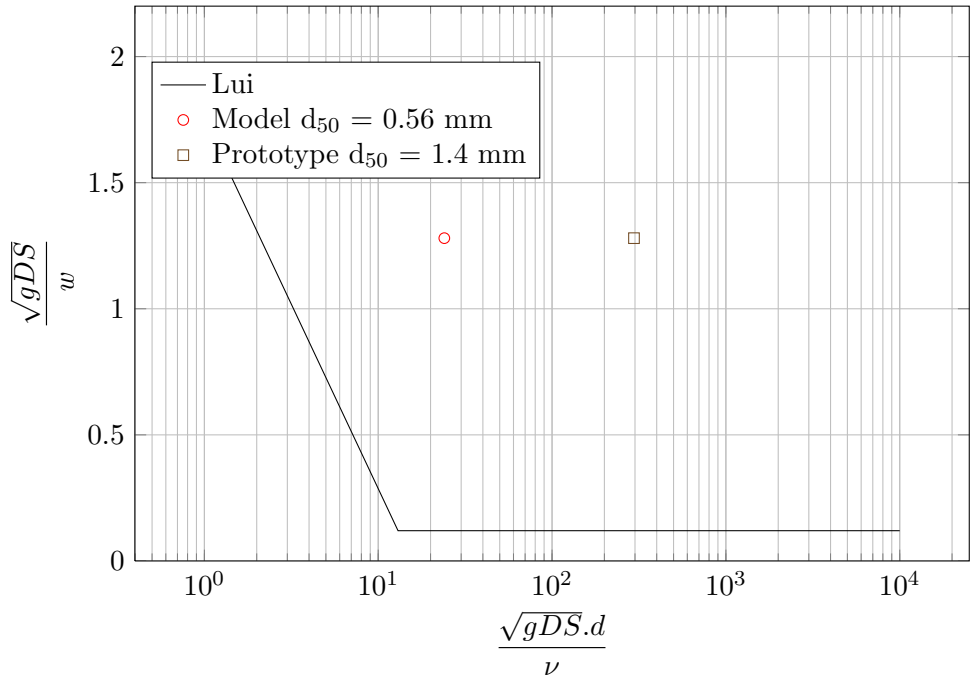

FIGURE C.1: Modified Lui Diagram with prototype Q_{riv} = 400 m^3/s and D = 3.1 m